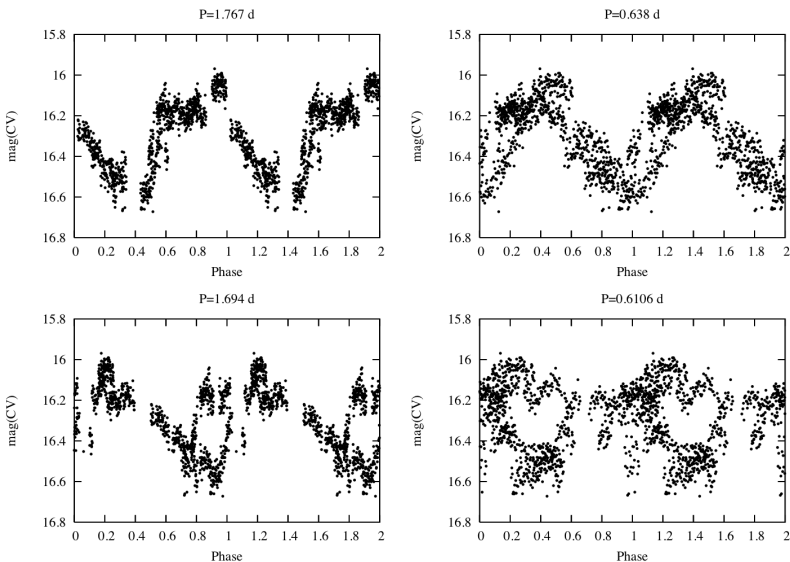


The Journal of the American Association
of Variable Star Observers

Optical Time-Series Photometry of a Peculiar Nova



The light curve of CSS081007 folded with four different periods.

Also in this issue...

- Further studies of "Irregularity" in Red Giants
- Ross 4—A Possible Recurrent Nova?
- Absolute Magnitudes and Distances of Recent Novae
- Observing Exoplanet Transits

Complete table of contents inside...



49 Bay State Road
Cambridge, MA 02138
U. S. A.

The Journal of the American Association of Variable Star Observers

Editor

John R. Percy
University of Toronto
Toronto, Ontario, Canada

Associate Editor

Elizabeth O. Waagen

Assistant Editor

Matthew Templeton

Production Editor

Michael Saladyga

Editorial Board

Priscilla J. Benson
Wellesley College
Wellesley, Massachusetts

David B. Williams
Indianapolis, Indiana

Douglas S. Hall
Vanderbilt University
Nashville, Tennessee

Thomas R. Williams
Houston, Texas

The Council of the American Association of Variable Star Observers 2009–2010

Director
President
Past President
1st Vice President
Secretary
Treasurer
Clerk

Arne A. Henden
Jaime R. Garcia
Paula Szkody
Mike Simonsen
Gary Walker
Gary W. Billings
Arne A. Henden

Councilors

Pamela Gay
Edward F. Guinan
Katherine Hutton
Michael Koppelman

Arlo U. Landolt
Jennifer Sokoloski
David Turner
Christopher Watson

ISSN 0271-9053

JAAVSO

The Journal of
The American Association
of Variable Star Observers

Volume 38
Number 2
2010



ISSN 0271-9053

49 Bay State Road
Cambridge, MA 02138
U. S. A.

The *Journal of the American Association of Variable Star Observers* is a refereed scientific journal published by the American Association of Variable Star Observers, 49 Bay State Road, Cambridge, Massachusetts 02138, USA. The *Journal* is made available to all AAVSO members and subscribers.

In order to speed the dissemination of scientific results, selected papers that have been refereed and accepted for publication in the *Journal* will be posted on the internet at the *eJAAVSO* website as soon as they have been typeset and edited. These electronic representations of the *JAAVSO* articles are automatically indexed and included in the NASA Astrophysics Data System (ADS). *eJAAVSO* papers may be referenced as *J. Amer. Assoc. Var. Star Obs., in press*, until they appear in the concatenated electronic issue of *JAAVSO*. The *Journal* cannot supply reprints of papers.

Page Charges

Unsolicited papers by non-Members will be assessed a charge of \$15 per published page.

Instructions for Submissions

The *Journal* welcomes papers from all persons concerned with the study of variable stars and topics specifically related to variability. All manuscripts should be written in a style designed to provide clear expositions of the topic. Contributors are strongly encouraged to submit digitized text in LATEX+POSTSCRIPT, MS WORD, or plain-text format. Manuscripts may be mailed electronically to journal@aaavso.org or submitted by postal mail to *JAAVSO*, 49 Bay State Road, Cambridge, MA 02138, USA.

Manuscripts must be submitted according to the following guidelines, or they will be returned to the author for correction:

Manuscripts must be:

- 1) original, unpublished material;
- 2) written in English;
- 3) accompanied by an abstract of no more than 100 words.
- 4) not more than 2,500–3,000 words in length (10–12 pages double-spaced).

Figures for publication must:

- 1) be camera-ready or in a high-contrast, high-resolution, standard digitized image format;
- 2) have all coordinates labeled with division marks on all four sides;
- 3) be accompanied by a caption that clearly explains all symbols and significance, so that the reader can understand the figure without reference to the text.

Maximum published figure space is 4.5" by 7". When submitting original figures, be sure to allow for reduction in size by making all symbols and letters sufficiently large.

Photographs and halftone images will be considered for publication if they directly illustrate the text.

Tables should be:

- 1) provided separate from the main body of the text;
- 2) numbered sequentially and referred to by Arabic number in the text, e.g., Table 1.

References:

- 1) References should relate directly to the text.
- 2) References should be keyed into the text with the author's last name and the year of publication, e.g., (Smith 1974; Jones 1974) or Smith (1974) and Jones (1974).
- 3) In the case of three or more joint authors, the text reference should be written as follows: (Smith *et al.* 1976).
- 4) All references must be listed at the end of the text in alphabetical order by the author's last name and the year of publication, according to the following format:
Brown, J., and Green, E. B. 1974, *Astrophys. J.*, **200**, 765.
Thomas, K. 1982, *Phys. Report*, **33**, 96.
- 5) Abbreviations used in references should be based on recent issues of the *Journal* or the listing provided at the beginning of *Astronomy and Astrophysics Abstracts* (Springer-Verlag).

Miscellaneous:

- 1) Equations should be written on a separate line and given a sequential Arabic number in parentheses near the right-hand margin. Equations should be referred to in the text as, e.g., equation (1).
- 2) Magnitude will be assumed to be visual unless otherwise specified.
- 3) Manuscripts may be submitted to referees for review without obligation of publication.

Journal of the American Association of Variable Star Observers

Volume 38, Number 2, 2010

Optical Time-Series Photometry of the Peculiar Nova CSS 081007:030559+054715 Matthew Templeton, Robert Koff, Patrick Wils, Arne A. Henden	147
Photometric Variability Properties of 21 T Tauri and Related Stars From AAVSO Visual Observations John R. Percy, Samantha Esteves, Jou Glasheen, Alfred Lin, Junjiajia Long, Marina Mashintsova, Emil Terziev, Sophia Wu	151
Further Studies of "Irregularity" in Pulsating Red Giants John R. Percy, Junjiajia Long	161
Two New Variable Stars in the Fields of Nova Cygni 2006 and Nova Cygni 2007 David Boyd	168
Ross 4—A Possible Recurrent Nova? Samantha J. Brown, O. F. Mills, Wayne Osborn, Vivian Hoette	176
Recent CCD Minima of 185 Eclipsing Binary Stars Gerard Samolyk	183
Absolute Magnitudes and Distances of Recent Novae Yitping Kok	193
Differential Ensemble Photometry by Linear Regression Kevin B. Paxson	202
Observing Exoplanet Transits With Digital SLR Cameras Colin Littlefield	212
A Simple, Portable Apparatus to Measure Night Sky Brightness at Various Zenith Angles Jennifer Birriel, James Kevin Adkins	221
Abstracts of Papers and Posters Presented at the 99th Spring Meeting of the AAVSO, Held in Mendoza, Argentina, April 15–18, 2010	
Introduction to Variable Star Astronomy Sebastián Otero	230
Current Hot Variable Star Topics Arne A. Henden	230
History of Variable Stars Rafael Girola, Nestor Vinet	230
Activities of the SEV/LIADA Raúl Roberto Podestá, María Dolores Suárez de Podestá	231
Mira Observations by Brazilício Alexandre Amorim	231

Table of Contents continued on following pages

King Charles' Star: A Multidisciplinary Approach to Dating Cassiopeiae A Martin Lunn, Lila Rakoczy	231
Near-infrared Observations of Cepheid Variables in the Large Magellanic Cloud Lucas Macri	232
Minima of Some Eclipsing Binaries Alexandre Amorim	233
New Variable Stars in the Southern Cross Victor Angel Buso	233
Didactics on Education in Astronomy Sebastián Musso	233
Starting Research Projects at Buenaventura Suárez Observatory in San Luis Province (poster) Eric González	234
New Equipment for Variable Star Research at the Instituto Copernico Observatory Jaime García, Federico García	234
<i>Observational Techniques Workshop</i>	
Visual Observing Techniques Sebastián Otero	234
An Introduction to CCD Photometry of Variable Stars Jaime García	235
Advanced CCD Observing Techniques Arne A. Henden	235
<i>Data Mining in Astronomy Workshop</i>	
An Introduction to Data Mining Michael Koppelman	235
Tips to Succeed in Using the ASAS-3 Database Sebastián Otero	235
Mining for Rare Variable Stars in Photometric Databases Doug Welch	236
<i>Data Reduction Workshop</i>	
Uncertainty Analysis in Photometric Observations Michael Koppelman	236
Using the AAVSO International Database Arne A. Henden	236

Table of Contents continued on next page

How to Use MAXIM DL for CCD Image Reduction Federico García	237
Period Search Techniques in Variable Stars Jaime García	237
An Introduction to PHOTOMETRICA Michael Koppelman	237
Index to Volume 38	238

Optical Time-Series Photometry of the Peculiar Nova CSS081007:030559+054715

Matthew Templeton

AAVSO Headquarters, 49 Bay State Road, Cambridge, MA 02138; matthewt@aavso.org

Robert Koff

980 Antelope Drive West, Bennett, CO 80102; bob@antelopehillsobservatory.org

Patrick Wils

Aarschotsebaan 31, Hever B-3191, Belgium; patrickwils@yahoo.com

Arne A. Henden

AAVSO, 49 Bay State Road, Cambridge, MA 02138; arne@aavso.org

Received July 31, 2009; revised December 10, 2009; accepted May 10, 2010

Abstract We present an analysis of optical photometry of the transient optical and X-ray source CSS081007:030559+054715. Unfiltered CCD observations were made between 2008 December 17 and December 30 (JD 2454817.5 to 2454830.5), showing variability at the level of 0.5 magnitude. Time-series analyses of these data confirm the existence of the 1.77-day period detected in X-ray, UV, and optical wavelengths by the Swift satellite. The maxima of the optical and X-ray emission appear to be out of phase.

1. Introduction

The variability of CSS081007:030559+054715 (hereafter CSS081007) was discovered after its significant brightening was detected by the Catalina Real-time Transient Survey (CRTS; Drake *et al.* 2009a) on 2008 October 7. The object was observed spectroscopically by Pejcha *et al.* (2008), who found broad emission lines of H- α , HeII, and [OIII] with multiple, high-velocity components indicative of nova ejecta. Schwarz *et al.* (2008) observed this object with the Swift satellite in both X-rays and ultraviolet; the X-ray spectrum indicated this object is a supersoft source, which is a common feature of accreting white dwarfs undergoing current or recent thermonuclear burning. Further X-ray observations by Beardmore *et al.* (2008) and Osborne *et al.* (2009) indicated both a significant brightening of the source in X-rays, along with an apparent periodicity of about 1.77 days. Analysis of pre-outburst photometry from CRTS by Drake *et al.* (2009b) indicated that the progenitor was highly variable, but that there was no evidence for a period of 1.77 days in the optical data, and dedicated *BVRc* photometry by Goranskij and

Metlova (2009) obtained over thirteen sparsely-distributed nights between 2008 December 3 and 2009 February 19 indicated marginal evidence for periodicity at 1.694 and 0.6106 days.

2. Data

The AAVSO requested observations of this star on 2008 December 12 (Templeton 2008), and R. Koff commenced a two-week series of nightly time-series of CSS081007. Unfiltered observations were made using a 0.25-meter SCT with an Apogee AP-47 CCD camera; the telescope is located near Bennett, Colorado. Differential photometry was performed using GSC 00061-01278 as the comparison star and GSC 00061-01257 as the check star. The unfiltered magnitudes are relative to the V -band zero point of 14.862 for the comparison star, as obtained by calibration data by A. Henden. We note that a full $BVRcIc$ calibration of this field was obtained by Henden using the Sonoita Research Observatory, and is available from the AAVSO website.

Eleven nights of photometry were obtained between JD 2454817.55 (2008 December 17.05) and 2454830.66 (2008 December 30.16), yielding a total of 874 observations of the variable. Photometry of the comparison and check stars showed that both were constant with standard deviations of about 0.02 magnitude throughout the two-week run. The resulting light curve of CSS081007 is shown in Figure 1.

3. Analysis

The time-series data were analyzed using a deconvolving, cleaning Fourier transform (Roberts *et al.* 1987), and we found the strongest peak at $P = 1.767 \pm 0.001$ days. We found evidence for a weaker peak at 0.638 day. These two peaks are separated by one cycle per day in the frequency domain, and one is almost certainly an alias of the other. Based upon the phase diagrams of these data, and on the Swift results which do not have the same sampling issues, we believe the longer period of 1.767 days is the true period.

Figure 2 shows the data folded with four different periods using the X-ray zero phase point of HJD 2454807.1245 from Osborne *et al.* (2009). The plot at top left shows the optical data folded with the 1.767-day period, with the 0.638-day period at top right; the Goranskij and Metlova (2009) periods of 1.694 and 0.6106 days are shown at bottom left and right, respectively. The optical light curve phases most cleanly with the period of 1.767 days, which is a good indication that the periodicity exists and our calculated period is consistent with its real value. We note that the bright segment located at a phase of 0.95 to 1.0 was observed on 2454817, making it the earliest portion of the light curve. It is possible the object declined after this night; however, the remaining data appear to have a reasonably constant mean afterward. Our second period of 0.638 can

phase the data, but there is clearly more phase dispersion on the rising branch. Both of the Goranskij and Metlova periods are ruled out by both Fourier analysis and the phase diagrams.

The morphology of the light curve is difficult to characterize given the relatively small amount of data available, the (likely) aperiodic rapid variability, and the varying mean light level due to evolution of the nova outburst. The simplest interpretation is that the light curve consists of a single deep minimum lasting for nearly half a cycle, with little or no evidence of a secondary eclipse. There is a very weak dip at maximum, around phase 0.1, but it is well below the level of scatter in the data when binned. The main eclipse is not symmetrical; the decline to minimum is at least 30 percent of the orbit, while the rise to maximum is about 10 percent. Aside from the bright segment of data around phase 0.35–0.4, the light curve appears to be stable throughout the two-week span of observations; therefore the overall morphology of the system did not appear to change appreciably during the observing run. Osborne *et al.* (2009) noted that their ephemeris yields the time of *minimum* in the X-ray. Figure 2 shows that this corresponds to a *bright* phase of the optical light curve, which indicates that the optical and X-ray emission come from two different locations within the system that are eclipsed or obscured at different times.

4. Discussion

These optical data strongly support the presence of a 1.767-day period in CSS081007. We believe the weaker detection and slightly different period found by Goranskij and Metlova is a product of their sparser sampling covering a broader span of time. Given the underlying nova event, the longer span of data may be significantly affected by the evolution of the nova light, complicating the analysis of the time-series. The AAVSO data phase with essentially the same period as the Swift X-ray and UV periods, although there is a significant phase shift between the optical and X-ray. Further time-series observations of the system would provide additional useful constraints for light curve modeling in both the optical and X-ray. The slow optical evolution of this outburst suggests a peculiar nova, and stronger constraints on the geometry of the system and the nature of its components would greatly aid in our understanding of this system.

References

- Beardmore, A. P., Osborne, J. P., Page, K., Schwarz, G. J., Starrfield, S., and Ness, J. -U. 2008, *Astron. Telegram*, Nr. 1873.
- Drake, A. J., *et al.* 2009a, *Astrophys. J.*, **696**, 870.
- Drake, A. J., *et al.* 2009b, *Astron. Telegram*, Nr. 1940.
- Goranskij, V. P., and Metlova, N. P. 2009, *Astron. Telegram*, Nr. 1938.
- Osborne, J. P., Beardmore, A. P., Page, K. L., Ness, J. -U., Schwarz, G., Starrfield, S., Balman, S., and Wynn, G. 2009, *Astron. Telegram*, Nr. 1942.

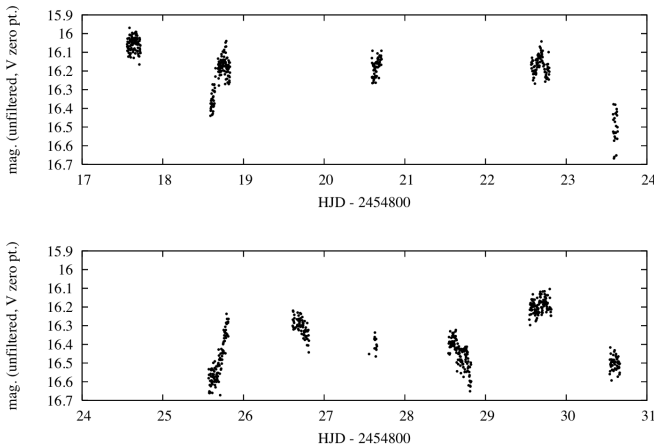


Figure 1. The unfiltered light curve of CSS081007 from 2008 December 12 to December 30 (JD 2454817.5 to 2454830.5). The average photometric error per point is about 0.025 magnitude.

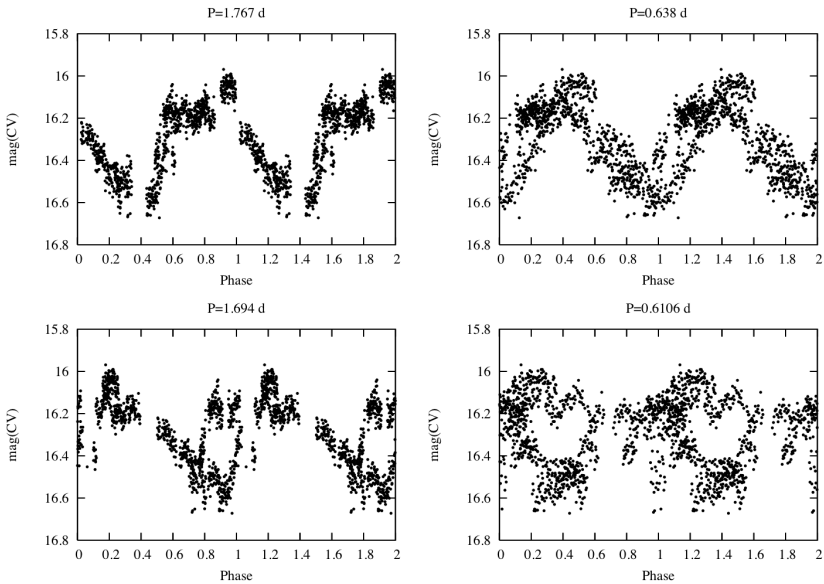


Figure 2. The light curve of CSS081007 folded with four different periods: (top left) 1.767 days; (top right) 0.638 day; (bottom left) 1.694 days; (bottom right) 0.6106 day. All four phase diagrams use the time of X-ray minimum (HJD = 2454807.1245) from Osborne *et al.* (2009) as the zero phase reference. The period of 1.767 phases much more cleanly than any of the other three. Comparison of the optical light in the 1.767-day period phase diagram shows that the optical light is near maximum during the X-ray minimum; phase=0.0 in the X-ray light is still optically bright.

Photometric Variability Properties of 21 T Tauri and Related Stars From AAVSO Visual Observations

John R. Percy

Samantha Esteves

Jou Glasheen

Alfred Lin

Junjiajia Long

Marina Mashintsova

Emil Terziev

Sophia Wu

Department of Astronomy and Astrophysics, University of Toronto, Toronto, ON M5S 3H4, Canada; john.percy@utoronto.ca

Presented at the 98th Annual Meeting of the AAVSO, November 7, 2009

Received February 19, 2010; revised April 9, 2010; accepted June 1, 2010

Abstract T Tauri variables are sun-like stars in various stages of their birth. We have analyzed long-term AAVSO visual observations of 21 T Tauri and related stars, using Fourier and self-correlation techniques. This follows our previous study of eleven such stars in *AAVSO* **35**, 290 (2006). Only a few of the variables showed periodic behavior, but self-correlation analysis makes it possible to construct a “variability profile”—amount of variability versus time scale—for *all* the stars, not just the periodic ones. For some of the periodic variables, we have studied the long-term behavior of the periods and amplitudes: T Cha and HT Lup appear to be rotating variables with stable periods less than 10 days; RU Lup, UX Ori, and TU Phe appear to show transient cycles of typically 50–500 days, probably arising in the accretion disc. R CrA has a stable 66-day period, which would be unusually long for a rotation period; its cause is not clear. We also discuss interesting but spurious low-amplitude one-year and one-month periodicities which occur in a few of the stars. Finally: we comment on the star AQ Dra, an RR Lyrae star, originally classified as a T Tauri star with a 5.5-day period.

1. Introduction

T Tauri stars are sun-like stars in various stages of birth, with or without an accretion disc still present. Although they are all photometrically variable, they are defined *spectroscopically*, on the basis of various emission lines and lithium lines being present in the spectrum. The types and causes of photometric variability include: (i) strict periodicity (periods 0.5 to several days) due to rotation of a spotted star; (ii) rapid flickering connected with accretion onto the star; (iii) slow variations due to variations in the rate of accretion; (iv) quasi-

periodic variations (periods 10s to 1000s of days), possibly due to effects of a companion, or inhomogeneities or other processes in the accretion disc. Herbst *et al.* (1994) have classified T Tauri stars into CTTS: classical T Tauri stars, with spectroscopically-visible accretion discs; WTTS: weak-lined T Tauri stars, without visible accretion discs; GTTS: G-type T Tauri stars; HAEBE: Herbig Ae/Be stars, more massive counterparts of T Tauri stars; and FUORs: FU Orionis stars, with long-lasting photometric outbursts.

There is an extensive literature on long-term CCD photometry of T Tauri stars, especially by Herbst (Wesleyan University) and his students and other collaborators (e.g. Herbst *et al.* (1994); Grankin *et al.* (2007); Grankin *et al.* (2008); Artemenko *et al.* (2010)). AAVSO visual observers have also measured T Tauri stars systematically for over three decades but, as explained by Percy and Palaniappan (2006), the data were only recently validated. Percy and Palaniappan (2006) analyzed the first few stars that were validated, as a pilot project, and showed that the visual data have definite scientific value. In the present paper, we report on the analysis of twenty-two more stars. We have also made a study of the long-term behavior of the period and amplitude of some of the periodic variables, especially those with unusually long periods.

2. Data and analysis

Visual measurements of the stars listed in Table 1 were made by AAVSO observers, validated by AAVSO staff, and made available in the AAVSO International Database. The stars in our sample are those which AAVSO staff considered to be promising. A preliminary pilot project analyzed a few stars which were classified as T Tauri in the AAVSO Validation File, and for which there were data available on the AAVSO website. Following Percy and Palaniappan (2006), the stars were analyzed by two time-series techniques: self-correlation analysis (Percy and Mohammed 2004, and references therein) and Fourier analysis as implemented in PERIOD04 (Lenz and Breger 2005). The Fourier analysis function in PERIOD04 is based on a discrete Fourier transform algorithm. It can plot the Fourier spectrum as power or amplitude; we chose to use the latter. There are many other useful functions built into this package.

The datasets were typically three decades long, and contained several hundred or more observations. Light curves of the stars in Table 1 can be inspected by using the light curve generator function on the AAVSO website: <http://www.aavso.org/lcg>

Self-correlation analysis was originally developed to analyze variable stars which were somewhat irregular and/or which had seasonal gaps which were of the same order of length as the period. Even if the variability is not periodic, the method can still provide a “profile” of the variability—the average variability as a function of time scale.

3. Results

The results are summarized in Table 1, which lists the star, the Herbst type (if known), the average observational error as determined from the intercept on the vertical axis of the self-correlation diagram, the half-range of variability as determined from the value of Δmag at large Δt in the self-correlation diagram, the period if any, the dominant time scales of variability (the time scales at which Δmag is increasing in the self-correlation diagram), and whether or not there is any evidence for periodicity on a time scale of one year (Y) or one month (M). Note that the Δmag , at any Δt , is approximately equal to half the peak-to-peak range; the exact relationship will depend on the exact form of the variation.

4. Spurious periods of one year and one month

In a recent analysis of visual observations of irregular pulsating red giants (Percy *et al.* 2009), we had noticed the presence of low-amplitude variability, with a period of one year, in some stars. This period is spurious, and is due to a physiological process—the Ceraski effect—which is due to the changing orientation of the star field, relative to the observer’s eyes, at different times of year. In the present study, we have noticed several stars which have low-amplitude periods close to *one sidereal month*, a frequency of 0.0366 cycle/day. These are noted in Table 1. Figure 1 shows one example. Since observers do not usually observe a variable star when the moon is nearby in the sky, we hypothesize that the monthly periods are also spurious, and due to the changing orientation of the star field, observed at different times of the night at different times of the month.

5. True periods and profiles

For a few stars in Table 1, periods are given. Some are less than 10 days, and some are considerably more. See Paper I for examples of self-correlation diagrams and Fourier spectra of periodic variables. For the stars which do not have periods, and they are the majority, it is still possible to use the self-correlation diagram to show the “profile” of the variability—the amount of variability as a function of time. Figure 2 shows an example, T Cha. The diagram rises smoothly from the intercept, which is a measure of the average observational error plus any very rapid variability. It then reaches a plateau at Δt about 30 days, indicating that most of the variability takes place on time scales of 0 to 30 days.

6. Amplitude variations in periodic stars

Most periodic T Tauri stars have periods of 0.5 to 5 days. These are the stars’ rotation periods, and the stars vary in brightness because they have cool starspots. The amplitude of variability depends on the size, contrast, and distribution of

the starspots. Stelzer *et al.* (2003) carried out an intensive photometric study of V410 Tau (period 1.87 days), and showed that the amplitude rose and fell on a time scale of 3,000 days. Percy *et al.* (2010) analyzed CCD observations of several other short-period T Tauri stars, and found that the amplitudes also varied on time scales of 1,500 to 3,500 days.

In the course of our analysis of long-term visual and CCD observations of T Tauri stars, we have encountered several stars with periods *greater* than 10 days, or even greater than 100 days. While these could be unusually-slow rotators, it is possible that the periodic variability has some other cause. We were therefore curious to know whether and how the amplitudes of these stars varied with time.

6.1. R CrA

R CrA has a period of 66 days (Percy and Palaniappan 2006), which is significantly longer than for T Tauri stars that are rotational variables. We grouped the observations into sets of about a thousand days, because the lengths of individual seasons were not much longer than the period. We used Fourier and self-correlation techniques to determine the period and amplitude. The amplitude results are shown in Figure 3. The period was constant from season to season, within its error. The result was confirmed through wavelet analysis, using the *wwz* package on the AAVSO website. Detailed information about *wwz* can be found there. The amplitude behavior, in both Figure 3 and the wavelet analysis, was less clear, mostly because of the effect of the seasonal gaps. There are variations in amplitude which are marginally convincing, including a larger amplitude around JD 2450000–2455000. The change in amplitude appears significant in all three forms of analysis.

6.2. RU Lup

RU Lup has an average period of 230 days but, when we analyzed the data on a season-to-season basis, we found that its behavior was much more complicated. Because of the length of the period, we divided the data into bins of approximately a thousand days, and used Fourier and self-correlation analysis to determine the period and amplitude. We found that, in some intervals, there was no significant period but, in others, there was a significant period ranging from 90 to 350 days, with an amplitude of up to 0.5 magnitude! Self-correlation diagrams for four intervals are shown in Figure 4. This result was confirmed through wavelet analysis; there was no frequency at which there was a *sustained* signal.

The AAVSO visual light curve of RU Lup shows a discontinuity of about 0.5 magnitude at JD 2444200. AAVSO Headquarters staff are not aware of any possible spurious reason for this discontinuity, such as changes to the charts or comparison stars, so we must assume that the discontinuity is real (Templeton 2010).

6.3. TU Phe

The best period for this star, based on the entire dataset, was about 200 days, but it appears that the analysis was dominated by an interval—JD 2451000–

2452000—when there was a large-amplitude signal of about this length. From JD 2450000 to 2451000, there was a weak signal at about 100 days, and from JD 2452000 to 2454000 there was a weak signal at about 500 days. Wavelet analysis confirmed the presence of random transient signals at periods between 60 and 500 days.

6.4. UX Ori

The situation was very similar to that with TU Phe: the 200-day period in the entire dataset was dominated by the interval JD 2452000–2453000, when there was a very strong (amplitude 0.5 magnitude) signal with a period of 210 days. In the intervals before and after this, there was no strong signal at this or any other period. These results are confirmed by the wavelet analysis.

7. Discussion and conclusions

7.1. Periods and variability profiles

Three stars in Table 1 have periods of less than 10 days, and are almost certainly rotational variables; the period is the rotation period.

Three stars in Table 1 have periods of about 200 days, as derived from the whole dataset. When the datasets are subdivided into different intervals, however, it turns out that the periods are unstable and transient. They may arise from some transient phenomenon in the accretion disc, at a place where the orbital period takes these period values.

R CrA (Percy and Palaniappan 2006) is an interesting case. When the data are analyzed on a season-to-season basis, the 66-day period is stable. Perhaps the star is a rotational variable with an unusually long rotation period and starspots that do not change significantly over many years. Or perhaps the 66-day period is caused by some dynamical effect such as the presence of a companion star or planet. In fact, Kraus *et al.* (2009) present evidence for a puffed-up inner rim of the accretion disc, at about 0.4 AU from the star, where the orbital period would be close to 66 days.

For all of the stars, the self-correlation diagram provides a “profile” of the variability, including the range of time scales over which variability takes place. These are given in column 6 of Table 1. They are generally 0–100 days, although some stars vary on longer time scales also, and some only on shorter time scales.

7.2. Spurious periods

The spurious one-year period appears to be due to a known effect—the Ceraski effect; see Percy *et al.* 2009 for a discussion. The spurious one-month period may arise from the same effect if the stars are observed systematically at different times of night at different times of the sidereal month.

7.3. Amplitude variations

The long period stars UX Ori, TU Phe, and especially RU Lup seem to be dominated by the effect of intervals when there is a large-amplitude cyclic variation. In other intervals, there are either other cycle lengths present, or no obvious cyclic variability at all. This suggests that the variability arises from transient phenomena in the disc, with a time scale determined by the orbital period at a specific place in the disc.

RU Lup is a particularly interesting star. Herczeg *et al.* (2005) have reviewed its properties. Much of its light comes from accretion energy, so some photometric variability may be due to variability in the accretion rate. The underlying star is slightly cooler, less massive, and less luminous than the sun, but is slightly larger; it is still contracting to the main sequence. The distance is about 140 pc, and the age is 2–3 Myr. Claims of a 3.7- (or 5.6-) day photometric period have not been confirmed. The accretion disc is probably seen nearly (but not exactly) edge-on. Takami *et al.* (2001) have used spectro-astrometric observations to study gas motions near the star. They see evidence of a bipolar outflow, magnetically driven, and also a wind emanating from the disc. The infrared spectral energy distribution is consistent with the presence of a gap in the disc, with an outer radius of 3–4 AU. This gap could be induced by an unseen companion such as a young planet.

7.4. The interesting case of AQ Dra

AQ Dra, an apparent T Tauri star, showed a stable 5.5-day period, and amplitude variations that were typical of those of other short-period T Tauri stars, for which the periodic variability is assumed to be due to rotation of a spotted star. The amplitude varied on a time scale of thousands of days, indicating that the inhomogeneities (spots) on the star varied on that time scale.

The referee, however, pointed out an interesting problem with this star. In the AAVSO Validation File, this star was listed as a type IS variable (rapid irregular variable) with a period of 5.5 days and an F2 spectral type. In the *General Catalogue of Variable Stars* (via SIMBAD), it is listed as ISB (rapid irregular variable of mid to late type), but claimed to be an RR Lyrae star! RR Lyrae stars have periods less than a day. Both Fourier and self-correlation analysis *seemed* to show that the period of AQ Dra is was 5.474 days, with variable amplitude. George Herbig (1960), a pioneering expert on T Tauri and related stars, had assigned this star to the RW Aur type, which is another name for IS type variables. In classifying its spectrum as F2, he notes that “absorption H β is absent, as if filled in by emission.” This would also be evidence for its IS or T Tauri nature.

AAVSO Science Director Dr. Matthew Templeton, however, pointed out to us that this star was *definitely* an RR Lyrae star! NSVS (Northern Sky Variability Survey) data clearly showed this to be the case, and the star is listed as such in the most recent catalogues of RR Lyrae stars, having a period of 0.55025 day. It is instructive, therefore, to see how we mis-analyzed the AAVSO data.

T Tauri stars may have periods as short as a few hours but, since the AAVSO visual observations were mostly made once a night, we did not look for periods shorter than about 2 days, since it would be inappropriate to do so. However, if a star with a period of 0.55025 day is sampled once a night, at approximately the same time, it will *appear* to have a period of about 5.5 days. This is a classic example of an “alias period” (e.g. Fullerton 1986, Figure 2). When we re-examined the AAVSO data with both Fourier and self-correlation analysis, looking for periods less than a day, we indeed found the 0.55025-day period, though the data were not well-suited to this purpose. In future, we will analyze the AAVSO visual data on AQ Dra in a way that is appropriate for an RR Lyrae star. The variable amplitude may be due to a Blazhko effect.

7.5. The value of visual observations of T Tauri stars

Visual observations are capable of revealing periodic variability, both real and spurious, even though the precision of individual observations is low; that is the power of time-series analysis, especially when applied to datasets that are large and long. Even for the stars that are not periodic, the observations provide a “profile” of the variability which may, with sufficient analysis and interpretation, provide further information about the stars. The long datasets provide information on the *long-term* changes in period and amplitude which could not be determined from shorter datasets. AAVSO visual data *definitely* have value!

8. Acknowledgements

We thank the Natural Sciences and Engineering Research Council of Canada and the Ontario Work-Study Program for research support. This project would not have been possible without the sustained efforts of dozens of AAVSO observers, and the help of AAVSO staff. We especially thank Dr. Matthew Templeton for clarifying the nature of AQ Dra, and the referee for first pointing out the discordant classifications. This research has made use of the AAVSO wwz wavelet analysis package, and the SIMBAD database, operated at CDS, Strasbourg, France.

References

- Artemenko, S. A., Grankin, K. N., and Petrov, P. P. 2010, *Astron. Reports*, **54**, 163.
Fullerton, A. W. 1986, in *The Study of Variable Stars using Small Telescopes*, ed. J. R. Percy, Cambridge University Press, Cambridge, U.K., 201.
Grankin, K. N., Bouvier, J., Herbst, W., and Melnikov, S. Yu. 2008, *Astron. Astrophys.*, **479**, 827.
Grankin, K. N., Melnikov, S. Yu., Bouvier, J., Herbst, W., and Shevchenko, V. S. 2007, *Astron. Astrophys.*, **461**, 183.
Herbig, G. H. 1960, *Astrophys. J.*, **131**, 632.
Herbst, W., Herbst, D. K., Grossman, E. J., and Weinstein, D. 1994, *Astron. J.*, **108**, 1906.
Herczeg, G. J., et al. 2005, *Astron. J.*, **129**, 2777.

- Kraus, S., Hofmann, K. -H., Malbet, F., Meilland, A., Natta, A., Schertl, D., Stee, P., and Weigelt, G. 2009, *Astron. Astrophys.*, **508**, 787.
- Lenz P., and Breger, M. 2005, *Comm. Asteroseismology*, **146**, 53
- Percy, J. R., Esteves, S., Lin, A., Menezes, C., and Wu, S. 2009, *J. Amer. Assoc. Var. Star Obs.*, **37**, 71.
- Percy, J. R., and Mohammed, F. 2004, *J. Amer. Assoc. Var. Star Obs.*, **32**, 9.
- Percy, J. R., and Palaniappan, R. 2006, *J. Amer. Assoc. Var. Star Obs.*, **35**, 290.
- Percy, J. R., et al. 2010, *Publ. Astron. Soc. Pacific*, in press.
- Stelzer, B., et al. 2003, *Astron. Astrophys.*, **411**, 517.
- Takami, M., Bailey, J., Gledhill, T. M., Chrysostomou, A., and Hough, J. H. 2001, *Mon. Not. Roy. Astron. Soc.*, **323**, 177.
- Templeton, M. 2010, private communication.

Table 1. Time-Series analysis of T Tauri stars and related objects.

<i>Star</i>	<i>Type</i>	<i>Error</i>	<i>Half-Range</i>	<i>P (d)</i>	<i>Timescales (d)</i>	<i>Comments</i>
SU Aur	GTTS	0.16	0.25	—	1–800	—
YZ Cep	—	0.23	0.26	—	1–100	Y
DI Cep	GTTS	0.21	0.28	—	1–50	—
T Cha	HAEBE	0.25	1.5!	3.3	1–20	M, no Y
T CrA	HAEBE	0.22	0.5:	—	1–1000	M?, Y?
AQ Dra	see text	0.2:	0.5	0.55	—	no M or Y
RU Lup	CTTS	0.24	0.4	230	1–100	Y, M
GQ Lup	—	0.33	0.55	—	1–100	Y
HT Lup	WTTS	0.08	0.23	6.25	1–100	Y
T Ori	HAEBE	0.34	0.6	—	1–40	—
RY Ori	—	0.35	0.7	—	1–1000	—
UX Ori	HAEBE	0.30	0.0	200	1–100	no M or Y
BF Ori	HAEBE	0.28	0.7	6:	1–30	Y
BN Ori	HAEBE	0.18	0.30	—	1–150	—
V350 Ori	—	0.21	0.5	—	1–10, 10–100	Y, no M
TU Phe	—	0.10:	0.25	200	—	—
RZ Psc	—	0.15	0.20	—	1–2000	no M
NX Pup	—	0.15	0.38:	—	1–70	Y?
AK Sco	HAEBE	0.16	0.24	—	1–100	Y
V856 Sco	—	0.15:	0.5	—	1–100	no M or Y
RR Tau	HAEBE	0.27	0.7	—	1–20	Y, no M
RY Tau	GTTS	0.22	0.5:	—	1–150	Y

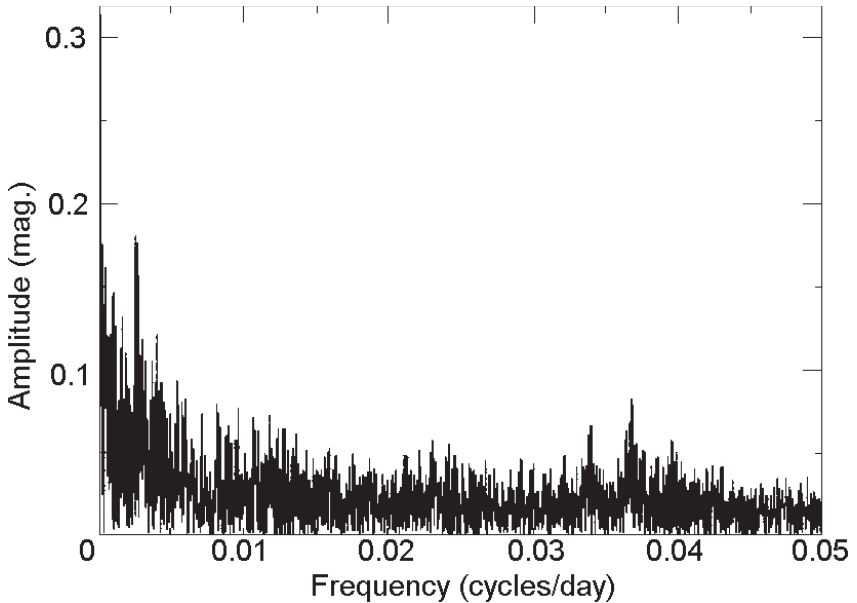


Figure 1. Fourier spectrum (PERIOD04) for RY Tau, showing spurious peaks at frequencies of 0.036 (one month) and 0.00274 (one year) cycle per day. See text for a discussion of possible origins of these features.

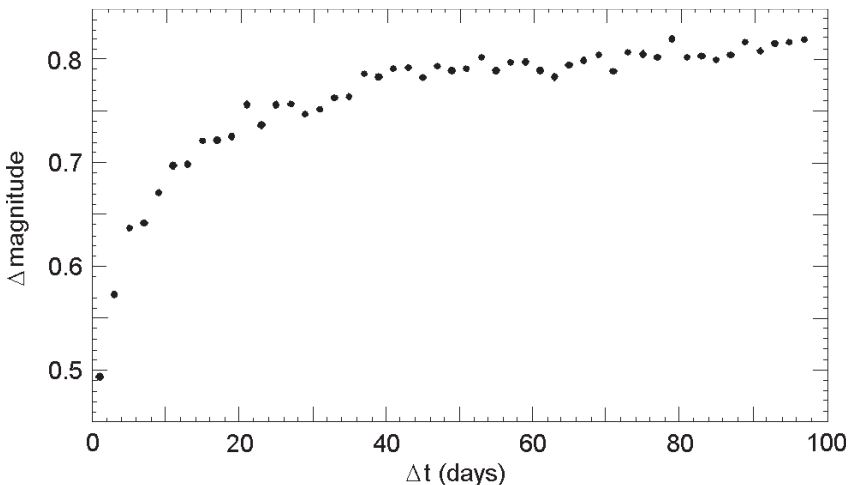


Figure 2. Self-correlation diagram for T Cha. The diagram rises smoothly from the intercept on the vertical axis to a plateau. There are no repeating minima which would indicate that a period was present, though a low-amplitude 3.3-day period is clearly visible in the Fourier spectrum. However, the diagram does provide a “profile” of the variability, indicating that most of the variability occurs on time scales of 0 to 30 days.

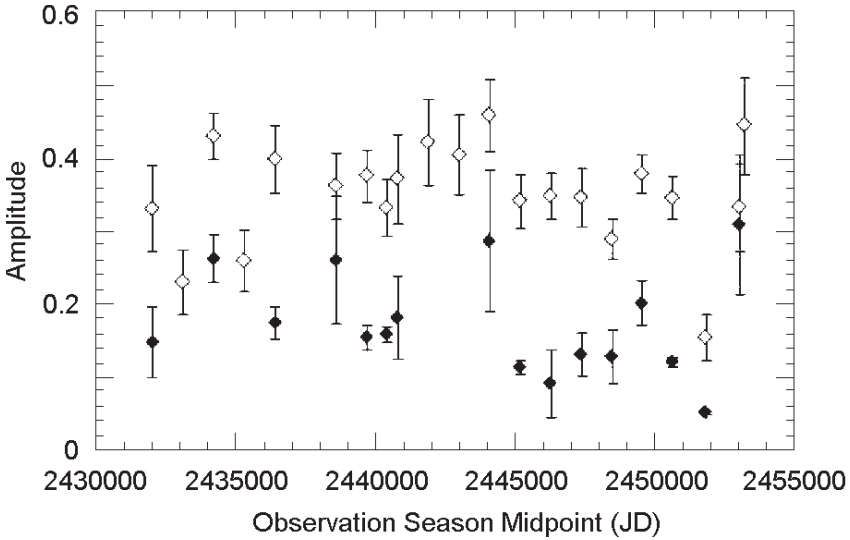


Figure 3. The amplitude variation of R CrA over several seasons; open diamonds are from PERIOD04, filled diamonds are from self-correlation. The former are higher than the latter because they include a contribution from noise. See section 6.1.

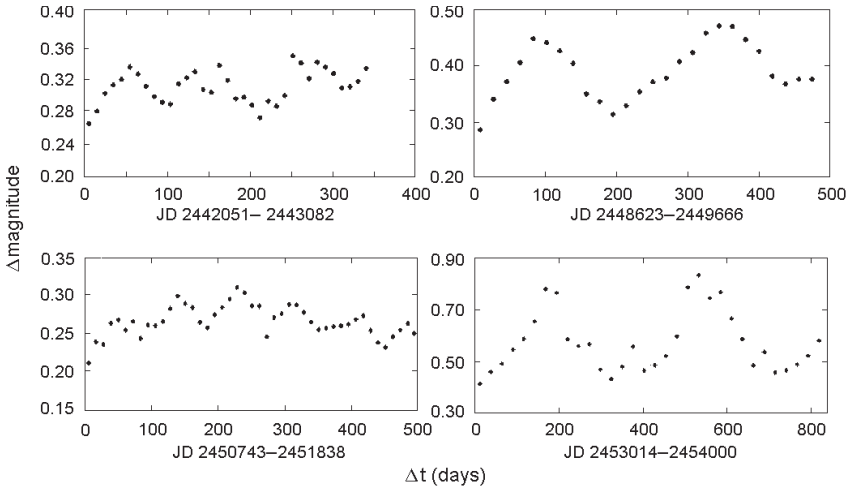


Figure 4. The self-correlation diagrams for RU Lupi over several intervals of time. The period is variable: about 105 days (upper left), 225 days (upper right), 90 days (lower left), and 360 days (lower right).

Further Studies of “Irregularity” in Pulsating Red Giants

John R. Percy

Junjiajia Long

Department of Astronomy and Astrophysics, University of Toronto, Toronto, ON M5S 3H4, Canada; john.percy@utoronto.ca

Received March 5, 2010; accepted March 16, 2010

Abstract In a previous paper (*JAAVSO* 37, 2009, p. 71) we used self-correlation to analyze AAVSO visual observations of twenty-three L-type (irregular) pulsating red giants, and found that they exhibited a continuous spectrum of behavior, from truly irregular to semiregular. In this paper, we carry out Fourier analysis of the same stars, partly to investigate whether some of their irregularity might be due to multiperiodicity, and partly to look for evidence of possible spurious periods of one year and one month, due to the methodology of visual observing. We find evidence of such spurious periods in many stars. We have also analyzed an additional seventeen L-type pulsating red giants, using both self-correlation and Fourier techniques. Several show evidence of spurious one-month or one-year periods. Only XY Lyr, VY UMa, and possibly DY Vul and BU Gem show evidence of intrinsic periodicity. Several show little or no variability. The rest vary irregularly on time scales of a few hundred days. We find no evidence that irregularity in L-type variables is due to multiperiodicity.

1. Introduction

Cool red giants are all variable in brightness. They are classified in the *General Catalogue of Variable Stars* (GCVS; Kholopov *et al.* 1985) as Mira (M), semiregular (SR), or irregular (L). In a previous paper (Percy *et al.* 2009, hereinafter Paper 1), we showed, through self-correlation analysis of AAVSO visual observations, that the L-type variables show a spectrum of behavior, from truly irregular to semiperiodic. We also found evidence of a spurious one-year period in some of the stars, presumably due to a physiological phenomenon called the Ceraski effect. In a similar analysis of AAVSO visual observations of T Tauri stars (Percy *et al.* 2010), we found evidence of a spurious one-month period in some of the stars, presumably due to the same effect. The purposes of the present paper are several-fold: (i) to use Fourier analysis to confirm the results of Paper 1; (ii) to investigate whether the irregularity of some of the stars in Paper 1 is due to multiperiodicity, since self-correlation is not well suited for this purpose; (iii) to look for further evidence of spurious one-year and one-month periods in these stars; and (iv) to analyze some additional L-type variables which have sufficient visual observations in the AAVSO International Database. Please see Paper 1 for a more complete introduction to L-type variables.

2. Sources of data

Visual measurements of the twenty-three L-type stars, listed in Table 1 and taken from Paper 1, and of the seventeen L-type stars, listed in Table 2, came from the AAVSO International Database, spanning up to several decades. There are dozens of L-type red giant variables in the database but, for most of them, the data are sparse. Richard Kinne, AAVSO Headquarters, kindly provided us with a list of L-type stars in the database, listed in order of decreasing number of observations. The numbers of observations of the stars in Table 2 range from 19,863 (VY UMa) down to 3,642 (CT Del). The lengths of the datasets are typically 20,000 days.

The precision of visual measurements is known to be about 0.2 to 0.3 magnitude. The intercept on the vertical axis of the self-correlation diagram (e.g. Figure 1, top) is a measure of the average precision of the measurements and, for the stars in our samples, is consistent with the estimate above.

3. Analysis

Self-correlation is a simple method of time-series analysis that determines the characteristic time scale and amplitude of the variability, averaged over the dataset. For a discussion of its nature, strengths, and weaknesses, see Percy and Mohammed (2004) and references therein, and for its application to the present project, see Paper 1. Self-correlation analysis also provides a “profile” of the variability—the amount of variability as a function of time scale. As indicated in Paper 1, our self-correlation software and manual are publicly available. Fourier analysis was carried out using PERIOD04 (Lenz and Breger 2005).

4. Results

Figure 1 shows a sample self-correlation diagram and PERIOD04 Fourier spectrum. See Paper 1 for other examples of self-correlation diagrams of L-type variables. The results of the present paper are summarized in Tables 1 and 2. The columns in Table 1 give: the star name, the spectral type (generally from SIMBAD), the period(s) determined in Paper 1, and comments about the occurrence of spurious periods. Please see Paper 1 for more information about these stars.

There are no stars in Table 1 for which the Fourier spectrum contains two or more significant periods which might indicate multiperiodicity. By “significant,” we mean having a signal-to-noise ratio greater than 3.

In Table 2, the columns give: the star name, the spectral type, the self-correlation Δ mags at 0 and 1,000 days, and comments. The value of Δ mag. at 0 days is a measure of the average observational error; it ranges from 0.21 to 0.38. The difference between the Δ mags at 0 and 1,000 days is a measure of the amount of true variability on time scales less than 1,000 days.

In the “comments” column: Y and M indicate the presence or possible presence of a spurious period of one year or one month. Over half of the stars show a possible one-month signal, and over half show a possible one-year signal. Specifically: the following stars show a signal or suspected signal at a period of one year: SV Aur, RT Car, IZ Cas, AD Cen, DM Cep, XY Lyr, T Cyg, SV Cyg, V449 Cyg, CT Del, and WY Gem. The following stars show a signal or suspected signal at a period of one sidereal month: RT Car, AD Cen, DM Cep, W CMA, T Cyg, SV Cyg, CT Del, and BU Gem.

Four stars show a phenomenon that we have occasionally seen in the self-correlation diagrams of other stars: very weak minima at Δt of 200, 550, and 900 days: W CMA, WY Gem, TX Psc, and DY Vul. The amplitudes, however, are less than 0.02 magnitude. We suspect that this is a spurious effect—the Ceraski effect or something similar—somehow related to the lengths of the seasons, and of the seasonal gaps.

The following stars show less than 0.03-magnitude variability on time scales of up to 1,000 days, according to the self-correlation diagrams: SV Aur, IZ Cas, AD Cen, DM Cep, V449 Cyg, WY Gem, and TX Psc.

The only stars that appear to have a genuine period are: XY Lyr (121.6 days), VY UMa (121.8 days), and possibly DY Vul (95 days), and BU Gem (2,000 days). The amplitudes, in each case, are only 0.02 to 0.03 magnitude. The self-correlation diagram of SV Cyg shows some evidence for a low-amplitude period of 230 days, but it is not present in the Fourier spectrum.

The other stars show no repeating minima in the self-correlation diagram, only a profile that rises smoothly from $\Delta t = 0$ to $\Delta t =$ a few hundred days or beyond. These stars are variable but truly irregular. As with the stars in Table 1, there are no stars which have two or more significant periods in the Fourier spectrum, which might be indicative of multiperiodicity.

None of the stars in Table 2 show evidence of long secondary periods, which are an order of magnitude longer than the pulsation periods (Nicholls *et al.* 2009), though most of the stars show some low-frequency (long period) noise.

5. Discussion and conclusions

Many stars in Tables 1 and 2 show signals at periods of one year and one sidereal month. As discussed by Percy *et al.* (2009, 2010), these are spurious, and due to the Ceraski effect, a physiological effect which results from the technique of visual observing. The stars are observed at different times of night during the year and month, and therefore in different orientations relative to the horizon. When the stars with and without this effect are plotted on the sky, there is no apparent pattern.

Several stars in Table 2 show only marginal variability, on time scales of 0 to 1,000 days, and are candidates for removal from the AAVSO visual observing program. Many of the stars in both Tables are “orphans,” in that they have not

been studied or classified in detail, and have been observed relatively sparsely. There are dozens of other L-type stars in the AAVSO International Database which have been observed even less frequently. Analysis of these stars may not produce meaningful results, but it would be worth doing in any case. It might reveal a few stars of special interest. For the rest, it would confirm that there is no particular need to continue observing them.

There are no irregular variables in Table 1 or 2 which show two or more significant peaks in their Fourier spectrum, which would be an indication of multiperiodicity. Thus there is no evidence that multiperiodicity causes some or all of the irregularity in these stars. For most of these stars, the amplitudes are small, and the irregular variability may be due to the effects of random convection cells and/or a complex mixture of low-level radial and non-radial pulsation modes.

Even for stars which show no minima, it is possible to define a characteristic time scale on the basis of how fast the self-correlation diagram rises to its plateau, i.e., by comparing the rise to plateau with the rise to first maximum in a star that is periodic. To a first approximation, the time scale would be of the order of the value of Δt at which the diagram reached the plateau. The characteristic time scales, for the stars in Tables 1 and 2, are several hundred days.

The analysis of the stars in Tables 1 and 2 supports the main conclusion of Paper 1: L-type variable red giants show a continuous spectrum of behavior, from irregular, to marginally periodic, to semi-periodic. The analysis also shows the value of systematic, long term visual observations of variable stars, especially those which are not periodic, or which may have long term variability.

6. Acknowledgements

We thank the Natural Sciences and Engineering Research Council of Canada for research support, and the AAVSO observers and headquarters staff, without whose efforts this project would not have been possible. This research has made use of the SIMBAD database, operated at CDS, Strasbourg, France.

References

- Kholopov, P. N. *et al.* 1985, *General Catalogue of Variable Stars*, 4th ed., Moscow.
- Lenz, P., and Breger, M. 2005, *Commun. Asteroseismology*, **146**, 53.
- Nicholls, C. P., Wood, P. R., Cioni, M. -R. L., and Soszynski, I. 2009, *Mon. Not. Roy. Astron. Soc.*, **399**, 2063.
- Percy, J. R., and Mohammed, F. 2004, *J. Amer. Assoc. Var. Star Obs.*, **32**, 9.
- Percy, J. R., Esteves, S., Lin, A., Menezes, C., and Wu, S. 2009, *J. Amer. Assoc. Var. Star Obs.*, **37**, 71.
- Percy, J. R., *et al.* 2010, *J. Amer. Assoc. Var. Star Obs.*, submitted.

Table 1. Self-correlation analysis of L-type variables.

<i>Star</i>	<i>Spectrum</i>	<i>Period</i>	<i>Comments</i>
U Ant	C5,3(NB)	350, 2000	—
V Aps	MB	irr.	—
VW Aql	M5III:D	800	M
UX Cam	M6	1000	—
AA Cas	M6III: D	75	—
PY Cas	M5III: D	irr.	M:
WW Cas	C5,5(N1)	irr.	—
ST Cep	M3Iab:C	300-400	—
AT Dra	M4IIID	333, 4000	M:, Y:
UW Dra	K5pvC	360 (?)	Y
GN Her	M4IIID	irr.	—
OP Her	M5II-III C	75, 650	—
TT Leo	M7D	irr.	Y:
HK Lyr	C6,4(N4)	250	Y:, M
T Lyr	C6,5(R6)	400	Y:, M
TU Lyr	M6	150	Y:, M
X Lyr	M3.5III:D	200, 6500	M
TY Oph	C5,5(N)	irr.	—
EX Ori	M7III	100, 500	—
ST Psc	M5D	700	—
τ^4 Ser	M5II-III	100, 1200	M
CP Tau	C5,4(N)	1250	M
X Tra	C5,5(NB)	500	Y:

Note: In Comments field, Y or M indicates the presence or possible presence of a spurious period of one year (Y) or one month (M).

Table 2. Time-series analysis of 17 additional L-type variables.

<i>Star</i>	<i>Spectrum</i>	$\Delta m(0)$	$\Delta m(1000)$	<i>Comments</i>
SV Aur	M1	0.22	0.23	Y
RT Car	M2Iab:	0.30	0.39	Y, M
IZ Cas	K8	0.33	0.36	Y, no M
AD Cen	K3(II)-M3e	0.21	0.23	Y, M:
DM Cep	M3D	0.32	0.35	Y:, M:
W CMa	C6,3(N)	0.38	0.44	M
T Cyg	KIIIC	0.22	0.30	Y:, M:
SV Cyg	C5,5-C7,4(N3)	0.38	0.45	Y:, M:
V449 Cyg	M1-4	0.23	0.26	Y
CT Del	M7	0.31	0.36	Y:, M:
BU Gem	M1-2Ia-Iab	0.27	0.37	M
WY Gem	M2epIab + B	0.26	0.28	Y:, no M
XY Lyr	M4-5Ib-II	0.23	0.29	no M
BL Ori	C6,3(Nb,Tc)	0.28	0.36	
TX Psc	C7,2(N0,Tc)	0.26	0.28	M
VY UMa	C6,3(N0)	0.27	0.29	no Y, M
DY Vul	M3-6	0.24	0.28	no M

Note: In Comments field, Y or M indicates the presence or possible presence of a spurious period of one year (Y) or one month (M).

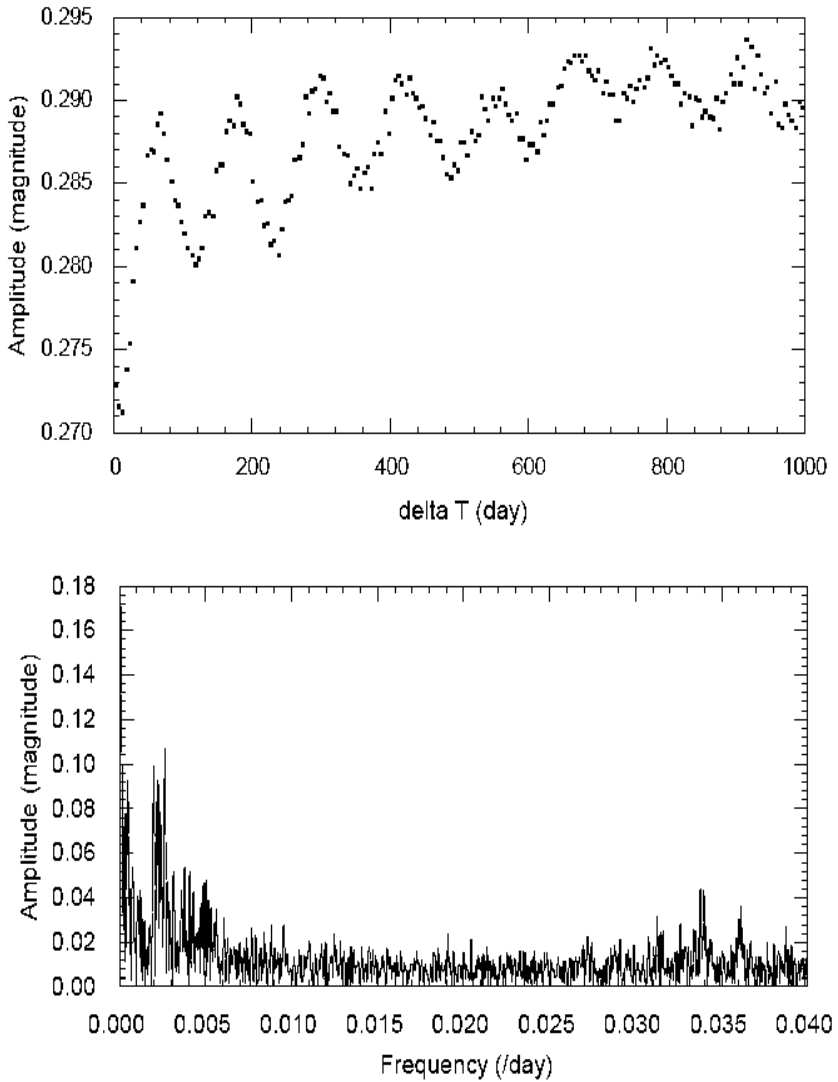


Figure 1. Top: self-correlation diagram for VY UMa, showing minima at multiples of 121.8 days, the period. Bottom: the `PERIOD04` Fourier spectrum for RT Car, showing spurious periods at one year ($f = 0.00274$) and one sidereal month ($f = 0.0366$), but no periods that are intrinsic to the star.

Two New Variable Stars in the Fields of Nova Cygni 2006 and Nova Cygni 2007

David Boyd

5 Silver Lane, West Challow, Wantage, OX12 9TX, UK; drsboyd@dsl.pipex.com

Received January 20, 2010; revised March 16, 2010; accepted March 25, 2010

Abstract Two new variable stars have been identified close to the recent novae V2362 Cygni (Nova Cyg 2006) and V2467 Cygni (Nova Cyg 2007). VSX J211145.0+444530 is likely to be a magnitude 11.6 γ Doradus variable with principal period 1.459(6) day and full amplitude 0.047 magnitude. VSX J202751.9+414727 is probably a magnitude 12.7 δ Scuti variable with period 0.05951(2) day and full amplitude 0.012 magnitude.

1. VSX J211145.0+444530

VSX J211145.0+444530 is not listed in SIMBAD but VIZIER reveals that it has already been catalogued under the names TYC 3181 1907, GSC 03181-01907, GSC 2.2 N0331312630, GSC 2.3 N31Y000630, USNO-A2.0 1275-14959662, USNO-B1.0 1347-0415391, 3UC 270-212234, and 2MASS J21114500+4445303. Its variability has not previously been recognized. Its position was measured as R.A. 21^h 11^m 45.00^s, Dec. +44° 45' 30.4" (J2000.0) using Astrometrica (Raab 2010) and UCAC3. It is 3.4 arcmin SE of the nova V2362 Cygni (= Nova Cygni 2006), see Figure 1.

11,997 *V*-filtered CCD observations were made of VSX J211145.0+444530 on eleven nights between 2006 June 5 and 2006 November 16 using a 0.35-m SCT operating at *f*/5.3 and an SXV-H9 CCD camera. Image scale was 1.4 arcsec/pixel with a typical FWHM of 2.5-3 pixels. Images were dark-subtracted and flat-fielded, and instrumental magnitudes were measured by aperture photometry using AIP4WIN (Berry and Burnell 2000). The magnitude of VSX J211145.0+444530 was measured relative to an ensemble of TYC 3181 1401 (C1, *V* = 11.24, (*V*-*I*) = 0.39) and GSC 03181-00369 (C2, *V* = 12.48, (*V*-*I*) = 0.68). Comparison star magnitudes were obtained from field photometry by Henden accessed through the AAVSO VSP service. The standard deviation of the zero points of these stars with respect to the mean ensemble zero point for each image averaged over all images was 0.007 magnitude. All times of observation were converted to HJD. Example light curves from two nights are shown in Figure 2.

Period analysis using the Lomb-Scargle (Lomb 1976; Scargle 1982) method in PERANSO (Vanmunster 2010) gives the power spectrum shown in Figure 3. The strongest signal is at frequency 0.685(3) c/d, period 1.459(6) days, with multiple-day aliases as expected from the spectral window. Removing the signal at 0.685 c/d leaves the power spectrum shown in Figure 4. The most prominent remaining

signals in order of decreasing strength are at 0.212 c/d, 0.789 c/d, 0.143 c/d, and 0.710 c/d plus aliases of these. Removing either of the signals at 0.212 c/d or 0.789 c/d also removes the other signals plus their aliases leaving only signals a factor of four lower in power. Figure 5 shows the phase diagram of the data for a period of 1.459 days. The full amplitude of variation is 0.047 magnitude.

This variable could potentially be interpreted either as an eclipsing binary system or a pulsating variable. If it is the former, we would expect a significant signal at twice the above period, namely 2.92(1) days, but the nearest prominent signal is at 3.10(2) days. Folding the light curve on the expected binary period gives the phase diagram in Figure 6. This has too many gaps to be able to discriminate between the two interpretations. On balance, the absence of a clear signal at the expected binary period and the presence of multiple periods in the spectrum favor interpreting it as a pulsating variable.

We measured the ($V-I$) color of the variable as 0.49 magnitude. Other published colors of the star are Henden ($B-V$) = 0.36, TYC2 ($B-V$) = 0.34, TASS ($V-I$) = 0.47, 2MASS ($J-H$) = 0.064, and ($H-K$) = 0.059. These suggest an early F spectral type assuming the star is unreddened. To give the observed apparent V -magnitude, a main sequence star with this spectral type would lie at a distance of ~ 600 parsecs. As the star is only 2.4° from the galactic plane, it will inevitably have suffered some degree of reddening. Galactic dust reddening and extinction data from Schlegel *et al.* (1998) give a cumulative reddening in this direction of ~ 0.7 magnitude. More helpful are measurements of the open cluster NGC 7039, which is less than a degree from the variable on the sky and has reddening of 0.13 magnitude and a distance of 951 parsecs (WEBDA 1). The relative distances of the cluster and variable suggest a reddening of ~ 0.08 magnitude for the variable, which makes its intrinsic color ($B-V$)_o ~ 0.28 . This places the star at the lower end of the instability strip in the region occupied by the γ Doradus stars and close to the red edge of the distribution of δ Scuti stars (Henry *et al.* 2007). The observed period of 1.459 days is too long for a δ Scuti star but is consistent with γ Doradus (Percy 2007) so, subject to spectroscopic confirmation, we consider it likely that VSX J211145.0+444530 is a new γ Doradus variable.

2. VSX J202751.9+414727

VSX J202751.9+414727 is also not listed in SIMBAD but has been catalogued as GSC03160-01853, GSC2.2N0331103671, GSC2.3N30Z000671, USNO-A2.0 1275-13940451, USNO-B1.0 1317- 0417130, UC3 264-197075, and 2MASS J20275193+4147278. It has not previously been recognized as variable. Its position was measured as R.A. $20^{\text{h}} 27^{\text{m}} 51.94^{\text{s}}$, Dec. $+41^\circ 47' 27.8''$ (J2000.0). It is 4.0 arcmin SW of the nova V2467 Cygni (= Nova Cygni 2007), see Figure 7.

3,185 V -filtered CCD observations of VSX J202751.9+414727 were made on ten nights between 2007 August 26 and 2007 November 12 using a 0.35-m SCT

operating at $f/5.3$ and an SXV-H9 CCD camera. Image scale was 1.4 arcsec/pixel with a typical FWHM of 2.5-3 pixels. Images were dark-subtracted and flat-fielded, and instrumental magnitudes were measured by aperture photometry using AIP4WIN (Berry and Burnell 2000). The magnitude of VSX J202751.9+414727 was measured relative to an ensemble of GSC 03160-01807 (C1, $V = 13.12$, $(V-I) = 0.60$), and GSC 03181-01708 (C2, $V = 13.64$, $(V-I) = 0.74$). Comparison star magnitudes were obtained from field photometry by Henden accessed through the AAVSO VSP service. The standard deviation of the zero points of these stars with respect to the mean ensemble zero point for each image averaged over all images was 0.005 magnitude. All times of observation were converted to HJD. Example light curves from two nights are shown in Figure 8.

Period analysis using the Lomb-Scargle method in PERANSO gives the power spectrum in Figure 9. There is a strong signal at frequency 16.803(4) c/d, period 0.05951(2) day, with the expected multiple-day alias signals. Removing the signal at 16.803 c/d leaves the signals shown in Figure 10. The remaining signals are all relatively weak with the strongest being at 6.556 c/d, 0.695 c/d, 24.42 c/d, and 20.47 c/d plus aliases of these. Removing each of these in turn does not diminish the others.

Figure 11 shows the phase diagram of the data for a period of 0.05951 day. The full amplitude of variation is 0.012 magnitude.

We measured the $(V-I)$ color of the variable as 0.43 magnitude. Other published colors of this star are Henden $(B-V) = 0.37$, TASS $(V-I) = 0.37$, 2MASS $(J-H) = 0.104$, and $(H-K) = 0.040$. These suggest an early F spectral type for this variable also, again assuming no reddening. To give the observed V -magnitude, a main sequence star with this spectral type would lie at a distance of ~ 1000 parsecs. Since the star is only 1.8° from the galactic plane, it will also have experienced reddening. Galactic dust reddening and extinction data from Schlegel *et al.* (1998) give a cumulative reddening in this direction of > 5 magnitudes. We get more useful information from the open cluster Collinder 421, which is less than a degree from the variable on the sky and coincidentally has very similar measured parameters to NGC 7039 with reddening of 0.10 and a distance of 950 parsecs (WEBDA 2). The relative distances of the cluster and variable suggest a reddening of ~ 0.11 magnitude for the variable, which makes its intrinsic color $(B-V)_0 \sim 0.26$. This places the star among the δ Scuti variables at the lower end of the instability strip (Breger and Montgomery 2000). The observed period of 0.06 day, its small amplitude, and the sinusoidal nature of the light curve are all consistent with the interpretation of VSX J202751.9+414727 as a new δ Scuti variable.

3. Acknowledgements

We acknowledge with thanks use of the SIMBAD and VIZIER services operated by CDS Strasbourg and the VSP service provided by the AAVSO. We also thank

the anonymous referee for helpful comments. This research has made use of NASA's Astrophysics Data System Service.

References

- Berry, R., and Burnell, J. 2000, *Handbook of Astronomical Image Processing*, Willmann-Bell, Richmond, VA.
- Breger, M., and Montgomery, M., eds. 2000, *Delta Scuti and Related Stars, Reference Handbook and Proceedings of the 6th Vienna Workshop in Astrophysics, held in Vienna, Austria, 4–7 August, 1999*. ASP Conf. Ser., **210**, Astron. Soc. Pacific, San Francisco.
- Henry, G. W., Fekel, F. C., and Henry, S. M. 2007, *Astron. J.*, **133**, 1421.
- Lomb, N. R. 1976, *Astrophys. Space Sci.*, **39**, 447.
- Percy, J. R. 2007, *Understanding Variable Stars*, Cambridge Univ. P., Cambridge.
- Raab, H. 2010, *Astrometrica*, <http://www.astrometrica.at>
- Scargle, J. D. 1982, *Astrophys. J.*, **263**, 835.
- Schlegel, D. J., Finkbeiner, D. P., and Davis, M. 1998, *Astrophys. J.*, **500**, 525, <http://irsa.ipac.caltech.edu/applications/DUST/>
- Vanmunster, T. 2010, PERANSO, period analysis software, <http://www.peranso.com>
- WEBDA 1, http://www.univie.ac.at/webda/cgi-bin/ocl_page.cgi?cluster=ngc+7039
- WEBDA 2, http://www.univie.ac.at/webda/cgi-bin/ocl_page.cgi?dirname=cr421

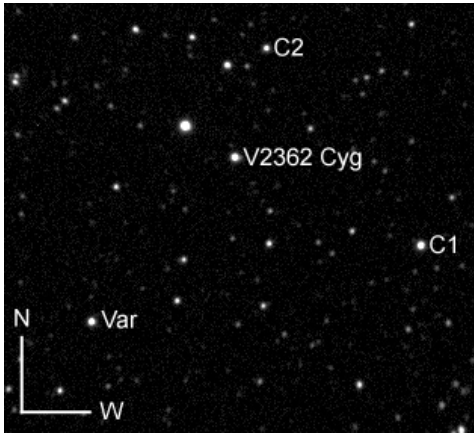


Figure 1. Location of the variable VSX J211145.0+444530 and comparison stars C1 and C2 ($6' \times 6'$).

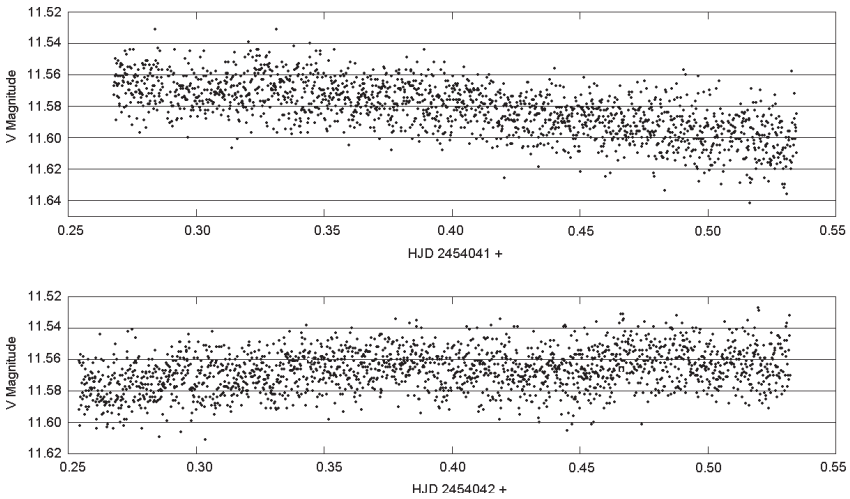


Figure 2. Example light curves of VSX J211145.0+444530 from 2006 November 1 and November 2.

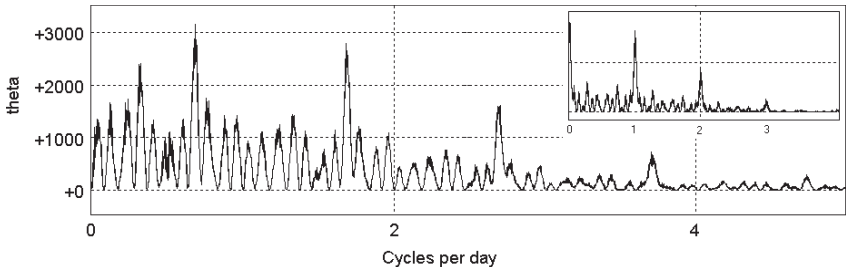


Figure 3. Power spectrum of VSX J211145.0+444530 also showing the spectral window.

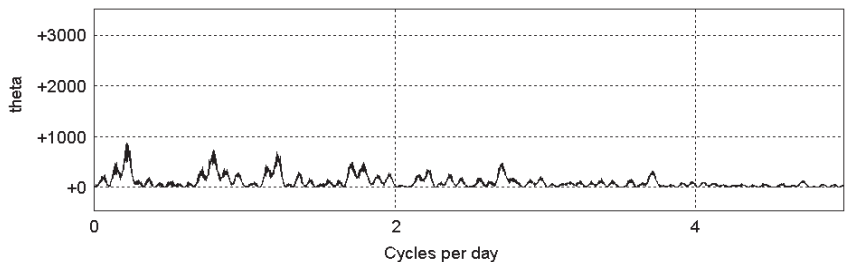


Figure 4. Power spectrum after removal of the signal at 0.685c/d.

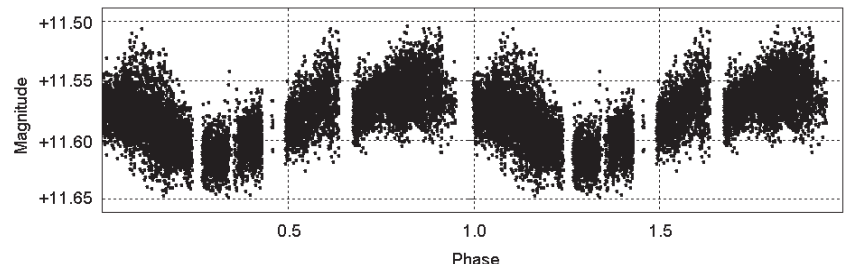


Figure 5. Phase diagram of VSX J211145.0+444530 for a period of 1.459 days.

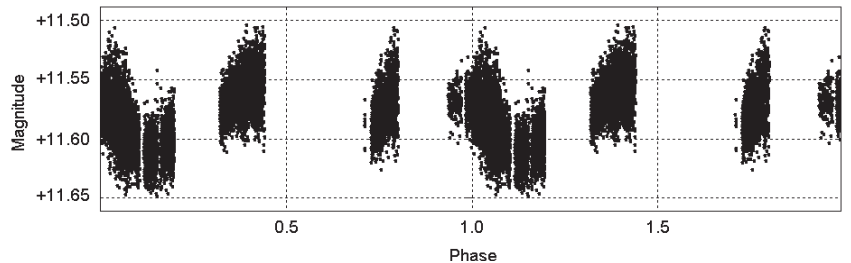


Figure 6. Phase diagram of VSX J211145.0+444530 for a period of 2.918 days.

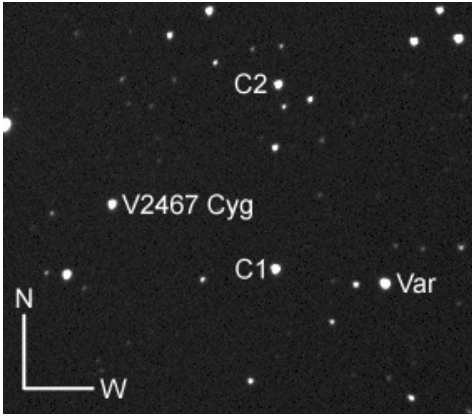


Figure 7. Location of the variable VSX J202751.9+414727 and comparisons stars C1 and C2 ($7' \times 6'$).

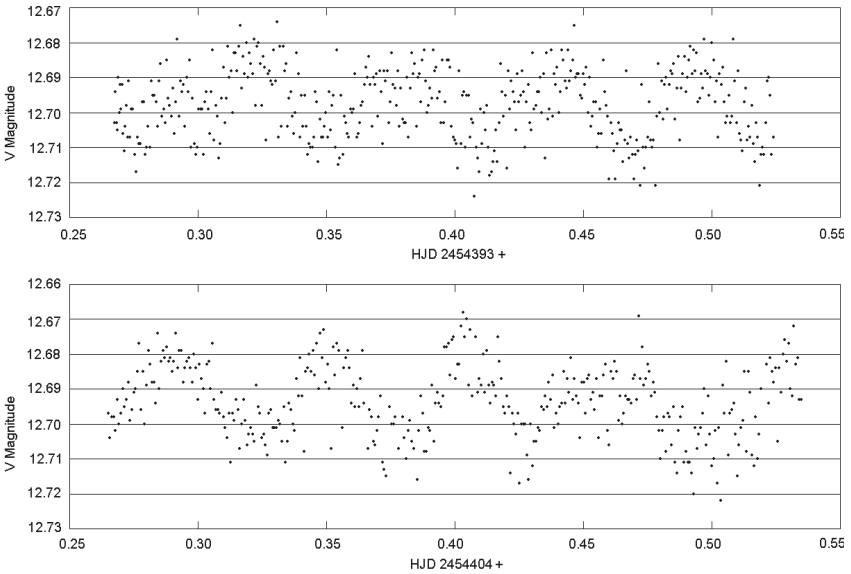


Figure 8. Example light curves of VSX J202751.9+414727 from 2007 October 19 and October 30.

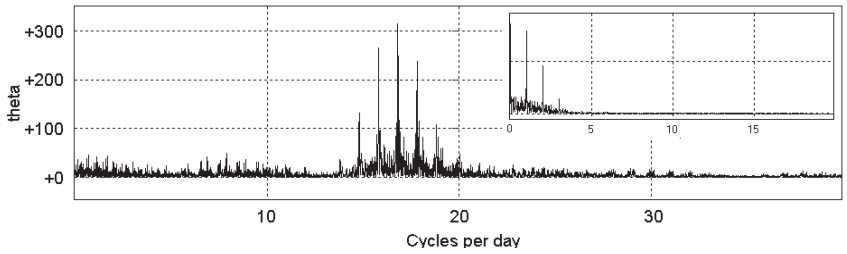


Figure 9. Power spectrum of VSX J202751.9+414727 also showing the spectral window.

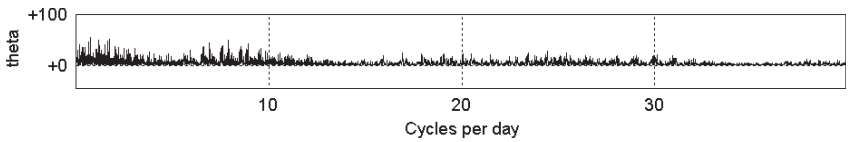


Figure 10. Power spectrum after removal of the signal at 16.803c/d.

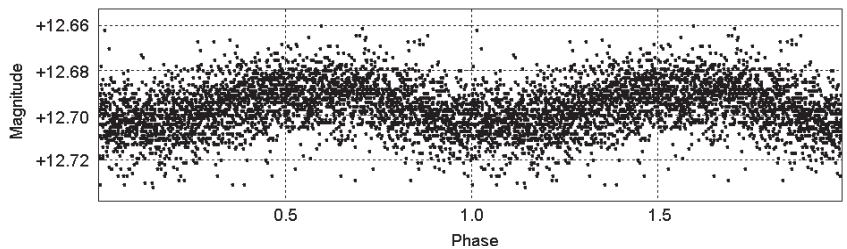


Figure 11. Phase diagram of VSX J202751.9+414727 for a period of 0.05951 day.

Ross 4—A Possible Recurrent Nova?

Samantha J. Brown

Intern, Yerkes Observatory, from Williams Bay High School, Williams Bay, WI

O. F. Mills

Wayne Osborn

Vivian Hoette

Yerkes Observatory, 373 W. Geneva St. Williams Bay, WI 53191; email correspondence should be sent to Wayne.Osborn@cmich.edu

Received August 9, 2010; accepted September 2, 2010

Abstract Archival photographic data have been used to study the suspected variable Ross 4 = NSV 1436. The star is found generally to be fainter than 15th magnitude but occasionally becomes brighter than 13. The available data suggest the object is a cataclysmic variable, possibly of the recurrent nova type.

1. Introduction

Between 1925 and 1931 F. Ross of Yerkes Observatory published ten lists of suspected new variable stars. Now known as the Ross variables, these objects were discovered when Ross compared photographic plates he had taken with plates taken with the same telescope some ten to twenty years earlier by E. E. Barnard.

The plates were taken with a telescope that actually consisted of three instruments on the same mounting: 10-inch and 6-inch refractors for photographs and a guide telescope (Barnard 1905). Because both Barnard and Ross obtained simultaneous exposures with the 10-inch and 6-inch telescopes, Ross could confirm that a suspected variable was not a plate defect. This was particularly important in the many cases when the object was clearly visible at one epoch but not seen at the other.

Most of the Ross variables have since been confirmed, while a few of the suspects seen at just one epoch have been found to be minor planets (Bedient 2003; Marsden 2007). There remain, however, a number of objects that are still unconfirmed or for which the variability is uncertain. One of these is Ross 4 (NSV 1436). This was one of the first variables Ross discovered, when he noticed that an object located at R.A. $03^{\text{h}} 54^{\text{m}} 01^{\text{s}}$, Dec. $+42^{\circ} 29.5'$ (1875) was at 11th magnitude on Barnard's plate taken 1904 November 1 but only 15th magnitude on his comparison plate of 1925 Jan. 14 (Ross 1925). Ross 4 is seen as a blend of two close stars on the digitized Palomar Sky Survey.

Bedient (2004) was the first to notice that the Ross 4 coordinates precessed to J2000 (R.A. $04^{\text{h}} 02^{\text{m}} 38^{\text{s}}$, Dec. $+42^{\circ} 50' 38''$) coincide with those of an X-ray

source (1RXS J040239.4+425037). He gathered brightness data from archival images as well as from new observations with the Hawaii 2.2-m telescope. The 2.2-m images showed the star blend is composed of three stars in a line running roughly north-south. All archival data identified by Bedient showed Ross 4 below 15th magnitude. The magnitudes from the recent images, presumably from CCD photometry, had it varying between 16 and 19.

Because Yerkes Observatory has the original discovery plates, as well as a number of other images of this field, we decided to review this material to confirm the exceptionally bright 1904 observation and to see what could be learned about this star.

2. Observations

We first verified Ross's findings. We used his own identification card and his markings on the 1925 plate to unambiguously identify the star and confirm his coordinates. The star was indeed bright on the two 1904 plates taken with the 10-inch and 6-inch cameras and faint on both 1925 plates. We next established a comparison sequence to be used to make eye estimates of the variable. A print was made of the field and ten nearby stars that ranged in B magnitude from 11.7 to 17.3 were selected. The B magnitudes were determined from the *Tycho* catalogue (Høg *et al.* 2000) when available, otherwise by averaging the values in the *USNO B1.0* (Monet *et al.* 2003) and *GSC 2.3* (Bucciarelli *et al.* 2008) catalogues. Our comparison stars and adopted magnitudes are given in Table 1. We believe the relative magnitudes of our sequence are accurate to 0.2m, but there may be a zero point error that is larger.

The Yerkes plate collection contains plates taken with the various Yerkes telescopes as well as a number of plate sets from instruments at McDonald Observatory, Dearborn Observatory, and the University of Illinois Observatory. We were able to locate the field of Ross 4 on eighty plates taken with five different instruments. All but six of the plates are unfiltered blue (photographic) exposures. Ross also recorded one visual observation with the Yerkes 40-inch refractor. The observation dates ranged from 1904 to 1952, but a sizable number of the plates are pairs taken on the same night. While some shorter-exposure plates only go to about $B = 12$, most plates recorded stars fainter than $B = 14.5$ and the forty-three deepest plates reach $B = 15.5$ –17.

The magnitude of Ross 4 (or its upper brightness limit) was estimated independently by three of us. Estimates were made by linearly interpolating between two convenient comparison stars when the star was seen, otherwise by determining the faintest comparison star visible. Ross 4 and its two companion stars are blended on our plates and our estimates correspond to their combined light. The adopted magnitudes along with the corresponding heliocentric Julian Dates are given in Table 2. We estimate they have uncertainties of 0.3m relative to the comparison sequence. The few estimates not from blue sensitive plates are given at the end of the table.

3. Results

The derived light curve is shown in Figure 1. Points indicate magnitudes where the blended stars were seen; dashes indicate a few of the “fainter-than” limits. One sees that the Ross 4 blend is usually below 15.8m but there are occasional outbursts when the star becomes brighter than 13m. In particular, two outbursts were observed—the one in 1904 and another in 1948. The 1904 event was recorded only on two plates taken simultaneously with the 10-inch and 6-inch cameras. The 1948 outburst was recorded on three plates taken on two different nights. There is some suggestion of variability during quiescence. The few visual, photovisual, and red observations give little useful information.

The 1948 pre-outburst, outburst, and post-outburst observations provide some sparse data on the eruption time scale. These data are plotted in Figure 2. On HJD 2432852 the star was at about 16.5. The next observation was thirty-three days later when the star was at 12.7. The brightness had fallen to 14.3 two days after and 109 days after maximum the star was again fainter than 15.5. Thus, the duration of the outburst was less than 140 days and likely much less. The blue magnitude change was at least 4 magnitudes, and perhaps as large as 6. The rapid and large magnitude changes suggest Ross 4 is a cataclysmic variable. This is supported by the X-ray emission. Our time coverage is insufficient to say how frequently outbursts occur, but it is possible the star is a recurrent nova. Searches for additional outbursts would obviously be worthwhile.

4. Acknowledgements

We thank Dr. Matthew Templeton, AAVSO, and the University Archives, Northwestern University, for providing some valuable information regarding Ross 4. This research has made use of the SIMBAD database, operated at CDS, Strasbourg, France.

References

- Barnard, E. E. 1905, *Astrophys. J.*, **21**, 35.
- Bedient, J. R. 2003, *Inf. Bull. Var. Stars*, No. 5478.
- Bedient, J. R. 2004, <http://www2.hawaii.edu/~bedient/svr004.html>.
- Bucciarelli, B., et al. 2008, in *A Giant Step: from Milli- to Micro-arcsecond Astrometry*, Proc. IAU, IAU Symp. 248, 316.
- Høg, E., et al. 2000, *Astron. Astrophys.*, **355**, L27.
- Marsden, B. G. 2007, *Perem. Zvezdy*, **27**, 3.
- Monet, D. G., et al. 2003, *Astron. J.*, **125**, 984.
- Ross, F. E. 1925, *Astron. J.*, **36**, 99.

Table 1. Comparison sequence.

<i>GSC 2.3 number</i>	<i>Adopted B (B-V)</i>		<i>GSC 2.3 number</i>	<i>Adopted B (B-V)</i>	
NCEH000476	11.7	1.0	NCEH000561	15.5	0.9
NCEH000514	14.1	1.5	NCEH004305	15.8	1.0
NCEH000480	14.4	0.7	NCEH000534	15.8	1.7
NCEH000553	14.6	1.9	NCEH005343	16.6	0.9
NCEH000552	15.2	1.5	NCEH004954	17.3	1.0

Table 2. Observed magnitudes for Ross 4.

<i>Plate number¹</i>	<i>Local Date</i>	<i>Exp. (min)</i>	<i>HJD – 2400000</i>	<i>Mag.</i>
Barnard plates				
10B-127	1904-11-01	136	16786.674	13.0
6B-127	1904-11-01	136	16786.674	12.8
10B-437	1907-10-28	140	17877.637	<15.8
6B-437	1907-10-28	140	17877.637	<15.8
10B-915	1914-09-19	67	20395.797	<15.8
6B-915	1914-09-19	64	20395.797	<14.1
10B-916	1914-09-20	98	20396.762	<15.8
6B-916	1914-09-20	98	20396.762	<15.8
10B-918	1914-09-24	51	20400.743	16.1:
6B-918	1914-09-24	51	20400.743	15.8:
10B-920	1914-10-20	120	20426.643	<15.8
6B-920	1914-10-20	120	20426.643	<15.5
10B-926	1914-10-24	270	20430.775	<15.8
6B-926	1914-10-24	270	20430.775	<14.6
10B-934	1914-11-22	200	20459.821	16.0:
6B-934	1914-11-22	200	20451.821	16.0
10B-1386	1919-12-19	140	22312.571	<14.4
6B-1386	1919-12-19	140	22312.571	<14.4
10B-1465	1920-08-20	97	22588.802	<14.1
6B-1465	1920-08-20	97	22588.802	<14.4
Ross plates				
6R-19	1924-12-27	120	24147.559	<14.6
10R-22	1925-01-14	120	24165.560	16.4
6R-22	1925-01-14	120	24165.560	16.2
10R-191	1927-01-23	120	24904.657	<14.6
3R-191	1927-01-23	120	24904.657	16.4

Table 2 continued on following pages

Table 2. Observed magnitudes for Ross 4, cont.

<i>Plate number^d</i>	<i>Local Date</i>	<i>Exp. (min)</i>	<i>HJD – 2400000</i>	<i>Mag.</i>
10R-402	1928-10-24	120	25544.810	<15.5
6R-402	1928-10-24	120	25544.810	16.0
3gR-402	1928-10-24	120	25544.810	<14.6
10R-412	1928-11-12	120	25563.740	<15.8
3gR-412	1928-11-12	120	25563.740	<14.6
10R-622	1929-12-05	90	25951.760	<15.2
3gR-622	1929-12-05	90	25951.760	<15.8
3pgR-757	1930-07-30	20	26188.839	<14.4
3pgR-760	1930-07-31	20	26189.833	<11.7
5R-786	1930-10-18	180	26268.839	16.1
10R-1260	1934-10-10	240	27722.000	17.3:
Illinois plates				
383	1940-09-27	60	29900.899	<16.6
384	1940-09-27	10	29900.924	<14.6
422	1940-10-26	60	29929.690	16.8:
423	1940-10-26	10	29929.715	<14.6
424	1940-10-26	60	29929.741	16.7
425	1940-10-26	10	29929.766	<14.1
426	1940-10-26	60	29929.792	17.4
427	1940-10-26	10	29929.817	<14.6
445	1940-11-01	60	29935.757	<15.5
446	1940-11-01	10	29935.787	<11.7
919	1947-11-08	10	32498.668	<11.7
920	1947-11-11	60	32501.551	<11.7
921	1947-11-11	60	32501.600	<14.6
922	1947-11-11	10	32501.625	<11.7
929	1947-12-08	60	32528.658	16.6:
930	1947-12-08	10	32528.684	<14.4
933	1947-12-13	30	32533.6 ²	<15.5
941	1948-01-14	60	32565.666	<15.8
942	1948-01-14	10	32565.691	<14.4
973	1948-03-04	60	32615.571	<14.6
1047	1948-10-05	50	32830.771	<15.2
1048	1948-10-05	9	32830.792	<15.2
1051	1948-10-25	60	32850.627	<15.5
1052	1948-10-25	10	32850.657	<14.1
1059	1948-10-26	60	32851.734	16.8:
1060	1948-10-26	10	32851.760	<15.2

Table 2 continued on next page

Table 2. Observed magnitudes for Ross 4, cont.

<i>Plate number¹</i>	<i>Local Date</i>	<i>Exp. (min)</i>	<i>HJD – 2400000</i>	<i>Mag.</i>
1061	1948-10-26	50	32851.786	<15.8
1062	1948-10-28	60	32853.689	<15.8
1063	1948-10-28	10	32853.714	<14.1
1079	1948-11-29	60	32886.610	12.5
1083	1948-11-29	60	32885.794	12.9
1097	1948-12-01	60	32887.622	14.5
1123	1949-03-18	60	32994.614	<15.8
1124	1949-03-18	10	32994.639	<11.7
McDonald plates				
C 076	1952-01-26	10	34037.590	15.8
C 078	1952-01-26	10	34037.642	15.8
C 080	1952-02-01	10	34043.593	15.8
C 082	1952-02-01	10	34043.691	15.8
Non-pg data ³				
Yerkes visual	1925-12-07	—	24492.6 ²	14.8
3vR-402	1928-10-24	120	25544.810	<12.7
3vR-412	1928-11-12	120	25563.740	<12.6
3vR-622	1929-12-05	90	25951.760	<12.7
3pvR-757	1930-07-30	20	26188.839	<10.7
3pvR-760	1930-07-31	20	26189.833	<10.7
Dearborn 1637	1942-10-07	5	30640.748	<12.7

Notes: 1. Initial number in Barnard and Ross plate designations indicates the telescope aperture in inches; Illinois plates with a 4-inch camera; McDonald plates with the 82-inch reflector; Dearborn plate with the 10.5-inch red camera. 2. Time not recorded so Julian Date is approximate. 3. Visual, photovisual and red magnitude estimates.

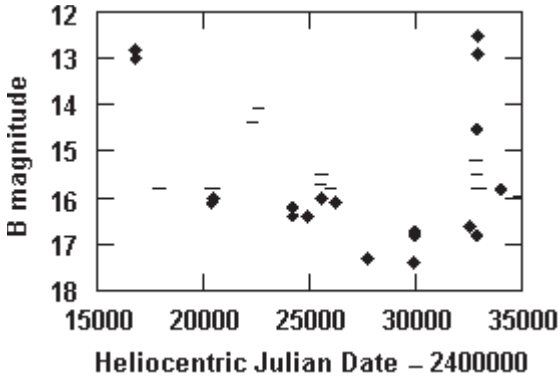


Figure 1. The light curve for Ross 4 from 1904 to 1952. Diamonds represent observed magnitude; lines represent brightness upper limit (fainter-than).

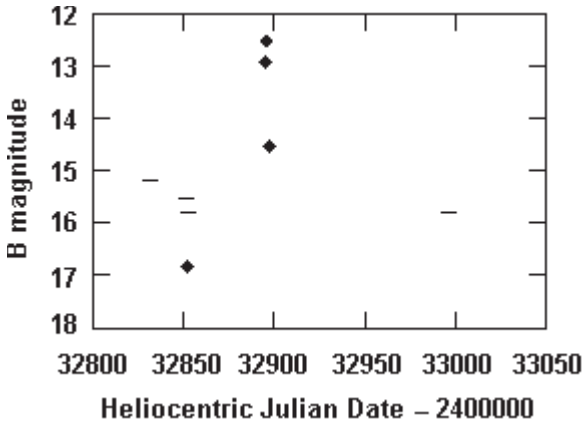


Figure 2. The light curve around the 1948 outburst. Diamonds represent observed magnitude; lines represent brightness upper limit (fainter-than).

Recent CCD Minima of 185 Eclipsing Binary Stars

Gerard Samolyk

P.O. Box 20677, Greenfield, WI 53220; gsamolyk@wi.rr.com

Received March 15, 2010; accepted March 15, 2010

Abstract This paper continues the publication of times of minima for eclipsing binary stars from observations reported to the AAVSO Eclipsing Binary section. Times of minima from observations made from September 2009 through February 2010 are presented.

1. Recent observations

The accompanying list contains times of minima calculated from recent CCD observations made by participants in the AAVSO's eclipsing binary program. This list will be web-archived and made available through the AAVSO ftp site at <ftp://ftp.aavso.org/public/datasets/gsamoj381.txt>. This list, along with eclipsing binary data from earlier AAVSO publications, is also included in the Lichtenknecker database administrated by the Bundesdeutsche Arbeitsgemeinschaft für Veränderliche Sterne e. V. (BAV) at <http://www.bav-astro.de/LkDB/index.php?lang=en>. These observations were reduced by the observers or the writer using the method of Kwee and van Woerden (1956). The standard error is included when available.

The linear elements in the *General Catalogue of Variable Stars* (GCVS; Kholopov *et al.* 1985) were used to compute the O–C values for most stars. For a few exceptions where the GCVS elements are missing or are in significant error, light elements from another source are used: CD Cam (Baldwin and Samolyk 2007), AC CMi (Samolyk 2008), CW Cas (Samolyk 1992a), Z Dra (Danielkiewicz-Krośniak and Kurpińska-Winiarska 1996), DF Hya (Samolyk 1992b), DK Hya (Samolyk 1990), EF Ori (Baldwin and Samolyk 2005), GU Ori (Samolyk 1985). O–C values listed in this paper can be directly compared with values published in recent numbers of the *AAVSO Observed Minima Timings of Eclipsing Binaries* series.

References

- Baldwin, M. E., and Samolyk, G. 2005, *Observed Minima Timings of Eclipsing Binaries No. 10*, AAVSO, Cambridge, MA.
- Baldwin, M. E., and Samolyk, G. 2007, *Observed Minima Timings of Eclipsing Binaries No. 12*, AAVSO, Cambridge, MA.
- Danielkiewicz-Krośniak, E., Kurpińska-Winiarska, M., eds. 1996, *Rocznik Astronomiczny* (SAC 68), **68**, 1.

- Kholopov, P. N., *et al.* 1985, *General Catalogue of Variable Stars*, 4th ed., Moscow.
 Kwee K. K., and van Woerden, H. 1956, *Bull. Astron. Inst. Netherlands*, **12**, 327.
 Samolyk, G. 1985, *J. Amer. Assoc. Var. Star Obs.*, **14**, 12.
 Samolyk, G. 1990, *J. Amer. Assoc. Var. Star Obs.*, **19**, 5.
 Samolyk, G. 1992a, *J. Amer. Assoc. Var. Star Obs.*, **21**, 34.
 Samolyk, G. 1992b, *J. Amer. Assoc. Var. Star Obs.*, **21**, 111.
 Samolyk, G. 2008, *J. Amer. Assoc. Var. Star Obs.*, **36**, 171.

Table 1. Recent times of minima of stars in the AAVSO eclipsing binary program.

<i>Star</i>	<i>HJD(min)</i> 2400000+	<i>Cycle</i>	<i>O-C</i> (<i>day</i>)	<i>Observer</i>	<i>Standard</i> <i>Error (day)</i>
RT And	55157.5733	22285	-0.0099	G. Samolyk	0.0001
TW And	55115.6907	3904	-0.0294	G. Samolyk	0.0001
WZ And	55086.7118	20433	0.0501	G. Samolyk	0.0002
WZ And	55093.6688	20443	0.0505	K. Menzies	0.0001
WZ And	55210.5403	20611	0.0515	G. Samolyk	0.0001
XZ And	55084.8180	22919	0.1720	K. Menzies	0.0001
XZ And	55239.5488	23033	0.1731	G. Samolyk	0.0001
AB And	55136.6008	57329	-0.0235	G. Samolyk	0.0001
AD And	55092.6659	16315.5	-0.0633	G. Samolyk	0.0002
AD And	55206.5701	16431	-0.0647	G. Samolyk	0.0001
BD And	55115.7907	43537	0.0133	G. Samolyk	0.0001
BD And	55124.5879	43556	0.0153	G. Samolyk	0.0002
BX And	55241.5719	30671	-0.0534	G. Samolyk	0.0003
DS And	55087.6133	18748	0.0021	G. Samolyk	0.0004
RY Aqr	55105.7244	7262	-0.0952	G. Samolyk	0.0001
CX Aqr	55094.6689	33528	0.0086	G. Samolyk	0.0003
CZ Aqr	55086.7622	13579	-0.0434	G. Samolyk	0.0002
XZ Aql	55076.6943	6158	0.1567	G. Samolyk	0.0002
KO Aql	55093.7025	4611	0.0725	G. Samolyk	0.0003
KP Aql	55078.6872	4360	-0.0150	G. Samolyk	0.0002
OO Aql	55081.3579	32495	0.0440	L. Corp	0.0003
OO Aql	55119.3688	32570	0.0458	L. Corp	0.0001
V342 Aql	55116.5285	4659	-0.1717	G. Samolyk	0.0002
V343 Aql	55112.6323	14458	-0.0549	G. Samolyk	0.0001
V1692 Aql	55112.2819	4877	-0.0391	Y. Ogmen	0.0003
RX Ari	55147.5569	16267	0.0611	G. Samolyk	0.0003
SS Ari	54750.6448	38726	-0.2584	G. Samolyk	0.0001
SS Ari	54840.5697	38947.5	-0.2610	G. Samolyk	0.0002
SS Ari	55076.8509	39529.5	-0.2681	G. Samolyk	0.0003
SS Ari	55146.6799	39701.5	-0.2700	R. Poklar	0.0002

Table continued on following pages

Table 1. Recent times of minima of stars in the AAVSO eclipsing binary program, cont.

<i>Star</i>	<i>HJD(min)</i> <i>2400000+</i>	<i>Cycle</i>	<i>O-C</i> <i>(day)</i>	<i>Observer</i>	<i>Standard</i> <i>Error (day)</i>
SS Ari	55163.5282	39743	-0.2704	N. Simmons	0.0003
SX Aur	55238.7379	12459	0.0132	G. Samolyk	0.0002
TT Aur	55177.6720	25463	-0.0157	K. Menzies	0.0001
TT Aur	55253.6396	25520	-0.0140	G. Samolyk	0.0005
AP Aur	55087.8747	22207.5	1.2584	G. Samolyk	0.0002
AP Aur	55188.6561	22384.5	1.2714	K. Menzies	0.0002
AP Aur	55210.5759	22423	1.2727	G. Samolyk	0.0002
AP Aur	55246.7339	22486.5	1.2794	G. Samolyk	0.0002
AR Aur	55209.5951	4065	-0.1233	G. Samolyk	0.0005
AR Aur	55240.6057	4072.5	-0.1229	G. Samolyk	0.0002
CL Aur	55110.8640	17795	0.1357	K. Menzies	0.0001
CL Aur	55231.5696	17892	0.1380	G. Samolyk	0.0001
EM Aur	54720.7908	13024	-1.1037	K. Menzies	0.0004
EM Aur	55183.5754	13278	-1.1029	G. Samolyk	0.0006
EP Aur	55183.6798	48856	0.0110	R. Poklar	0.0002
EP Aur	55186.6349	48861	0.0110	G. Samolyk	0.0002
EP Aur	55231.5532	48937	0.0127	G. Samolyk	0.0001
HP Aur	55147.6829	8709	0.0552	G. Samolyk	0.0002
HP Aur	55184.6746	8735	0.0538	R. Poklar	0.0001
HP Aur	55206.7296	8750.5	0.0552	G. Samolyk	0.0001
HP Aur	55241.5885	8775	0.0552	G. Samolyk	0.0002
HP Aur	55246.5697	8778.5	0.0565	G. Samolyk	0.0003
TY Boo	54982.6806	64645.5	0.0840	H. Gerner	0.0002
TY Boo	55225.9331	65412.5	0.0842	G. Samolyk	0.0003
TY Boo	55232.9097	65434.5	0.0835	K. Menzies	0.0001
TZ Boo	55246.8419	52543.5	0.0686	G. Samolyk	0.0001
Y Cam	55123.6826	3679	0.3629	G. Samolyk	0.0002
SV Cam	55112.5956	21107	0.0530	G. Samolyk	0.0001
AL Cam	55136.7001	21625	-0.0316	G. Samolyk	0.0001
CD Cam	55105.6877	3066	0.0003	G. Samolyk	0.0006
CD Cam	55246.6840	3250.5	0.0046	G. Samolyk	0.0004
RT CMa	55175.8061	22068	-0.7014	G. Samolyk	0.0003
RT CMa	55210.7378	22095	-0.7015	G. Samolyk	0.0001
SX CMa	55184.8143	16678	0.0330	G. Samolyk	0.0003
SX CMa	55228.6705	16705	0.0343	R. Poklar	0.0002
TU CMa	55174.7937	25002	-0.0094	G. Samolyk	0.0002
TZ CMa	55138.8674	14656	-0.1562	G. Samolyk	0.0003
TZ CMa	55182.7816	14679	-0.2052	G. Samolyk	0.0004
UU CMa	55183.7477	4886	-0.1061	G. Samolyk	0.0002

Table continued on following pages

Table 1. Recent times of minima of stars in the AAVSO eclipsing binary program, cont.

<i>Star</i>	<i>HJD(min)</i> <i>2400000+</i>	<i>Cycle</i>	<i>O-C</i> <i>(day)</i>	<i>Observer</i>	<i>Standard</i> <i>Error (day)</i>
XZ CMi	55190.9376	22022	-0.0069	G. Samolyk	0.0002
XZ CMi	55236.6652	22101	-0.0053	R. Poklar	0.0001
YY CMi	55246.7470	24884	0.0138	G. Samolyk	0.0002
AC CMi	55191.7892	3705	0.0010	G. Samolyk	0.0003
AC CMi	55238.6192	3759	0.0013	G. Samolyk	0.0001
AC CMi	55244.6903	3766	0.0018	R. Poklar	0.0001
AK CMi	55163.7587	21315	-0.0185	G. Samolyk	0.0001
AK CMi	55206.7665	21391	-0.0189	G. Samolyk	0.0001
AK CMi	55239.5888	21449	-0.0187	G. Samolyk	0.0001
AM CMi	55246.6244	29437	0.1931	G. Samolyk	0.0005
RZ Cas	55114.5892	9968	0.0608	G. Samolyk	0.0002
TW Cas	55084.6827	9155	-0.0108	G. Samolyk	0.0002
TW Cas	55167.5255	9213	-0.0108	G. Samolyk	0.0002
TW Cas	55174.6647	9218	-0.0132	R. Poklar	0.0007
AB Cas	55114.8430	9072	0.1012	G. Samolyk	0.0001
AB Cas	55199.5901	9134	0.1021	G. Samolyk	0.0001
CW Cas	55086.6041	42195	-0.0516	G. Samolyk	0.0002
CW Cas	55231.5244	42649.5	-0.0550	G. Samolyk	0.0002
CW Cas	55241.5694	42681	-0.0543	G. Samolyk	0.0001
DZ Cas	55153.6590	34042	-0.1768	R. Poklar	0.0004
GT Cas	55182.6681	9312	0.1883	R. Poklar	0.0005
IR Cas	55088.7957	18694	0.0088	K. Menzies	0.0001
IR Cas	55157.5441	18795	0.0080	G. Samolyk	0.0001
IR Cas	55238.5471	18914	0.0094	G. Samolyk	0.0001
IS Cas	55159.6758	14327	0.0646	R. Poklar	0.0002
IS Cas	55253.5927	14378	0.0644	G. Samolyk	0.0001
IT Cas	55138.8390	6769	0.0624	G. Samolyk	0.0002
IT Cas	55181.7020	6780	0.0624	R. Poklar	0.0003
MM Cas	55089.7734	16995	0.0927	K. Menzies	0.0001
OR Cas	55061.7598	8711	-0.0229	K. Menzies	0.0001
OR Cas	55086.6739	8731	-0.0231	C. Hesselteine	0.0002
OR Cas	55096.6397	8739	-0.0230	K. Menzies	0.0001
OR Cas	55253.5986	8865	-0.0237	G. Samolyk	0.0002
OX Cas	55086.7781	5550.5	0.0459	G. Samolyk	0.0007
PV Cas	55090.6099	8491	-0.0341	G. Samolyk	0.0002
V364 Cas	55093.7151	13454	-0.0198	G. Samolyk	0.0004
V364 Cas	55110.6855	13465	-0.0231	K. Menzies	0.0001
V364 Cas	55137.6886	13482.5	-0.0237	K. Menzies	0.0001
V364 Cas	55154.6632	13493.5	-0.0229	R. Poklar	0.0002

Table continued on following pages

Table 1. Recent times of minima of stars in the AAVSO eclipsing binary program, cont.

<i>Star</i>	<i>HJD(min)</i> <i>2400000+</i>	<i>Cycle</i>	<i>O-C</i> <i>(day)</i>	<i>Observer</i>	<i>Standard</i> <i>Error (day)</i>
V364 Cas	55239.5308	13548.5	-0.0240	G. Samolyk	0.0003
V375 Cas	55163.7002	13928	0.1485	N. Simmons	0.0002
V375 Cas	55253.5808	13989	0.1527	G. Samolyk	0.0002
V380 Cas	55175.6288	21757	-0.0649	R. Poklar	0.0004
V380 Cas	55209.5601	21782	-0.0654	G. Samolyk	0.0002
U Cep	55084.8674	4229	0.1664	G. Samolyk	0.0002
SU Cep	55138.7555	31965	0.0043	G. Samolyk	0.0001
WW Cep	52542.5744	17940	0.2954	G. Samolyk	0.0001
WW Cep	53232.7024	18390	0.3034	C. Hesseltine	0.0001
WW Cep	54396.7152	19149	0.3138	J. Bialozynski	0.0001
WW Cep	54626.7578	19299	0.3164	J. Bialozynski	0.0001
WW Cep	55077.6404	19593	0.3206	G. Samolyk	0.0002
WZ Cep	55114.6208	64856.5	-0.0930	G. Samolyk	0.0003
WZ Cep	55163.6693	64974	-0.0946	N. Simmons	0.0001
WZ Cep	55238.5985	65153.5	-0.0971	G. Samolyk	0.0002
XX Cep	55079.6137	4381	-0.0163	G. Samolyk	0.0003
XX Cep	55238.5548	4449	-0.0134	G. Samolyk	0.0005
ZZ Cep	55163.5670	12716	-0.0128	G. Samolyk	0.0004
DK Cep	55138.5668	21856	0.0335	G. Samolyk	0.0001
DL Cep	55157.5900	13009	0.0547	G. Samolyk	0.0003
EG Cep	55163.7236	23079	0.0139	G. Samolyk	0.0001
SS Cet	55087.7666	4249	0.0136	G. Samolyk	0.0002
TT Cet	55144.6899	46504	-0.0612	R. Poklar	0.0001
TW Cet	55114.7595	40212.5	-0.0255	G. Samolyk	0.0001
TW Cet	55168.6240	40382.5	-0.0259	R. Poklar	0.0001
TX Cet	55151.6727	16291	0.0099	R. Poklar	0.0003
TX Cet	55174.6399	16322	0.0110	G. Samolyk	0.0002
RW Com	55163.8833	63795	-0.0147	G. Samolyk	0.0002
RZ Com	55163.9053	60047.5	0.0441	G. Samolyk	0.0001
RZ Com	55253.7778	60313	0.0432	G. Samolyk	0.0001
SS Com	55238.7778	73246.5	0.7059	G. Samolyk	0.0003
W Crv	55191.9734	40054	0.0178	G. Samolyk	0.0001
V Crt	55183.9141	19638	-0.0031	G. Samolyk	0.0002
ZZ Cyg	55167.5444	16174	-0.0549	G. Samolyk	0.0002
AE Cyg	55105.7818	10854	-0.0049	G. Samolyk	0.0003
BR Cyg	55087.6453	10167	0.0002	G. Samolyk	0.0002
CG Cyg	54996.6956	24672	0.0627	N. Simmons	0.0002
DK Cyg	55088.5576	36306	0.0827	K. Menzies	0.0002
KR Cyg	55123.5772	30784	0.0143	G. Samolyk	0.0001

Table continued on following pages

Table 1. Recent times of minima of stars in the AAVSO eclipsing binary program, cont.

<i>Star</i>	<i>HJD(min)</i> <i>2400000+</i>	<i>Cycle</i>	<i>O-C</i> <i>(day)</i>	<i>Observer</i>	<i>Standard</i> <i>Error (day)</i>
V346 Cyg	55084.6388	7071	0.1418	K. Menzies	0.0002
V387 Cyg	55123.7070	42364	0.0201	G. Samolyk	0.0001
V388 Cyg	55138.6147	15349	-0.0846	G. Samolyk	0.0002
V401 Cyg	55056.7959	19257	0.0593	G. Samolyk	0.0003
V456 Cyg	55138.7206	11476	0.0459	G. Samolyk	0.0002
V466 Cyg	55080.5642	18904	0.0061	K. Menzies	0.0001
V548 Cyg	55096.5557	5894	0.0166	K. Menzies	0.0003
V704 Cyg	55086.8113	30046	0.0299	G. Samolyk	0.0003
V704 Cyg	55109.6389	30086	0.0294	K. Menzies	0.0003
V809 Cyg	55077.3397	11110	0.0344	Y. Ogmen	0.0001
V809 Cyg	55081.2687	11112	0.0345	Y. Ogmen	0.0001
TT Del	55094.6220	3435	-0.0908	G. Samolyk	0.0003
Z Dra	55253.7550	3985	-0.0273	G. Samolyk	0.0001
RZ Dra	55092.6168	19814	0.0478	G. Samolyk	0.0002
S Equ	55138.5616	3650	0.0644	G. Samolyk	0.0002
TZ Eri	55147.7882	4886	0.2901	G. Samolyk	0.0001
YY Eri	55114.8943	42094.5	0.1348	G. Samolyk	0.0001
YY Eri	55147.8467	42197	0.1341	G. Samolyk	0.0001
YY Eri	55210.5393	42392	0.1353	G. Samolyk	0.0001
RW Gem	55201.6642	12877	0.0018	R. Poklar	0.0002
SX Gem	55146.8394	26422	-0.0547	G. Samolyk	0.0002
TX Gem	55181.7579	12619	-0.0308	G. Samolyk	0.0002
TX Gem	55223.7580	12634	-0.0309	K. Menzies	0.0002
TX Gem	55240.5578	12640	-0.0312	K. Menzies	0.0001
TX Gem	55240.5584	12640	-0.0306	G. Samolyk	0.0001
WW Gem	55206.5232	23608	0.0241	G. Samolyk	0.0005
WW Gem	55248.6060	23642	0.0213	K. Menzies	0.0004
AF Gem	55210.7045	22556	-0.0695	G. Samolyk	0.0001
AL Gem	55240.7038	20783	0.0691	N. Simmons	0.0001
SZ Her	55098.6601	16177	-0.0209	R. Sabo	0.0001
WY Hya	55192.9305	20421.5	0.0283	G. Samolyk	0.0002
AV Hya	55210.6743	27125	-0.0949	G. Samolyk	0.0004
AV Hya	55251.6795	27185	-0.0940	R. Poklar	0.0003
DF Hya	55163.8049	37434.5	-0.0129	G. Samolyk	0.0001
DF Hya	55188.9303	37510.5	-0.0135	G. Samolyk	0.0001
DF Hya	55238.6874	37661	-0.0124	G. Samolyk	0.0001
DK Hya	55181.9300	23640	0.0067	G. Samolyk	0.0004
SW Lac	55085.6160	30588.5	-0.1029	G. Samolyk	0.0001
SW Lac	55124.5838	30710	-0.1027	G. Samolyk	0.0001

Table continued on following pages

Table 1. Recent times of minima of stars in the AAVSO eclipsing binary program, cont.

<i>Star</i>	<i>HJD(min)</i> 2400000+	<i>Cycle</i>	<i>O-C</i> (<i>day</i>)	<i>Observer</i>	<i>Standard</i> <i>Error (day)</i>
VX Lac	55110.5750	9169	0.0717	K. Menzies	0.0001
AR Lac	55146.7644	6834	-0.0823	G. Samolyk	0.0005
AW Lac	55083.6441	24902	0.1764	G. Samolyk	0.0002
CO Lac	55088.6881	17867	-0.0061	K. Menzies	0.0001
CO Lac	55105.6536	17878	-0.0049	G. Samolyk	0.0003
CO Lac	55112.6002	17882.5	0.0018	G. Samolyk	0.0001
DG Lac	55080.6668	4791	-0.2246	K. Menzies	0.0003
Y Leo	55156.8125	5765	-0.0165	K. Menzies	0.0001
Y Leo	55210.7677	5797	-0.0166	G. Samolyk	0.0001
UU Leo	55193.8711	5832	0.1662	K. Menzies	0.0001
Z Lep	55138.8514	27890	-0.1709	G. Samolyk	0.0002
RR Lep	55157.7639	27070	-0.0341	G. Samolyk	0.0002
RY Lyn	55163.7229	8555	-0.0424	G. Samolyk	0.0002
UZ Lyr	55124.5491	6046	-0.0271	G. Samolyk	0.0001
EW Lyr	55087.7014	14670	0.2380	R. Sabo	0.0001
RU Mon	55147.8275	3739.5	-0.5361	G. Samolyk	0.0007
RU Mon	55178.7530	3748	-0.0810	G. Samolyk	0.0002
RU Mon	55239.6922	3765	-0.0825	R. Poklar	0.0001
RW Mon	55146.8101	11262	-0.0700	G. Samolyk	0.0001
RW Mon	55188.7436	11284	-0.0706	G. Samolyk	0.0001
AT Mon	55210.6002	14097	0.0053	G. Samolyk	0.0004
BB Mon	55138.8470	38839	-0.0045	G. Samolyk	0.0002
BB Mon	55240.6921	38978	-0.0045	G. Samolyk	0.0002
BB Mon	55240.6933	38978	-0.0033	R. Poklar	0.0002
EP Mon	55177.8076	19414	0.0318	G. Samolyk	0.0004
EP Mon	55246.6940	19474	0.0322	R. Poklar	0.0001
EF Ori	55210.5400	1766	0.0039	G. Samolyk	0.0004
EQ Ori	55209.5276	13614	-0.0354	G. Samolyk	0.0001
ER Ori	55147.7362	31935	0.0837	G. Samolyk	0.0002
ER Ori	55197.6989	32053	0.0854	R. Poklar	0.0001
ER Ori	55246.6027	32168.5	0.0866	G. Samolyk	0.0001
ET Ori	55144.8290	29929	-0.0056	K. Menzies	0.0001
FH Ori	55209.5803	13625	-0.3617	G. Samolyk	0.0003
FL Ori	55138.7785	6313	0.0346	G. Samolyk	0.0001
FL Ori	55211.6745	6360	0.0349	R. Poklar	0.0001
FL Ori	55239.5941	6378	0.0371	K. Menzies	0.0001
FT Ori	55153.8167	4382	0.0149	K. Menzies	0.0001
FZ Ori	55136.8273	27782	-0.0587	G. Samolyk	0.0010
FZ Ori	55147.8316	27809.5	-0.0541	G. Samolyk	0.0004

Table continued on following pages

Table 1. Recent times of minima of stars in the AAVSO eclipsing binary program, cont.

<i>Star</i>	<i>HJD(min)</i> <i>2400000+</i>	<i>Cycle</i>	<i>O-C</i> <i>(day)</i>	<i>Observer</i>	<i>Standard</i> <i>Error (day)</i>
FZ Ori	55154.8278	27827	-0.0576	K. Menzies	0.0001
FZ Ori	55210.6265	27966.5	-0.0570	R. Poklar	0.0002
GU Ori	55114.8208	25590.5	-0.0443	G. Samolyk	0.0005
GU Ori	55156.7104	25679.5	-0.0453	K. Menzies	0.0002
GU Ori	55206.6022	25785.5	-0.0457	G. Samolyk	0.0002
GU Ori	55210.6022	25794	-0.0465	G. Samolyk	0.0003
GU Ori	55253.6686	25885.5	-0.0474	R. Poklar	0.0005
U Peg	55077.8331	49539	-0.1328	G. Samolyk	0.0002
U Peg	55086.6428	49562.5	-0.1305	G. Samolyk	0.0002
U Peg	55175.6492	49800	-0.1347	G. Samolyk	0.0001
BB Peg	55089.6488	31328.5	-0.0031	K. Menzies	0.0001
BB Peg	55096.6981	31348	-0.0031	R. Sabo	0.0001
BB Peg	55146.5851	31486	-0.0034	G. Samolyk	0.0003
BG Peg	55112.6038	4907	-1.9112	G. Samolyk	0.0002
BG Peg	55157.5096	4930	-1.9180	K. Menzies	0.0003
BO Peg	55116.2506	16374	-0.0349	Y. Ogmen	0.0001
BX Peg	55087.6684	38843	-0.0938	C. Hesselstine	0.0001
BX Peg	55107.2959	38913	-0.0958	Y. Ogmen	0.0001
BX Peg	55146.5572	39053	-0.0934	G. Samolyk	0.0002
DI Peg	55085.7474	13893	-0.0114	G. Samolyk	0.0002
KW Peg	55146.5584	8559.5	0.1521	G. Samolyk	0.0004
Z Per	55087.7205	3085	-0.2304	G. Samolyk	0.0001
Z Per	55246.6448	3137	-0.2340	G. Samolyk	0.0001
RT Per	55138.6095	25621	0.0656	G. Samolyk	0.0001
RT Per	55240.5384	25741	0.0665	G. Samolyk	0.0001
RV Per	55239.7118	6685	-0.0005	G. Samolyk	0.0001
ST Per	55087.8035	4777	0.2947	G. Samolyk	0.0002
ST Per	55095.7499	4780	0.2962	K. Menzies	0.0001
ST Per	55156.6618	4803	0.2969	R. Poklar	0.0003
ST Per	55172.5519	4809	0.2971	K. Menzies	0.0001
XZ Per	55122.8078	10086	-0.0514	G. Samolyk	0.0001
XZ Per	55130.8691	10093	-0.0515	K. Menzies	0.0001
IU Per	55118.4273	11093	0.0119	J. Virtanen	0.0001
IU Per	55146.7118	11126	0.0145	G. Samolyk	0.0001
IU Per	55158.7101	11140	0.0145	R. Poklar	0.0002
IU Per	55207.5581	11197	0.0121	K. Menzies	0.0001
KW Per	55163.5209	13701	0.0115	G. Samolyk	0.0001
Beta Per	55146.7270	3315	0.0997	G. Samolyk	0.0001

Table continued on following pages

Table 1. Recent times of minima of stars in the AAVSO eclipsing binary program, cont.

<i>Star</i>	<i>HJD(min)</i> <i>2400000+</i>	<i>Cycle</i>	<i>O-C</i> <i>(day)</i>	<i>Observer</i>	<i>Standard</i> <i>Error (day)</i>
Y Psc	55147.5630	2526	-0.0054	G. Samolyk	0.0001
RV Psc	55058.7040	55375	-0.0525	C. Hesselstine	0.0003
RV Psc	55115.7673	55478	-0.0504	G. Samolyk	0.0002
RV Psc	55116.3158	55479	-0.0559	Y. Ogmen	0.0002
UZ Pup	55192.7650	13309.5	-0.0053	G. Samolyk	0.0002
UZ Pup	55235.6857	13363.5	-0.0066	R. Poklar	0.0002
AV Pup	55175.9443	43135	0.1348	G. Samolyk	0.0005
AV Pup	55232.7119	43237	0.1559	R. Poklar	0.0003
RS Ser	55105.5517	33744	0.0651	G. Samolyk	0.0002
RW Tau	55136.7759	3414	-0.2328	G. Samolyk	0.0003
RZ Tau	55157.8249	42055	0.0584	G. Samolyk	0.0002
RZ Tau	55178.6089	42105	0.0587	G. Samolyk	0.0001
TY Tau	55093.7931	31467	0.2526	K. Menzies	0.0001
TY Tau	55163.8207	31532	0.2521	G. Samolyk	0.0001
WY Tau	55198.5852	25689	0.0567	G. Samolyk	0.0002
AM Tau	55225.6784	4879	-0.0536	G. Samolyk	0.0001
AQ Tau	55157.6972	20974	0.5527	N. Simmons	0.0003
AQ Tau	55179.5846	20992	0.5538	G. Samolyk	0.0003
AQ Tau	55235.5163	21038	0.5539	K. Menzies	0.0002
CT Tau	55146.6965	14610	-0.0532	G. Samolyk	0.0002
CT Tau	55180.7050	14661	-0.0530	R. Poklar	0.0001
CT Tau	55240.7199	14751	-0.0529	G. Samolyk	0.0001
EQ Tau	55116.7448	43660.5	-0.0255	K. Menzies	0.0001
EQ Tau	55116.9156	43661	-0.0254	R. Sabo	0.0001
HU Tau	55239.6762	6791	0.0230	G. Samolyk	0.0001
V Tri	55115.6713	52360	-0.0042	G. Samolyk	0.0001
V Tri	55120.9374	52369	-0.0049	R. Sabo	0.0002
V Tri	55139.6633	52401	-0.0056	R. Sabo	0.0003
V Tri	55231.5420	52558	-0.0042	G. Samolyk	0.0001
X Tri	55090.8279	12957	-0.0747	G. Samolyk	0.0001
X Tri	55092.7709	12959	-0.0748	K. Menzies	0.0001
RS Tri	55206.6669	9045	-0.0353	G. Samolyk	0.0001
RV Tri	55146.6123	12092	-0.0308	G. Samolyk	0.0001
RV Tri	55161.6857	12112	-0.0307	R. Poklar	0.0001
W UMa	55157.7382	28150.5	-0.0625	G. Samolyk	0.0002
TY UMa	55163.8498	44088.5	0.2782	G. Samolyk	0.0002
TY UMa	55213.8412	44229.5	0.2797	K. Menzies	0.0003
XZ UMa	55209.8248	7397	-0.1022	K. Menzies	0.0001

Table continued on following page

Table 1. Recent times of minima of stars in the AAVSO eclipsing binary program, cont.

<i>Star</i>	<i>HJD(min)</i> <i>2400000+</i>	<i>Cycle</i>	<i>O-C</i> <i>(day)</i>	<i>Observer</i>	<i>Standard</i> <i>Error (day)</i>
XZ UMa	55247.7165	7428	-0.1025	K. Menzies	0.0002
ZZ UMa	54922.6757	8251	-0.0026	R. Poklar	0.0001
ZZ UMa	55223.8795	8382	-0.0018	K. Menzies	0.0001
W UMi	55157.5705	12624	-0.1660	G. Samolyk	0.0003
RU UMi	55239.6792	25991	-0.0136	G. Samolyk	0.0001
AH Vir	55253.8132	23162.5	0.2230	G. Samolyk	0.0002
AW Vir	55239.9052	28862.5	0.0232	K. Menzies	0.0001
AW Vir	55246.8076	28882	0.0227	G. Samolyk	0.0001
Z Vul	55079.7535	4942	-0.0080	G. Samolyk	0.0002
AX Vul	55147.6386	5084	-0.0308	G. Samolyk	0.0001
BK Vul	55120.2701	66934	0.0091	Y. Ogmen	0.0001
BO Vul	55105.6149	9824	-0.0332	G. Samolyk	0.0001
BS Vul	55146.5658	24949	-0.0244	G. Samolyk	0.0001
BU Vul	55094.5499	37893	0.0152	K. Menzies	0.0001

Absolute Magnitudes and Distances of Recent Novae

Yitping Kok

34/155 Abercrombie Street, Darlington, NSW, 2008, Australia; yitping.kok@gmail.com

and

Variable Stars South

Received March 19, 2010; accepted September 2, 2010

Abstract Using photometric data from the American Association of Variable Star Observers, peak absolute magnitudes and distances of some novae discovered in 2009 were calculated using the maximum-magnitude-rate-of-decline (MMRD) relationship. As these novae were only discovered recently, their distances have not been reported using any other method. In view of this, several older novae have been subjected to similar MMRD analysis. Their distances were then compared with other published work which used different methods of estimation. The distances found in this work correlate well, thus giving confidence in the estimates for the recent novae and the MMRD analysis.

1. Introduction

The relationship between the peak absolute magnitude, M_v , of a nova and its rate of decline of brightness from the maximum can be expressed by the following:

1. Nonlinear $M_v - t_2$ relation (Della Valle and Livio 1995; Downes and Duerbeck 2000).

$$M_v = -7.92 - 0.81 \arctan \left[\frac{1.32 - \log t_2}{0.23} \right] \quad (1)$$

$$M_v = -8.02 - 1.23 \arctan \left[\frac{1.32 - \log t_2}{0.23} \right] \quad (2)$$

2. Classical “linear” $M_v - t_2$ relation (Cohen 1985; Downes and Duerbeck 2000).

$$M_v = -(10.70 \pm 0.30) - (2.41 \pm 0.23) \log t_2 \quad (3)$$

$$M_v = -(11.32 \pm 0.440) - (2.55 \pm 0.323) \log t_2 \quad (4)$$

3. Conditional “linear” $M_v - t_2$ relation (Downes and Duerbeck 2000).

$$M_v = \begin{cases} -(10.79 \pm 0.92) - (1.53 \pm 1.15) \log t_2 & , \log t_2 < 1.2 \\ -(8.71 \pm 0.82) - (1.03 \pm 0.51) \log t_2 & , \log t_2 \geq 1.2 \end{cases} \quad (5)$$

4. Classical “linear” $M_v - t_3$ relation (Schmidt 1957; Downes and Duerbeck 2000).

$$M_v = -11.75 - 2.5 \log t_3 \quad (6)$$

$$M_v = -(11.79 \pm 0.56) - (2.54 \pm 0.35) \log t_3 \quad (7)$$

5. Conditional “linear” $M_v - t_3$ relation (Downes and Duerbeck 2000).

$$M_v = \begin{cases} -(11.26 \pm 0.84) - (1.58 \pm 0.78) \log t_3 & , \log t_3 < 1.5 \\ -(8.13 \pm 1.26) - (0.56 \pm 0.68) \log t_3 & , \log t_3 \geq 1.5 \end{cases} \quad (8)$$

where t_2 and t_3 are the time taken for the brightness of nova to decline by 2 and 3 magnitudes from its maximum, respectively. Both parameters can be extracted from the light curve of a nova. With absolute magnitude, the distance, D (in kiloparsec, kpc), of a nova can be found by using the following equation.

$$D = 10^{0.2(m_v - M_v + 5 - A_v)} \quad (9)$$

where m_v is the peak apparent magnitude of the nova and A_v is the interstellar extinction coefficient.

2. Analysis flow and results

At the time of writing there were five novae discovered in 2009: V5581 Sgr, V5582 Sgr, V1213 Cen, V5583 Sgr, and V2672 Oph. Observational data recorded at AAVSO for the first two novae were inadequate and hence were left out of this work. The remaining three novae were subjected to the following analysis flow to determine their peak absolute magnitude and distance. Three older novae, V351 Pup, V4633 Sgr, and V2467 Cyg, were used as references.

1. Collect data from AAVSO
2. Curve-fit data and extract light curve parameters
3. Calculate absolute magnitudes, M_v
4. Refer or estimate extinction coefficients, A_v
5. Calculate distances, D

2.1. Curve-fit observational data

Raw data downloaded from AAVSO were minimally processed. Only “visual” and “V” type observations were considered. “Fainter-than” observations were not considered. All three novae are fast (Downes and Duerbeck 2000) and their light curves past maximum brightness fitted very well to an exponential function in this general form.

$$m_v = P_1 - P_2 \exp(-P_3 t) \quad (10)$$

where m_v represents the observed brightness in magnitude and t is the time in Julian date. Parameters P_1 , P_2 , and P_3 are extracted from the data using non-linear least squares method. Figures 1 through 4 plot the function m_v with data of each of the 2009 novae and the old nova V4633 Sgr.

2.2. Extract light curve parameters

Maximum brightness, m_0 , and the time of maximum brightness, t_0 , of each nova were read off from the light curve. The uncertainties of both parameters due to chart reading were noted down as well. Subsequently, t_2 and t_3 are determined from equation (10). Uncertainties of both parameters were also determined from equation (10) by means of error propagation and variance-covariance matrix obtained during the non-linear least square fitting. Table 1 lists the light curve parameters extracted for the three recent novae of interest and also for the three older novae. The parameters of the three older novae extracted in this analysis are comparable with numbers reported in other work, which are listed for comparison in Table 2.

2.3 Calculate peak absolute magnitude, M_v

Peak absolute magnitudes for each nova were calculated using all equations from all the five $M_v - t_n$ relations listed earlier. Subsequently a final error weighted mean value is calculated. The mean peak absolute magnitude of each nova is listed in Table 3. Values from other work are also listed as reference. The novae were also categorized according to their speed type (Downes and Duerbeck 2000).

2.4. Calculate distance of nova, D

Before the distances of the novae can be calculated, the interstellar extinction coefficient has to be determined. The interstellar extinction coefficient, A_v , can be determined from photometric measurement of the reddening effect of the nova and calculating it from the following equation.

$$A_v = 3.1E(B-V) \quad (11)$$

Unlike the light curve data, $E(B-V)$ is not readily available from AAVSO or any other sources because the value is specific to that region of the sky where the nova of interest is found. Fortunately there are researchers who have created an interstellar extinction model or map of the whole sky.

A map by Schlegel *et al.* (1998) gives estimates of the maximum extinction on the line of sight in units of $E(B-V)$ or A_v . The map is presented in electronic form and is accessible from:

<http://nedwww.ipac.caltech.edu/forms/calculator.html>.

Application of the extinction value into the distance, D , equation is straightforward.

Another model considered is the work by Arenou *et al.* (1992) which gives a tridimensional mathematical model of the interstellar extinction. The extinction is modeled as a function of galactic longitude, latitude, and distance from the Sun. In general, the mathematical model is a mixture of quadratic and linear relation with distance.

$$A_v(r, l, b) = \begin{cases} \alpha(l, b)r + \beta(l, b)r^2 & , r \leq r_0 \\ \alpha(r_0, l, b) + \gamma(l, b)(r - r_0) & , r > r_0 \end{cases} \quad (12)$$

where r is the distance of object, l, b are galactic coordinates, α, β , and γ are coordinate-dependent constants. Since the extinction value is dependent on the distance of the object, the distance of nova, D , is solved numerically.

3. Discussion

There is a big variation in distance due to the values of A_v used. A better estimate of distance can be obtained only if one measures the $E(B-V)$ of the nova. This is especially true for the case of V2672 Oph. The $E(B-V)$ of V2672 Oph was reported to be +1.6 (Kato 2009), or $A_v \sim 4.96$. This gives an estimate of distance of 9.4 ± 2.3 kpc for V2672 Oph, which is closer to the number obtained with Schlegel *et al.* (1998) in Table 4. The range of distance estimated for V1213 Cen is large as well. It is difficult to narrow down the estimate without any $E(B-V)$ measurement. On the other hand, the distance estimate for V5583 Sgr is more meaningful. It is very likely that V5583 Sgr lies on the other side of the Galaxy since the distance of the Galactic center is ~ 8 kpc away from the Sun. At this distance, V5583 Sgr lies about 1.1–1.4 kpc above the Galactic plane. This is not unlikely, as it has been found that the distribution of fast novae exists beyond 1 kpc above the Galactic plane (Burlak 2008). Bulge novae are likely to belong to a spectroscopic class type of Fe II (Della Valle and Livio 1998) while novae that lie near the Galactic disk, like V1213 Cen and V2672 Oph, belong to the He/N class. Table 5 lists the height of the three recent novae with respect to the Galactic plane.

Another interesting observation from V2672 Oph is the mass of the white dwarf that is responsible for the nova. If the peak absolute magnitude in V band is assumed to be approximately equal to its magnitude in B band and according to the mass – magnitude relation below (Livio 1992), it is interesting to note

that the mass of white dwarf of V2672 Oph (at ~ 1.38 solar mass) is very close to the Chandrasekhar limit. The Chandrasekhar limit sets the theoretical maximum mass of a white dwarf to ~ 1.4 solar masses.

$$M_B^{max} \sim M_v^{max} = -8.3 - 10.0 \log \left(\frac{M_{WD}}{M_\odot} \right) \quad (13)$$

4. Conclusions

Absolute magnitudes and distances of three recent novae were found to a good degree of confidence by exploiting the relationship between maximum magnitude and rate of decline of classical novae and published papers on older novae. All three recent novae are fast with recent two likely to be located on the other side of the Galaxy.

5. Acknowledgement

The author would like express his gratitude to Alan Plummer, Stan Walker, and Thomas Richards from Variable Stars South for their encouragement in publishing this work.

References

- Arenou, F., Grenon, M., and Gomez, A. 1992, *Astron. Astrophys.*, **258**, 104.
 Burlak, M. A. 2008, *Astron. Lett.*, **34**, 468.
 Cohen, J. G. 1985, *Astrophys. J.*, **292**, 90.
 Della Valle, M., and Livio, M. 1995, *Astrophys. J.*, **452**, 704.
 Della Valle, M., and Livio, M. 1998, *Astrophys. J.*, **506**, 818.
 Downes, R. A., and Duerbeck, H. W. 2000, *Astron. J.*, **120**, 2007.
 Ikeda, Y., Kawabata, K. S., and Akitaya, H. 2000, *Astron. Astrophys.*, **355**, 256.
 Kato, T. 2009, vsnet-alert No. 11399.
 Lipkin, Y., Leibowitz, E., Retter, A., and Shemmer, O. 2001, *Mon. Not. Roy. Astron. Soc.*, **328**, 1169.
 Livio, M. 1992, *Astrophys. J.*, **393**, 516.
 Orio, M., Balman, S., Della Valle, M., Gallagher, J., and Oegelman, H. 1996, *Astrophys. J.*, **466**, 410.
 Poggiani, R. 2009, *Astron. Nachr.*, **330**, 77.
 Schlegel, D. J., Finkbeiner, D. P., and Davis, M. 1998, *Astrophys. J.*, **500**, 525.
 Schmidt, T. 1957, *Z. Astrophys.*, **41**, 182.
 Tomov, T., *et al.* 2007, *Inf. Bull. Var. Stars*, No. 5779, 1.

Table 1. Light curve parameters of novae.

<i>Nova</i>	m_0	t_0	t_2	t_3
V351 Pup	6.4 ± 0.5	0.0 ± 0.5	11.1 ± 5.5	27.2 ± 12.5
V4633 Sgr	7.6 ± 0.3	0.0 ± 0.5	19.5 ± 4.7	42.9 ± 11.2
V2467 Cyg	7.4 ± 0.5	0.0 ± 0.5	9.0 ± 3.6	17.8 ± 5.6
V1213 Cen	8.2 ± 0.5	0.0 ± 0.5	6.6 ± 2.8	15.3 ± 8.0
V5583 Sgr	7.0 ± 0.3	0.8 ± 0.5	4.5 ± 1.2	8.8 ± 1.7
V2672 Oph	10.0 ± 0.5	0.0 ± 0.5	1.0 ± 0.7	2.0 ± 0.7

Table 2. Comparison between parameters extracted (*c*) from curve fit and reported (*r*) by others.

<i>Nova</i>	$t_2(c)$	$t_2(r)$	$t_3(c)$	$t_3(r)$	<i>Reference</i>
V351 Pup	11.1 ± 5.5	10	27.2 ± 12.5	26	Downes and Duerbeck (2000)
V4633 Sgr	19.5 ± 4.7	19 ± 3	42.9 ± 11.2	42 ± 5	Lipkin <i>et al.</i> (2001)
V2467 Sgr	9.0 ± 3.6	7.6 ± 3.0	17.8 ± 5.6	14.6 ± 3.5	Poggiani (2009)

Table 3. Calculated (*c*) and cited (*r*) peak absolute magnitude of recent and older novae.

<i>Nova</i>	<i>Type</i>	$M_v(c)$	$M_v(r)$	<i>Reference</i>
V351 Pup	fast	-8.5 ± 0.3	-8.0 ± 0.4	Downes and Duerbeck (2000)
V4633 Sgr	slow	-7.7 ± 0.3	-7.7 ± 0.5	Lipkin <i>et al.</i> (2001)
V2467 Sgr	fast	-8.8 ± 0.2	-8.8 ± 0.3	Poggiani (2009)
V1213 Cen	fast	-9.1 ± 0.1		
V5583 Sgr	fast	-9.3 ± 0.1		
V2672 Oph	fast	-9.8 ± 0.1		

Table 4. Distances of novae in kpc.

<i>Nova</i>	$A_v(1)$	$D(1)$	$A_v(2)$	$D(2)$	$D(r)$	<i>Reference</i>
V351 Pup	4.20	1.4 ± 0.4	1.46	4.9 ± 1.3	4.7 ± 0.6	Orio <i>et al.</i> (1996)
V4633 Sgr	1.30	6.3 ± 1.2	0.71	8.3 ± 1.6	2 – 10	Ikeda <i>et al.</i> (2000)
V2467 Sgr	20.24	0.0 ± 0.0	2.00	7.0 ± 1.7	1.5 – 4	Tomov <i>et al.</i> (2007)
V1213 Cen	6.72	1.3 ± 0.3	1.89	12 ± 3		
V5583 Sgr	1.29	9.9 ± 1.5	0.76	13 ± 2		
V2672 Oph	5.02	9.2 ± 2.2	1.69	42 ± 10		

Table 5. Heights of novae, z (in kpc), above the Galactic plane.

<i>Nova</i>	<i>Type</i>	$b $	$z(1)$	$z(2)$
V1213 Cen	disk	-1.4	0.03 ± 0.01	0.3 ± 0.1
V5583 Sgr	bulge	-6.4	1.1 ± 0.2	1.4 ± 0.2
V2672 Oph	disk	2.5	0.4 ± 0.1	1.9 ± 0.5

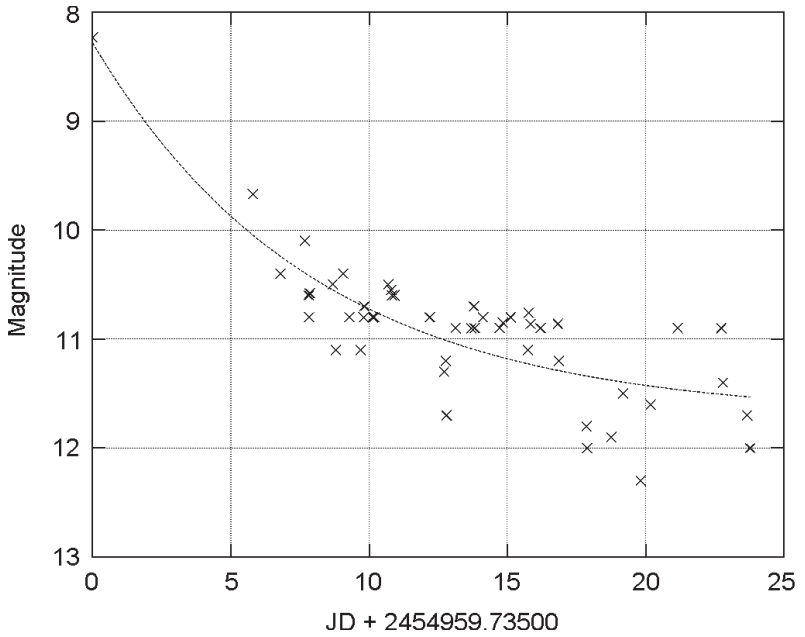


Figure 1. Light curve of V1213 Cen. Dashed line shows the fit of function m_v .

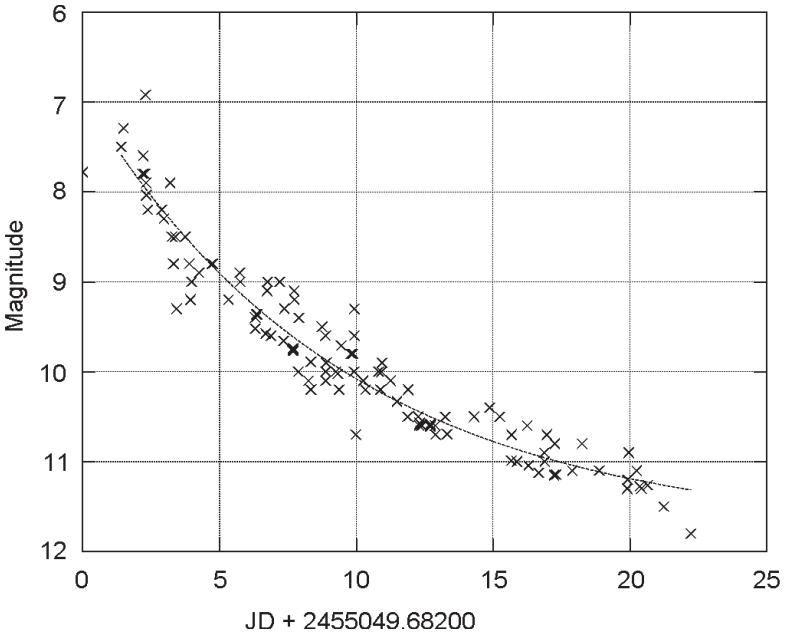


Figure 2. Light curve of V5583 Sgr. Dashed line shows the fit of function m_v .

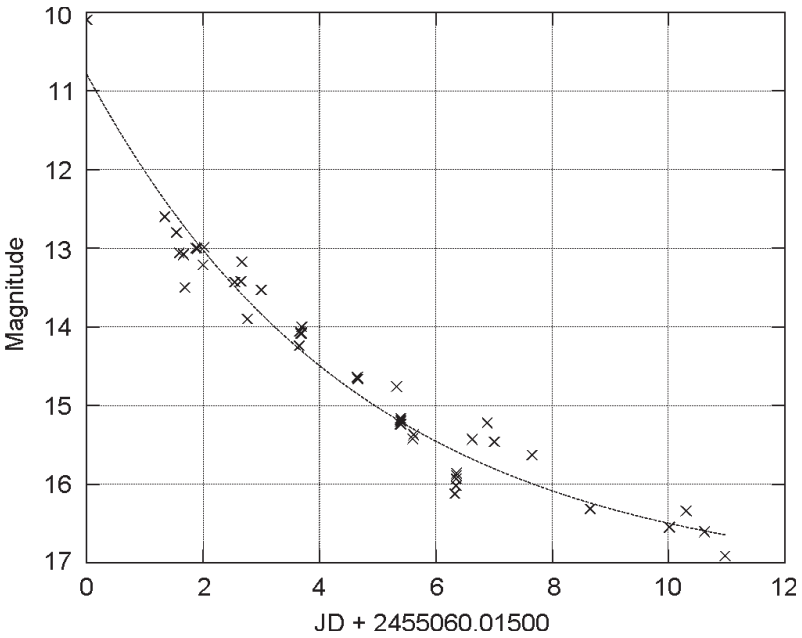


Figure 3. Light curve of V2672 Oph. Dashed line shows the fit of function m_v .

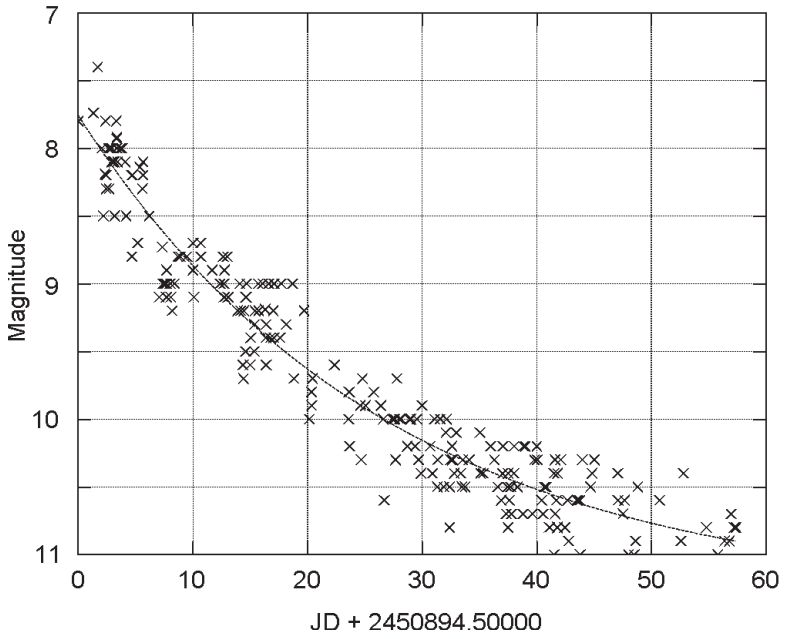


Figure 4. Light curve of V4633 Sgr. Dashed line shows the fit of function m_v .

Differential Ensemble Photometry by Linear Regression

Kevin B. Paxson

20219 Eden Pines, Spring, TX 77379; kbpaxson@aol.com

Received January 20, 2010; revised January 22, 2010; accepted January 25, 2010

Abstract A linear regression method for multiple star ensemble photometry by spreadsheet is presented. After initial spreadsheet setup and data entry, a differential ensemble magnitude estimate is calculated along with a total error. Ensemble photometry by linear regression allows one to see the distribution of comparison star errors, yields variable star estimates with enhanced confidence, and identifies potential problems with the comparison stars, validating the Johnson V magnitude sequence. Spreadsheet construction is described and two linear regression ensemble examples are illustrated and discussed.

1. Introduction

Over the past decade and a half, CCD variable star photometry by amateur astronomers has grown exponentially with the increased availability of larger CCD chips and less expensive commercially-made CCD cameras in the marketplace. Photometric reduction techniques have become more refined over time, including ensembles. Most ensemble reduction methods involve the use of multiple sets of variable star-comparison star differences, where differential magnitude and error calculations are computed using a variety of methods. These include the mean value method, the weighted average method, and the master star method (Crawford 2006). Of these, the mean value method is most popular.

Ensemble photometry methods using mainframe computer programs (Honeycutt 1992) or specialized programming languages such as C (Richmond 2006) and FORTRAN (Howell and Everett 2001) exist in the literature, but are beyond the access of and availability to most amateur astronomers. Most image processing software packages (MAXIM DL, AIP4WIN v2, and others) can perform photometry of a single star, an ensemble, or photometry over an entire image. These software programs use the mean value method for ensemble determination, but do not allow for the visualization of an individual photometric result. The author used the single star photometry function in both MAXIM DL5 and AIP4WIN in v2 for the ensemble examples presented in this article.

Most spreadsheet applications have been oriented towards photometric corrections (Warner 2006), system transformations (Warner 2006), time series light curve analysis of variable stars (Cook 1999), asteroids (Warner 2006), or exoplanets (Gary 2007). The spreadsheet-based linear regression methodology for multi-star ensemble photometry was described in concept by Buchheim (2007) and has been expanded using Microsoft Excel 2007[®] in this paper.

2. The linear regression method of ensemble photometry

The linear regression method for ensemble photometry is an algebraic and graphical presentation in which instrumental magnitude and Johnson V magnitude pairs for all measure comparison stars are linearly regressed and plotted. The result is a straight line and a linear regression equation that relates Johnson V magnitude to instrumental magnitude with minimized residual error (see Figure 1). This equation takes the form of

$$Y_N = a + B \times X_N \quad (1)$$

where (Y_N) is the calculated Johnson V magnitude of comparison star N, (a) is a constant offset, (B) is the slope of the linear regression solution, and (X_N) is instrumental magnitude of comparison N. Excel or other spreadsheet programs can readily derive and graph the linear regression equation of the trend line for all Johnson V and instrumental magnitude pairs.

The coefficient of determination, or R^2 , represents the statistical measure of how well the linear regression line represents the real data points. An R^2 value equal to 1 indicates that the regression line perfectly fits the observed data. With comparison star variation about the mean of the linear regression, R^2 is usually slightly less than 1, with the average distance from the line inversely related to R^2 . R^2 usually increases with increased number of comparison stars and increasing image SNR.

The estimated magnitude error from the linear regression method is the mean of the differences between the calculated values from the linear regression and true Johnson V magnitudes for all of the measured comparison stars. Poisson photon noise error, which is caused by statistical photon distribution over a given time interval, is another source of error. Poisson photon noise error (for one sigma error) is approximated by Equation 2 (Howell 2000; Berry and Burnell 2005):

$$\text{Poisson noise error} = 1.0857 / \text{SNR} \quad (2)$$

The linear regression error is combined in quadrature with the Poisson photon noise error to arrive at a final standard error estimate. This final total error is given by Equation 3:

$$\text{Final total error} = \text{Square root} (\text{Linear regression error}^2 + \text{Poisson noise error}^2) \quad (3)$$

Specifics about the linear regression ensemble method and error calculation are explained in the V723 Cas spreadsheet example given below.

3. Spreadsheet ensemble example for V723 Cas

An eight-star photometry ensemble spreadsheet (Figure 3) was created for V723 Cas from a single 180-second Johnson V filtered exposure taken with a remote internet based 24-inch (0.61-m) $f/10$ Cassegrain. This spreadsheet was constructed with Microsoft Office EXCEL 2007® by using the following steps. When entering text in the steps below, enter the text between the quotation marks only, not including the quotation marks. Quotation marks may also indicate an action, a keystroke, or a computed result. In specific cells, all text is center-justified and all numbers and calculated results are right justified.

1. Please view Figure 2 and replicate this skeleton spreadsheet.
2. Format the empty cell J15 by right clicking on this cell, selecting “Format cell” and selecting “Perimeter highlighting” and selecting the lightest weight line and then hitting <ENTER>.
3. Select cell J15, right mouse click to “Copy” it and then “Paste” it in all cells which are surrounded by a black perimeter as shown in Figure 2.
4. Type in the specific text from each cell in Figure 2 into your spreadsheet.
5. In cells C6 to C13, type “132, 142, 145, 147, 150, 154, 159, and 162,” respectively, hitting <ENTER> after each entry. These are the AAVSO chart comparison star V magnitudes to one decimal place for V723 Cas.
6. In cells D6 to D13, type “4.505, 5.550, 5.802, 6.045, 6.358, 6.732, 7.222 and 7.522,” hitting <ENTER> after each entry. These are the instrumental magnitudes from your calibrated CCD image and your photometry software program for each comparison star.
7. In cells E6 to E13, type “13.203, 14.226, 14.465, 14.726, 15.033, 15.390, 15.877 and 16.165,” hitting <ENTER> after each entry. These are the true Johnson V sequence magnitudes for each comparison star.
8. Highlight cells D6 through E13 (all 16 cells) and then go to the “Insert” column drop down menu and select a “Scatter Chart with Smooth Lines and Markers.”
9. In the newly created graph below the data cells, right mouse click on the line between the data points and select “Add a Trendline” under Chart.

10. Select the “Linear” regression type and select “Display Equation on chart” and “Display R-squared on chart.” Do not select “Set Intercept to 0.0” (all photometry software packages have their own specific zero magnitude offset). The resulting regression line equation in this newly created graph should read “ $y = 0.9838x + 8.7695$ ” and “ $R^2 = 0.9999$.”
11. In cell F6, type “ $=0.983*D6+8.769$ ” and hit <ENTER>. The result of “13.1974” is the calculated Johnson V magnitude for 132 comparison star.
12. Highlight cell F6 and then click the right mouse button to “Copy” this cell.
13. Highlight cells F7 to F13 and then right mouse click to “Paste” the regression equation in all these cells. The returned values in these cells are the calculated Johnson V magnitudes the remainder of the comparison stars.
14. In cell G6, type “ $=ABS(E6-F6)$ ” and then hit <ENTER>. The result of “0.0056” is the error between the calculated and true Johnson V magnitude for the 132 comparison star.
15. Highlight cell G6 and then click the right mouse button to “Copy” this cell.
16. Highlight cells G7 to G13 and then right mouse button to “Paste” this equation into all these destination cells. The resulting values are the errors between the calculated and true Johnson V magnitudes for the remainder of the comparison stars.
17. In cell G14, type “ $=AVERAGE(G6:G13)$ ” and hit <ENTER>. The result of “0.0072” is the average error between the calculated magnitudes and the true Johnson V magnitudes for each of the comparison stars.
18. In cell I6, type “6.428” and then hit <ENTER>. This is the instrumental magnitude of the V723 Cas from the calibrated CCD image and photometry reduction software.
19. In cell J6, type “ $=0.983*I6+8.769$ ” and hit <ENTER>. The result of “15.0877” is the calculated linear regression value for the differential V magnitude of V723 Cas.
20. In cell I9, type “199.66” and then hit <ENTER>. This is the SNR reading of V723 Cas from the calibrated CCD image and the photometry reduction software.

21. In cell J9, type “=1.0857/19” and then hit <ENTER>. The result of “0.0054” is the Poisson photon noise error (one sigma error in magnitude) of the V723 Cas SNR reading from the photometry reduction software.
22. In cell I12, type “=SQRT((J9^2+G14^2))” and then hit <ENTER>. The result of “0.0090” is the “Final V error.” The final V723 Cas magnitude estimate is 15.0877 V (cell J6) and the error is 0.0090 (cell I12).
23. Type in photometry software and annulus or radii information (I typed “MaxIm DL5 and 6, 16”) in cells I15 and J15.
24. Type in your specific details (I typed “V723 Cas, SSO 24”, V , 180 and 2454801.6952”) in cells F3, G3, H3, I3, and J3, hitting <ENTER> after each cell entry.
25. Save your file with a meaningful file name (for this example I called the Excel file “V723_Cas_01Dec2008.xls”) and put it in your Ensembles folder.
26. This ensemble spreadsheet can be copied and renamed with the “File,” and “Save As” options and later amended for any star in your observing program.

Please note that instrumental magnitudes by definition are negative, but most software packages express raw instrumental magnitudes as a positive number. These positive instrumental magnitudes are used in the spreadsheet.

4. The V723 Cas ensemble—results and methodology

The caption below Figure 3 explains the workings of the linear regression ensemble spreadsheet. Instrumental magnitude (X axis) and Johnson V (Y axis) pairs for all eight comparison stars are regressed and plotted, resulting in a very straight line with an X coefficient of 1.0373 and a very high R^2 (correlation coefficient) of 0.9999. The Johnson V magnitude estimate of 15.0877 with a total error of 0.0090 is an excellent photometric result. This is due to the high SNR (199.66) attained in the 180-second exposure taken by the 24-inch (0.61-m) $f/10$ Cassegrain.

5. Methodology

I typically use four to seven or eight comparison stars for my ensembles, ranging no more than two and a half magnitudes above and below the targeted variable’s estimated magnitude. Due to crowded star fields and/or the necessity

of picking a constant measuring aperture and outer (sky) annulus for all stars to be measured on a CCD image, one may not be able to use all of the comparison stars in a given sequence. Use as many comparison stars as possible. Using three comparison stars or less is not recommended. Three data points are an insufficient sample for this ensemble methodology and any two points define a straight line.

A good linear regression ensemble should yield a regression equation with an X coefficient of 0.985 to 1.015 and an R^2 value of 0.99 or greater. R^2 usually increases and comparison star data scatter usually decreases and with an increasing number of comparison stars and image SNR. Look for any outliers (0.1 magnitude or greater) that plot away from a straight line beyond average scatter. If measured SNR is high and no signs of comparison star contamination can be found, you may have discovered a potential variable star! If the brighter stars in a given sequence make the ensemble graph in a “hockey stick down” manner, pixel saturation may be the culprit.

Should a calculated Johnson *V* magnitude for one comparison star substantially fall off the linear regression line, that star should be considered suspect. Saturated pixels, hot or cold pixels, dust accumulation since the last flat was taken, cosmic ray hits in a comparison star image, or potential comparison star variability may be possible explanations for comparison star error. If all of the other comparison stars fall on a straight line, the one bad comparison star can be deleted with confidence. This procedure is explained below.

In the spreadsheet for V723 Cas shown in Figure 3, the comparison stars 4 and 5 (147 and 150) have the highest error. For illustrative purposes only, we will eliminate the comparison star 4 (147) and recalculate the ensemble result. Begin by highlighting cells B9 to G9 and hit <DELETE>. Highlight cells B10 to G14 and move them up one row vertically. A new equation is now in the regression graph, now reading “ $y = 0.9841 * x + 8.7663$ ” and the “ $R^2 = 1$ ” versus the old equation which read “ $y = 0.9838 * x + 8.7695$ ” and the “ $R^2 = 0.9999$.” In cell F6 type “ $=0.9841*16+8.7663$ ” and hit <ENTER>. “Copy” cell F6 and highlight cells F7 to F12 and right mouse click to “Paste” this new equation into these destination cells. All of the cells from F6 to F12 have new Johnson *V* magnitudes based on this new linear equation. Linear regression errors in cells G6 to G12 have also been updated. In cell J6, again type the equation “ $=0.9841*16+8.7663$ ” and hit <ENTER>. The recalculated ensemble magnitude for V723 Cas using seven comparison stars is now 15.0921 *V* (versus 15.0877 *V*) and the total error is now 0.0073 (versus 0.0090).

6. The 3C 66A ensemble—results

A nine-star photometric ensemble was created for the blazar 3C 66A from a single 180-second clear filtered exposure taken with a remote internet-based f/3.8 10-inch (0.25-m) astrograph. For brevity, the spreadsheet ensemble with all

of the photometric and sequence data values already entered into the appropriate cells is shown in Figure 4.

This linear regression ensemble is of good quality with an average X coefficient of 1.0373 and an R^2 value of 0.9994, especially when you consider this is an unfiltered image. The Johnson CV magnitude estimate of 14.820 with a total error of 0.031 is respectable. Comparison stars 8 (15.872 V) and 9 (16.520 V) have the highest error, due to decreasing SNR (17.808 and 10.988, respectively). These two comparison stars could be ignored for a better ensemble result if desired.

7. Conclusions

A linear regression based-method for ensemble differential photometry has been presented and described. By visualizing the distribution of the errors of the comparison stars in a sequence, confidence is increased in the variable star estimate. The linear regression methodology provides an objective method for ensemble magnitude estimates and to handle total error correctly. Good linear regression ensembles validate the accuracy of a variable star sequence, more so than simpler ensemble methods. A comparison star “outlier” that dramatically departs from the linear regression can be readily identified and investigated. If image quality sources of error are eliminated, the outlier may be a variable star. The linear regression ensemble method forces the observer to “look at the data,” and assess the quality of the sequence, resulting in a confident variable star magnitude estimate.

8. Acknowledgements

The author would like to recognize Arne Henden (2009) for his email suggestions concerning this methodology offered in late 2008 and Mike Simonsen and others for their comments during the preparation of this paper.

References

- Berry, R., and Burnell, J. 2005, *Handbook of Astronomical Image Processing*, Willmann-Bell, Richmond, VA, 278.
- Buchheim, R. K. 2007, *The Sky Is Your Laboratory*, Springer Praxis, Berlin, 107–112.
- Cook, L. L. 1999, AutoPlot—A Light Curve Plotting Excel Spreadsheet, <http://www.lewcook.com/autoplot.htm>.
- Crawford, T. R. 2006, Ensemble Photometry Options for AAVSO Amateur Observers Using AIP4WIN and Other Software, <http://homepage.mac.com/windwalker1/Public/Ensemble%20PhotometryV5.pdf>.
- Gary, B. L. 2007, Exoplanet Observing for Amateurs, http://brucegary.net/book_EOA/WebEOA/ExoplanetObservingAmateurs.html.
- Henden, A. A. 2009, Private communication.

Honeycutt, R. K. 1992, *Publ. Astron. Soc. Pacific*, **104**, 435.

Howell, S. B. 2000, *Handbook of CCD Astronomy*, Cambridge Univ. Press, Cambridge, 57.

Howell, S. B., and Everett, M. E. 2001, *Publ. Astron. Soc. Pacific*, **113**, 1428.

Richmond, M. 2006, Ensemble Software to Perform Inhomogeneous Ensemble Photometry, <http://spiff.rit.edu/ensemble>.

Warner, B. D. 2006, *A Practical Guide to Lightcurve Photometry and Analysis*, Springer, New York.

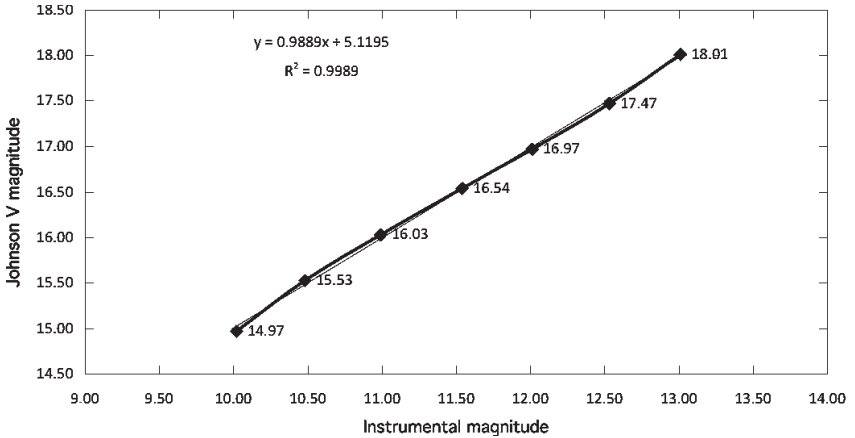


Figure 1. A sample graph showing the linear regression concept. X and Y pairs of Instrumental (X-axis) and Johnson V (Y-axis) magnitudes of all the comparison stars are put into a linear regression, yielding an equation which relates the pairs. In this particular example, Johnson V magnitude = 0.9889 × Instrumental Magnitude + 5.1195. The R² is 0.9985.

	A	B	C	D	E	F	G	H	I	J
1										
2						Variable	Telescope	Filter	Exp. In sec.	JD
3										
4										
5	Comp Star #	V m.	Instr. m.	V m.	Calc. V m.	Error V m.			Var. Inst. m.	Var. V m.
6	1									
7	2									
8	3								Var. SNR	Std. Error
9	4									
10	5									
11	6								Final V Err.	
12	7									
13	8									
14						Avg. V error			Software	Apertures
15										

Figure 2. The linear regression ensemble spreadsheet skeleton. Replicate this spreadsheet and follow the instructions in the text of Section 3 to recreate the spreadsheet and graph shown in Figure 3.

A	B	C	D	E	F	G	H	I	J	
1										
2					Variable	Telescope	Filter	Exp. In sec.	JD	
3					V723 Cas	SSO 24"	V	180	2454801.6952	
4										
5	Comp Star #	V m.	Instr. m.	V m.	Calc. V m.	Error V m.	Var. Inst. m.		Var. V m.	
6	1	132	4.505	13.203	13.1974	0.0056	6.428		15.0877	
7	2	142	5.550	14.226	14.2247	0.0014	Var. SNR		Std. Error	
8	3	145	5.802	14.465	14.4724	0.0074	199.66		0.0054	
9	4	147	6.045	14.726	14.7112	0.0148	Final V Err.			
10	5	150	6.358	15.033	15.0189	0.0141	0.0090			
11	6	154	6.732	15.390	15.3866	0.0034	Software		R1 and R2	
12	7	159	7.222	15.877	15.8682	0.0088	Maxim DL5		6, 16	
13	8	162	7.522	16.165	16.1631	0.0019				
14	Avg. V error					0.0072				
15										

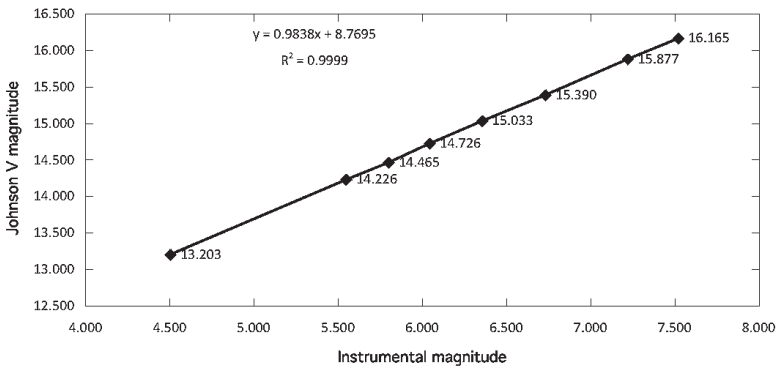


Figure 3. A linear regression ensemble spreadsheet for V723 Cas. Instrumental magnitudes (Column D data and plotted on the X-axis) and Johnson *V* magnitudes (Column E data and plotted on the Y-axis) are regressed for all of the measured comparison stars to yield a linear equation. The Johnson *V* magnitude estimate for V723 Cas = 0.9838×6.428 (the instrumental magnitude for V723 Cas given in cell I6) + $8.7595 = 15.0877$ (cell J6). Final total error is ± 0.0090 (cell I12). V723 Cas was not displayed on the graph in Figure 3 above, as only the comparison stars were regressed to establish the linear Instrumental to Johnson *V* magnitude relationship. V723 Cas would plot exactly on the linear regression line at $X = 6.428$ (instrumental magnitude) and $Y = 15.0877$ (the calculated Johnson *V* magnitude).

A	B	C	D	E	F	G	H	I	J
1									
2					Variable	Telescope	Filter	Exp. In sec.	JD
3					3C 66A	GRAS-005	V	180	2454806.65492
4									
5	Comp Star #	V m.	Inst. m.	V m.	Calc. V m.	Error V m.	Var. Inst. m.		Var. V m.
6	1	129	17.529	12.856	12.831	0.025	19.447		14.820
7	2	136	18.311	13.639	13.642	0.003	Var. SNR		Std. Error
8	4	142	18.861	14.182	14.212	0.030	46.112		0.235
9	5	144	19.074	14.424	14.433	0.009	Final V Error		
10	6	148	19.392	14.771	14.763	0.008	0.236		
11	7	153	19.915	15.308	15.306	0.002	Software		
12	8	159	20.505	15.872	15.918	0.046	AIP4WinV2		
13	9	165	21.042	16.520	16.475	0.045	Apertures		
14					Avg. V error		7, 10, 17		
15									

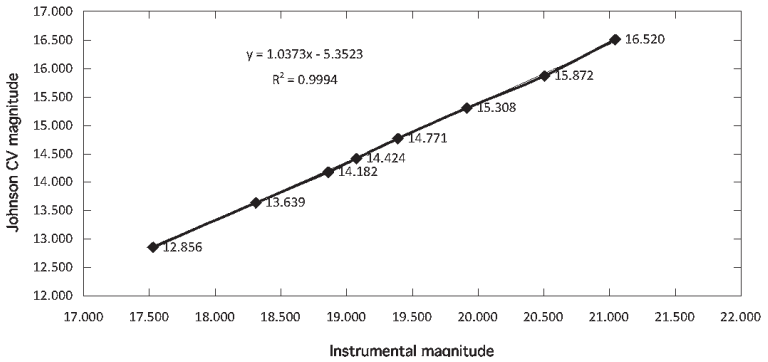


Figure 4. A linear regression ensemble spreadsheet for 3C 66A. The Johnson CV magnitude estimate for 3C 66A = 1.0373×19.447 (the instrumental magnitude for 3C 66A given in cell I6) $- 5.3523 = 14.820$ (cell J6). Final total error is ± 0.031 (cell I12). 3C 66A was not displayed on the graph in Figure 4 for reasons previously explained. 3C 66A would plot exactly on the linear regression line above at X = 19.447 (instrumental magnitude) and Y = 14.820 (the calculated Johnson CV magnitude).

Observing Exoplanet Transits With Digital SLR Cameras

Colin Littlefield

*Department of Physics, University of Notre Dame, Notre Dame, IN 46556;
clittlef@nd.edu*

Received April 6, 1020; revised June 4, 2010, accepted June 4, 2010

Abstract Using a digital single lens reflex (DSLR) camera, I observed a transit of exoplanet HD 189733 in order to determine the feasibility of using these types of cameras for high-precision photometry. The results were scientifically useful, showing that even though the camera is not explicitly designed for scientific applications, it can nevertheless produce high-quality differential photometry.

1. Introduction

DSLR cameras have revolutionized amateur astroimaging, but they are not optimized for photometry and present a variety of obstacles for obtaining useful data. First, DSLRs generally have a maximum bit depth of just 12 bits, which increases the risk of quantization errors caused by having relatively few steps with which to represent the dynamic range of an image. These errors can prevent the detection of subtle variations in the flux of a star. Second, the sensors in these cameras are overlaid with a matrix of color filters. This is particularly problematic because even though DSLRs have sensors with millions of pixels, only a fraction of those pixels will be covered by a particular color filter. In most cameras, half of the sensor's pixels are overlaid with green filters, one quarter with red filters, and the remaining quarter with blue filters. Thus, there are non-negligible gaps between pixels of a given color, which can create spurious features in light curves as star images drift over different-colored pixels. Third, DSLRs have low quantum efficiency, making them ill-suited for faint objects, and anti-blooming sensors, which can compromise the linearity of the camera's response.

This paper assesses the photometric capabilities of DSLRs by presenting the results of an observation of an exoplanet transit with a DSLR. I first verify that my DSLR's response curve is sufficiently linear for photometry before I describe the procedures that I used to successfully observe an exoplanet transit.

2. Overcoming DSLR limitations

As serious as the aforementioned limitations are, they do not prevent DSLRs from realizing a high level of photometric precision. The camera must be set to record images in its RAW mode, which, as its name implies, saves the raw image data without applying any form of processing. Consequently, it preserves the full 12-bit data from each pixel without compromising the data's photometric quality.

To lessen quantization error, the camera's gain can be decreased by increasing the ISO setting, which reduces the dynamic range and, therefore, the number of electrons which correspond to a single analog-to-digital unit (ADU). Meanwhile, the deleterious effects of the color filter matrix can be largely overcome by defocusing the image so that each star image covers hundreds of pixels. As an added benefit, defocusing the image allows for longer exposure times without the risk of saturation.

3. Linearity

One of the greatest photometric strengths of CCD cameras is their linear response to light, without which a camera would be nearly useless for photometry. Thus, characterizing a DSLR's response curve is of the utmost importance for photometry, a task which can be easily accomplished in an indoor setting. I tested the linearity of my Canon EOS 20Da DSLR by pointing it at an unvarying, indoor light source and taking a series of images, changing only the exposure time of each image. The camera was set to record the images using its 12-bit RAW mode, and to reduce the risk of quantization error inherent to 12-bit cameras, I used a relatively high ISO value of 1600. According to the analysis of planetary scientist and imaging expert Roger Clark, the ISO setting which best corresponds to the 20Da's unity gain—the ISO setting at which one electron is converted into one ADU—is ISO 1600 (Clark 2010; Clark finds that unity gain for the 20Da would occur at ISO 1200, but this setting is not available on the 20Da. Instead, I selected the next-highest setting, ISO 1600). Increasing the camera's ISO setting beyond unity gain merely decreases dynamic range without increasing the camera's ability to record a fainter signal.

The test data were analyzed in Iris, a free-but-powerful program developed by Christian Buil (2008) for processing astronomical images. Iris contains many useful features for processing DSLR data, including the ability to extract each of the four color channels—two green, one red, and one blue—from a RAW image. I split each image into its channels and measured the average intensity value of the same region in each image. A plot of average intensity against exposure time, which is reproduced in Figure 1, showed a linear response up to nearly 4,000 ADUs (the maximum value is 4,096 ADUs). These findings imply that the sensor's linearity is sufficient to provide useful photometry at ISO 1600 as long as the maximum ADU count is kept below approximately 4,000.

4. Transit of exoplanet HD 189733b

On September 19, 2009, exoplanet HD 189733b transited its star. With a V -magnitude of 7.67, a transit depth of 0.028 magnitude, and a number of suitable reference stars, HD 198733 is an ideal test object for detecting exoplanet transits. I detected and measured this transit of HD 189733b with the 20Da DSLR and a

polar-aligned Celestron CPC 800 telescope, an eight-inch Schmidt-Cassegrain. I used a piggybacked guidescope for autoguiding. The telescope was also heavily defocused, so that each star image was approximately 35 pixels in diameter. I obtained one hundred, ninety-second exposures at ISO 1600 of the transit before dew and fog forced an early shutdown.

I used Iris for reduction, image alignment, and photometry. I applied flat fields and dark frames to the images before splitting them into their red, green, and blue components. I then performed aperture photometry on each channel, using four nearby bright stars as references. To decrease noise, I averaged the two green channels. Additionally, an outlier identification algorithm rejected individual data points if they varied too far from the median value of nearby data points. This caused two green data points, one blue data point, and ten red data points to be removed from analysis.

Light curves from the green, red, and blue channels are shown in Figures 2, 3, and 4, respectively. To create these light curves and to perform a chi-square analysis of the data, I used a spreadsheet created by Bruce Gary (2010b), a retired professional astronomer who operates the Amateur Exoplanet Archive (AXA). A detailed description of the light curve fitting routine employed in Gary's spreadsheet (NASA 2009) can be found at:

<http://nsted.ipac.caltech.edu/NStED/docs/datasethelp/AXA/html>

Table 1 compares the observed data for each channel with accepted values found on the AXA. The green and blue channels showed comparable timing anomalies, but the red channel, which had the lowest signal-to-noise ratio, did not.

Depth is consistent in each band, but the measured length of the transit in the green band is longer than it is in the blue and red channels. Also, while the timing anomalies of the blue and green channels suggest that the transit was late, the red channel timing anomaly indicates that it came early. These differences between the three channels are probably attributable to systematic errors caused by image rotation across an imperfect flat field and differences in color between HD 189733 and the reference stars. Because there are relatively little out-of-transit data to provide a baseline, it is difficult to determine the effect of these systematic errors with a high degree of confidence.

5. Discussion

Defocusing and using a high ISO setting—that is, a low gain—were probably the two most important factors in the high quality of the photometry. Photometry of star images spread across hundreds of pixels is unlikely to be substantially impacted by image drift and changes in stars' point spread functions, even with measurable gaps between pixels, and the high ISO setting assures that quantization errors should be relatively minimal.

The transit light curve for the green channel showed the highest signal-to-noise ratio. The red channel had the worst signal-to-noise ratio, although it was still useable. This is not surprising, as most off-the-shelf DSLRs contain built-in infrared blocking filters to improve color balance for daylight photography. These filters also curtail the red response in DSLRs, and the 20Da's red sensitivity plummets after the hydrogen-alpha wavelength of 656 nm. In addition, since a RAW image contains two distinct green channels, both green channels can be averaged together to reduce noise. The relatively low scatter in the light curve of the combined green channels demonstrates that for moderately bright stars, very high-precision photometry is feasible with a DSLR camera. Even the red and blue channels, while noisier than the green channels, were still quite useable.

Much of the observed scatter in the light curves is likely attributable to electronic noise. Since DSLRs have peak sensitivities in the green part of the spectrum, the signal-to-noise ratios of the blue and red channels will tend to be worse than that of the green channel. Additionally, an examination of the 20Da's dark frames from the evening showed that the blue and red channels had standard deviations of 19.5 ADUs and 17.5 ADUs, respectively, whereas the corresponding figure for the averaged green channel was just 13.5 ADUs. Clearly, the green data are less noisy than the data from the other channels. Since sensors in DSLRs are not cooled, they will perform better on cooler nights than on warm ones.

6. Conclusion

Other people have demonstrated that DSLRs can provide precision, cost-effective photometry. For example, Buil (2009) has detected exoplanet transits with a DSLR, as have AXA contributors Nicolaj Haarup (2009) and Gregor Srdoc (Gary 2010a). In addition, DSLRs can provide very accurate photometry of bright variable stars with only a standard camera lens and tripod, and many AAVSO observers have obtained excellent DSLR photometry of the ongoing eclipse of Epsilon Aurigae. DSLRs offer wider fields of view than CCD cameras of comparable cost and can be run without either a computer or an external power supply. Although they have lower quantum efficiencies than CCD cameras and lack cooling, internal guiding, and true photometric color filters, they are eminently capable of the precision necessary to observe exoplanet transits.

Finally, I originally submitted photometry of this particular transit to the AXA within days of the event. However, I subsequently reprocessed the data with different photometric apertures, which resulted in better photometry. Consequently, the data presented here are slightly different from the earlier version that I sent to the AXA.

7. Acknowledgements

I wish to express my gratitude to the Physics Department of the University of Notre Dame, which provided some of the equipment necessary to perform the observations described in this paper. In particular, Professors Peter Garnavich and Terrence Rettig provided invaluable guidance. Lastly, the resources made available by Bruce Gary through the AXA greatly facilitated these observations and the subsequent analysis.

References

- Buil, C. 2008, Iris image processing software, <http://astrosurf.com/buil/us/iris/iris.htm>
- Buil, C. 2009, "Extrasolar Planet Observations by Radial Velocity Method," <http://astrosurf.com/buil/extrasolar/obs.htm>
- Clark, R. 2010, "Digital Camera Sensor Performance Summary," <http://www.clarkvision.com/imagedetail/digital.sensor.performance.summary/>
- Gary, B. 2010a, "Aperture versus Technique," http://brucegary.net/AXA/x.htm#Aperture_versus_Technique
- Gary, B. 2010b, "Light Curve Creation Spreadsheet," http://brucegary.net/book_EOA/xls.htm
- Haarup, N. 2009, "Exo Planets," <http://starworks.dk/exo.php>
- NASA/IPAC/NEExSci 2009, "Star and Exoplanet Database, Summary Details for Amateur Light Curves," <http://nsted.ipac.caltech.edu/NStED/docs/datasethelp/AXA.html>
- Poddany, S., Brat, L., and Pejcha, O. 2010, *New Astron.*, **15**, 297.

Table 1. HD 189733 transit parameters derived from blue, green, and red channels.

	<i>Depth (mmag)</i>	<i>Length (hrs)</i>	<i>Timing Anomaly (min)</i>
Blue Channel	28.5 ± 1.0	1.71 ± 0.05	3.0 ± 1.6
Green Channel	28.5 ± 0.9	1.79 ± 0.04	4.6 ± 1.3
Red Channel	28.8 ± 1.2	1.67 ± 0.05	-3.2 ± 1.5
Accepted Values	29.0 ± 0.4	1.70 ± 0.03	—

A chi-square analysis of the data was performed using Bruce Gary's Light Curve Creation Spreadsheet (Gary 2010b). The timing anomaly estimates assume an orbital period of 2.2185733 days and a transit epoch of HJD 2453988.80336. Both figures were obtained from the Exoplanet Transit Database of the Czech Astronomical Society (Poddany et al.; <http://var2.astro.cz/ETD/index.php>).

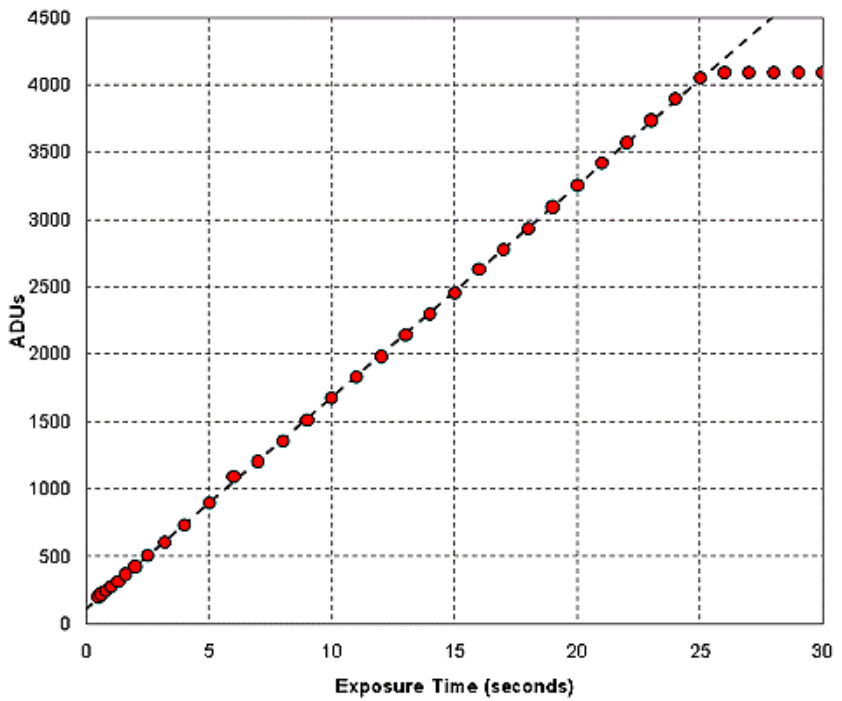


Figure 1. Linearity of the Canon 20Da. I tested the linearity of the Canon 20Da by pointing it at a constant light source and increasing exposure time in successive images. This graph plots average intensity of the same region in each image as a function of exposure time. The relationship between intensity and exposure time is linear to approximately 4,000 ADUs at ISO 1600, which is very close to the limit of 4,096 ADUs of the 12-bit camera.

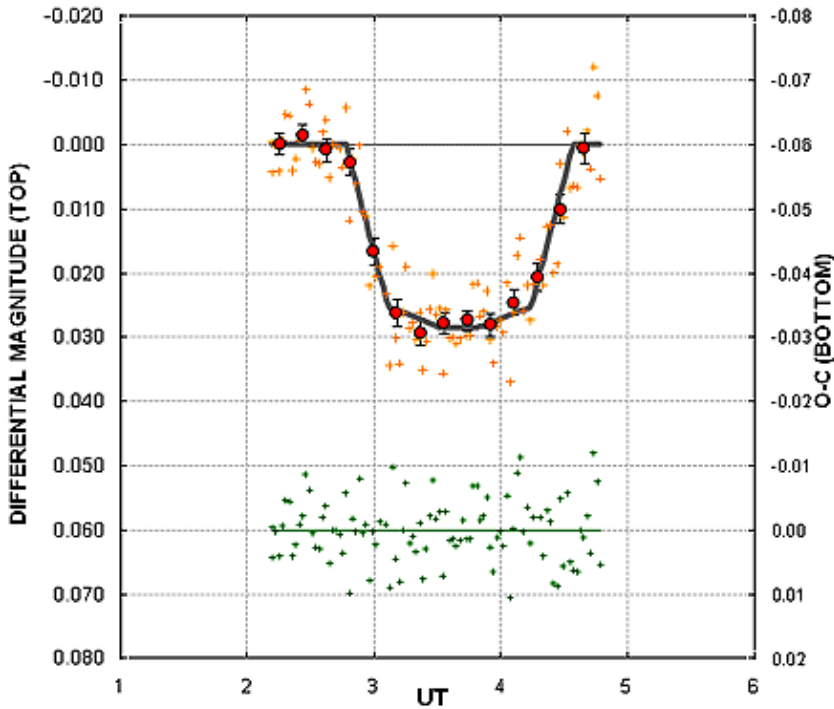


Figure 2. HD 189733b Transit, DSLR Green Channel. I measured the flux of HD 189733 and compared it to the sum of the fluxes of four nearby reference stars to produce this light curve of the differential magnitude of the transit of HD 189733b. The small crosses represent individual images, which were 90 seconds long at ISO 1600 with the telescope significantly defocused. Larger circles with error bars denote five-image, non-overlapping averages, and the plot below the light curve shows the residuals from the transit model. Finally, systematic errors, such as air mass curvature caused by differences in star colors, have been removed. All three light curves were created with Bruce Gary's Light Curve Creation Spreadsheet, version 9908 (Gary 2010b).

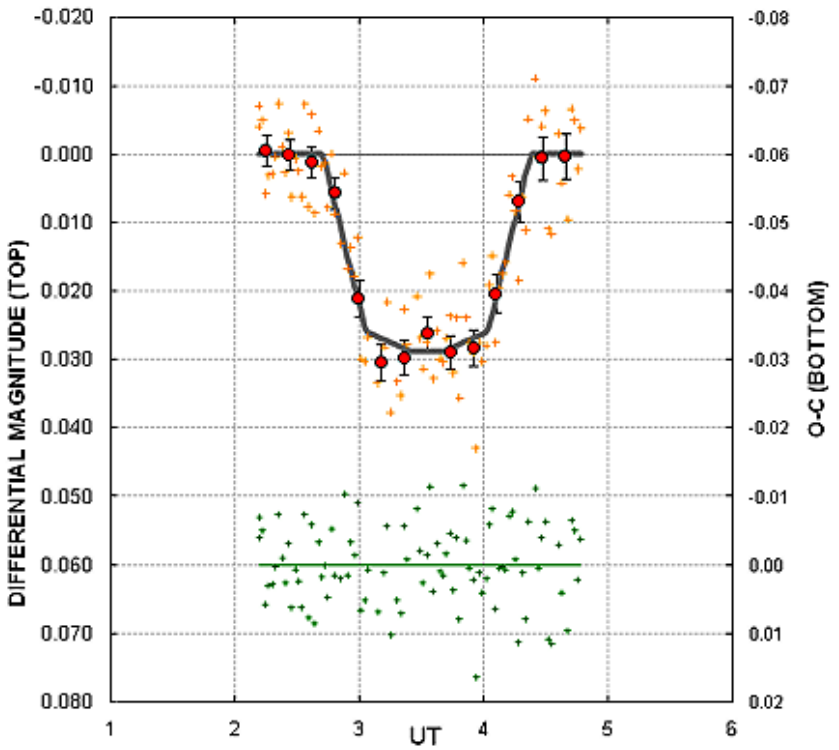


Figure 3. HD 189733b Transit, DSLR Red Channel. Individual images are 90 seconds long, and the bins combine five non-overlapping images. Residuals are shown beneath the light curve.

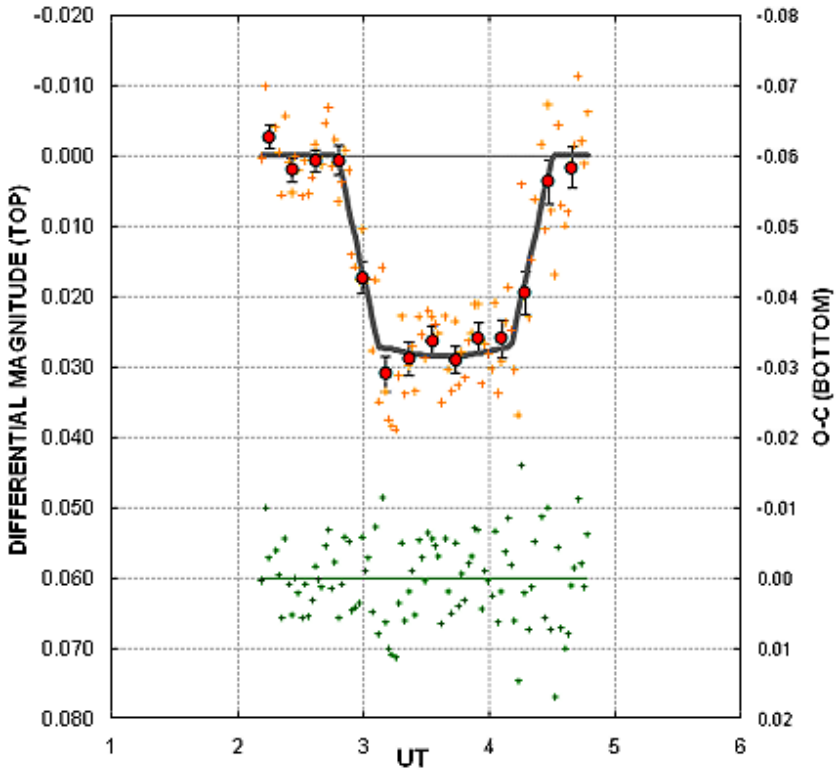


Figure 4. HD 189733b Transit, DSLR Blue Channel. Individual images are 90 seconds long, and the bins combine five non-overlapping images. Residuals are shown beneath the light curve.

A Simple, Portable Apparatus to Measure Night Sky Brightness at Various Zenith Angles

Jennifer Birriel

James Kevin Adkins

Department of Mathematics, Computer Science, and Physics, Morehead State University, Morehead, KY 43051; j.birriel@morehead-st.edu

Received May 4, 2010; revised May 17, 2010; accepted July 17, 2010

Abstract We describe a simple apparatus for making measurements of night sky brightness as a function of zenith and azimuth using “off-the-shelf” equipment: a Unihedron Sky Quality Meter with Lens, a protractor with plumb-line, a tripod, and a hand-held compass. Compared to a photoelectric or CCD photometric system, this apparatus is simple to set up and use and does not require complex data reduction procedures. Thus, this apparatus makes measurements of night sky brightness as a function of zenith and azimuthal angles quite amenable to students.

1. Introduction

The natural brightness of the night sky originates predominantly from the integrated light of faint stars within our own galaxy, airglow, and zodiacal light (e.g. Leinert *et al.* 1998). Other sources include starlight scattered by interstellar dust which produces a diffuse glow along the galactic plane and a weak contribution from extragalactic light (Leinert and Mattila 1998). Airglow, the visible emission produced when atmospheric atoms and molecules (e.g. O, Na, O₂) previously excited by ultraviolet solar radiation during the day decay, is the dominant source of night sky brightness (Benn and Ellision 2010). Airglow increases with zenith angle due to the thicker air column along the line of sight. Zodiacal light, sunlight scattered by interplanetary dust, is the second largest contributor to night sky brightness and increases towards the ecliptic. The third major contribution to night sky brightness results from the integrated light of stars not individually accounted for; this is strongest toward the galactic equator and decreases toward the galactic poles (e.g. Leinert and Mattila 1998).

Garstang (1989) developed a detailed model for the natural sky background in the context of a larger study to predict the brightness of the night sky caused by a city. At zenith, the faint star and galaxy light contributes about 40 percent to the total night sky brightness while airglow contributes the remaining 60 percent (Garstang 1989); Garstang’s model is consistent with earlier photometric observations (e.g. Pike 1976, Berry 1976): natural night sky brightness at sea level increases by some 0.5 mag/arcsec² from zenith to 85° zenith angle primarily due to increased airglow. Measurements of actual night sky brightness as a function of zenith angle can be compared to the Gargstang model of natural night sky

brightness. Such measurements can serve as a useful quantitative measure of light pollution at a given location.

A number of methods can be used to measure the brightness of the night sky as a function of both zenith and azimuth. Upgren (1991) used multiple, naked eye observations of bright stars to determine changes in night sky brightness near the horizon over a period of 14 years. This method has the distinct advantage of being simple and cheap but such measurements will also be somewhat subjective, varying from observer to observer. Portable, wide-field CCD systems have been successfully employed (e.g. Cinzano and Falchi 2003; Duriscoe *et al.* 2007) to record mosaic images of night sky brightness from zenith to horizon in all azimuth angles. Such systems have the advantages of being fast, quantitative, and repeatable, however, neither the data reduction process nor the cost (roughly \$15,000 U.S.) is trivial. More recently, several authors have experimented with DSLR systems equipped with a “fish-eye” lens (Zotti 2007). Such systems are relatively inexpensive, roughly \$1,000 for a modest DSLR camera, and can obtain an image of nearly the whole sky in a single image. These systems can also give calibrated data with a high degree of accuracy, however, the data reduction and analysis of such images is still rather complex.

The advent of inexpensive, hand-held sky quality light meters presents another opportunity to “map” night sky brightness as a function of zenith angle and azimuth. The Unihedron Sky Quality Meter with lens, hereafter the SQM-L, was originally designed to take measurements at zenith. However, the fairly narrow observation cone of this device allows one to measure sky brightness at angles well below zenith. The SQM-L allows users to make simple, reliable measurements of the night sky in the visible region of the spectrum in only a few seconds. It has already been incorporated into the Globe-at-Night observing campaign in America (Walker 2010). We report on our use of the SQM-L as part of a simple, inexpensive apparatus to measure night sky brightness as a function of zenith angle and altitude. This apparatus improves and simplifies night sky brightness measurements using the SQM-L in two respects: 1) previously this device was designed for zenith only measurements; our setup allows observers to make measurements at various zenith angles, and 2) mounting the device on a tripod ensures that the device is always pointed in the same direction, increasing the accuracy of any individual measurement as compared to simply holding the device by hand.

2. Apparatus and measurement method

The core of our apparatus is the Unihedron SQM-L. The SQM-L is nearly identical to its predecessor the SQM; both devices are equipped with the same light sensor (the TAOS TSL237S) and the same infrared blocking filter (a HOYA CM-500). Each device is a small ($3.6 \times 2.6 \times 1.1$ in.), portable light meter powered by a 9-volt battery. Both the SQM and the SQM-L are equipped with

an infrared blocking filter and measure only visible light (from red to blue). Both devices measure the ambient temperature and all photometric measurements are automatically corrected for temperature effects. Measurement with either device requires a few seconds in heavily light polluted areas to no more than 80 seconds under the darkest skies. Each individual SQM/SQM-L device is calibrated using a NIST-traceable light meter. The Unihedron Corporation reports the precision of ± 0.10 mag/arcsec² for measurements made with a single device; this precision is consistent with field observations (e.g. Craine *et al.* 2008; Smith *et al.* 2008). For a full report of the performance characteristics of the SQM, see Cinzano 2005.

The main difference between the SQM and SQM-L is the field of view. The SQM has a full-cone width of 84 degrees while the SQM-L is fitted with a lens which reduces the full-cone width to 20 degrees. The addition of the lens means that zenith measurements taken with the SQM-L are not affected by lights or shading on the horizon. The smaller field of view also makes the SQM-L useful for making measurements of sky brightness at various zenith angles, whereas the SQM is really only useful for zenith measurements.

Our apparatus is shown in Figure 1. The SQM-L is mounted on the shoe pad of a tripod using a wide rubber band. One must take care to avoid placing the rubber band on or near the sensor lens. Velcro tape is used to mount a protractor (equipped with a plumb-line) along the side of the SQM-L; this allows us to measure zenith angles. A compass is used to determine the direction in which the device points. The total cost of the device is under \$250 US; the most expensive components of the device are the SQM-L (\$135 US) and a sturdy tripod (\$100 U.S.).

Before proceeding to take measurements, it is necessary confirm that the night sky is clear. This can be achieved by examining both infrared and water vapor satellite images; such images are available from the National Oceanic and Atmospheric Administration website (NASA 2010) at:

http://www.weather.gov/sat_tab.php?image=ir.

In infrared satellite images, high altitude clouds appear bright. However, low altitude clouds and fog are similar in temperature to the ground and hence infrared images will not be useful for identifying these. Low altitude clouds and fog can be identified using a new product, the GEOS 4-km shortwave albedo IR4 cloud images, available at:

http://rammb.cira.colostate.edu/ramsd/online/goes-west_goes-east.asp.

Measurements were taken at two different sites on July 15, 2010; on this date the Moon age was 3.0 days. Measurements were taken after the Moon set. Measurements were taken at zenith angle zero and then at zenith angles of 0°, 20°, 40°, 60°, and 80°. At each particular zenith angle, five individual measurements were taken and then averaged. A compass was used to establish the cardinal directions for each set of azimuthal data. Here, we note that one must take care to correct for the magnetic “declination” of a given observation site; magnetic “declination” is the angle between geographic north pole and the magnetic pole

and varies with latitude. The magnetic declination of a site can be quite large and this should be determined prior to making measurements in the field by consulting a good topographical map or consulting a magnetic “declination” calculator (e.g. see the National Oceanic and Atmospheric Administration’s Geophysical Data Center www.ngdc.noaa.gov/geomagmodels/struts/calcDeclination).

All data were recorded by hand using a notebook, pen, and flashlight. However, it should be noted that the Unihedron Corporation does offer a SQM-L with USB connectivity (\$189.99 US). The “SQM-LU” allows for continual, connected measurements of sky brightness. It comes supplied with a USB cable and applications for reading data in Perl.

3. Results

Using a standard spreadsheet program, we plot our brightness measurements in magnitudes per square arcsecond as a function of zenith angle. Observations along each of the four major cardinal lines serve as a measure of azimuth. (Note that here we are measuring brightness in a fairly specific direction. If one wishes to document sky glow along the horizon due to distant cities, this can be achieved by closer spacing of each azimuth reading, about every 20 degrees or so; this would require the use of a mounted compass or a second protractor mounted horizontally on the SQM-L.) From a previous study (Birriel, Wheatley, and McMichael 2010) we identified two sites of interest for our study: Cave Run Lake near Morehead, Kentucky, which serves as our local “dark-sky” site with a zenith SQM-L reading of 21.7 mag/arcsec², and a location at the edge of the Morehead State University Campus near Eagle Lake with a SQM-L zenith reading of 19.3 mag/arcsec².

In both cases, we compare our readings to the Garstang (1989) model of the dark sky site for Mount Graham Junipero Serra Peak in Boulder, Colorado; this model is for a moonless night at solar minimum in the photometric *V* band. Cinzano (2005) found a slight mismatch between the SQM-L spectral response and the Johnson *V* band. He determined that SQM readings can be converted to *V* band readings via the simple expression $V = \text{SQM} - 0.17$. We have made this adjustment to all our measured values.

The Cave Run Lake and Morehead sites are in Rowan County, Kentucky, nestled in the foothills of the central Appalachian Mountains. The region is characterized by largely forested, hilly, and highly dissected terrain with elevation ranging between 208 m and 404 m. The Cave Run Lake site is about 20 kilometers from the town of Morehead and is effectively shielded from much of the light from town. Readings taken with our device at the Cave Run Lake site are shown in Figure 2. One feature that immediately stands out on this plot are the small differences (± 0.1 to ± 0.2 mag/arcsec²) between individual azimuth measurements; these results are well within the expected precision of the SQM-L. The overall dependence of sky brightness on zenith angle is close to what is predicted by

the Garstang model, although the curves are systematically shifted upward with respect to a true dark-sky site at solar minimum. Given that our measurements were taken shortly after solar minimum (NASA 2010), this most likely arises simply from elevated light levels due to artificial light sources. This site does exhibit a systematic brightening near the horizon in the southerly directions due to the presence of a light from the nearby dam reflecting off the lake. In the opposite direction, the decline in brightness near the horizon results from the presence of hills towards the north.

The Eagle Lake site is located in the town of Morehead. It is located at the northern edge of the Morehead State University campus at the crest of a hill. The campus and town extend to the south while north lies the Daniel Boone National Forest. As seen in Figure 3, the brightness of the sky increases dramatically looking toward the southerly direction of town and campus. In fact, the presence of artificial lighting is clearly evidenced by the rapid increase in brightness.

4. Summary and future

The results obtained with our apparatus show that one can document night sky brightness as a function of both zenith angle and azimuth without expensive equipment. Measurements can be obtained quickly and results easily analyzed. This makes the apparatus a particularly useful tool for experimental projects at both the high school and college levels. We envision employing this apparatus as a laboratory tool for undergraduate astronomy and physics courses. In addition, measurements from such a device should prove valuable for science fair projects and college student research projects on light pollution. We also plan to use this device to evaluate Walker's law (Walker 1973), taking measurements of sky brightness at a zenith angle of 45 degrees at various distances from nearby large cities.

Acknowledgement

The authors would like to thank the anonymous referee for the many helpful suggestions that helped improve the clarity and quality of this paper.

References

- Benn, C. R., and Ellison, S. L. 2010, "La Palma Night sky Brightness", <http://www.ing.iac.es/Astronomy/observing/conditions/skybr/skybr.html#top>, accessed, 7/15/2010.
- Berry, R. 1976, *J. Roy. Astron. Soc. Canada*, **70**, 97.
- Birriel, J., Wheatley, J., and McMichael, C. 2010, *J. Amer. Assoc. Var. Star Obs.*, **38**, 132.
- Cinzano, P. 2005, *ISTIL Internal Report, No. 9, Vol. 1.4*, www.unihedron.com/projects/darksky/, accessed July 15, 2010.

- Cinzano, P., and Falchi, F. 2003, *Mem. Soc. Astron. Ital.*, **74**, 458.
- Craine, E. M., Culver, R. B., Craine, J. C., and Tucker, R. A. 2008, in *The Society for Astronomical Sciences 27th Annual Symposium on Telescope Science*, held May 20–22, 2008, Big Bear Lake, CA, Soc. Astron. Sci., Rancho Cucamonga, CA, 157.
- Duriscoe, D. M., Luginbuhl, C. B., and Moore, C. A. 2007, *Publ. Astron. Soc. Pacific*, **119**, 192.
- Garstang, R. H. 1989, *Publ. Astron. Soc. Pacific*, **101**, 306.
- Leinert, Ch., et al. 1998, *Astron. Astrophys., Suppl. Ser.*, **127**, 1, 1.
- Leinert, Ch., and Mattila, K. 1998, in *Preserving The Astronomical Windows, Proceedings of Joint Discussion Number 5 of the 23rd General Assembly of the International Astronomical Union held in Kyoto, Japan 22–23 August 1997*, eds. S. Isobe and T. Hirayama, ASP Conf. Ser. 139, Astron. Soc. Pacific, San Francisco, 17.
- NASA 2010, Solar Physics Website, <http://solarscience.msfc.nasa.gov/predict.shtml>, accessed July 15, 2010.
- Pike, R. 1976, *J. Roy. Astron. Soc. Canada*, **70**, 116.
- Pike, R., and Berry, R. 1978, *Sky & Telescope*, **55**, 126.
- Smith, M. G., Warner, M., Orellana, D., Munizaga, D., Sanhueza, P., Bogglio, H., and Cartier, R. 2008, in *Preparing for the 2009 International Year of Astronomy: A Hands-On Symposium*, ASP Conf. Ser., 400, Astron. Soc. Pacific, San Francisco, 152.
- Ungren, A. R. 1991, in *Light Pollution, Radio Interference, and Space Debris*, ed. D. L. Crawford, ASP Conf. Ser., 17, Astron. Soc. Pacific, San Francisco, 79.
- Walker, C. E. 2010, *Bull. Amer. Astron. Soc.*, **42**, 409.
- Walker, M. F. 1973, *Publ. Astron. Soc. Pacific*, **85**, 508.
- Zotti, G. 2007, in *DarkSky: 7th European Symposium for the Protection of the Night Sky*, held Oct. 5–6, Bled, Slovenia, <http://www.darksky2007.si/2.html>



Figure 1a. Mounting the SQM-L on the tripod shoe pad can be done quite simply and quickly with the use of a thick rubber band.



Figure 1b. To measure zenith angles, we attached a simple protractor with plumb-line to the side of the SQM using adhesive Velcro tape.

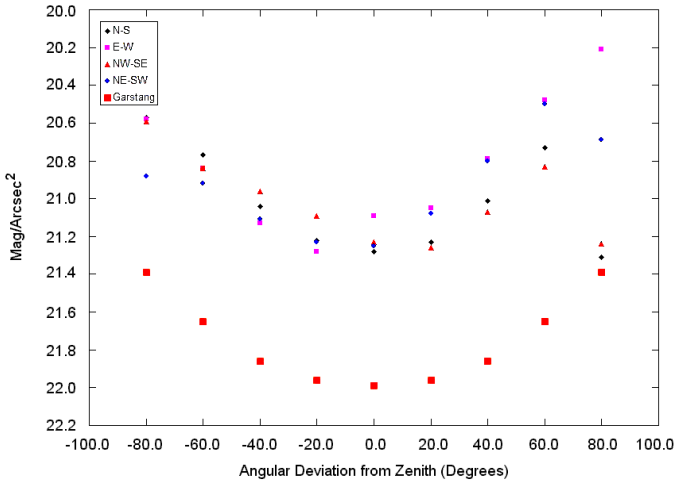


Figure 2a. A plot of night sky brightness in mag/arcsec² as a function of zenith angle and azimuth for the Cave Run Lake site. Zenith angles pointing North along the N-S line and East along the E-W line are positive. Zenith angles along the NE-SW line are positive when point NE and along the NW-SE line the angles are positive when pointing NW. The Garstang model for natural night sky brightness is also plotted. The ± 0.2 mag/arcsec² uncertainty in the SQM-L device is clearly visible in readings near zenith.

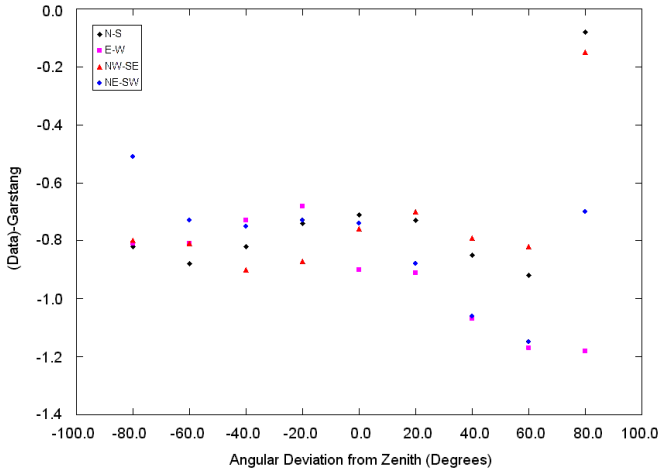


Figure 2b. The difference between the observed sky brightness (at Cave Run Lake) and the Garstang model. Note that sky brightness at this site is comparatively low, with an increase in brightness at zenith of less than one magnitude.

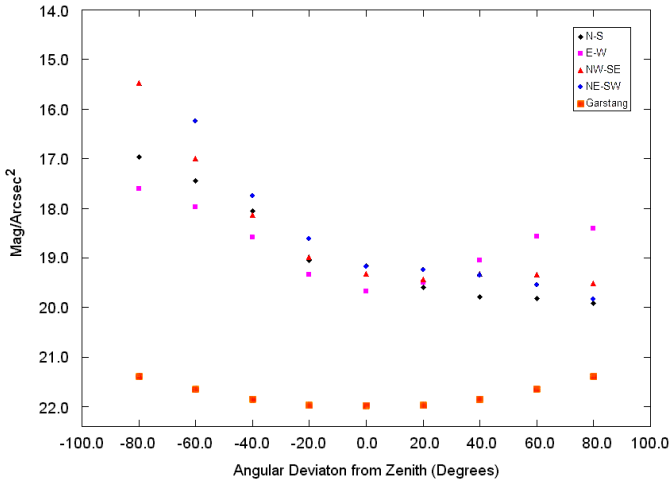


Figure 3a. A plot of night sky brightness in mag/arcsec² as a function of zenith angle and azimuth for the Eagle Lake site at the edge of the Morehead State University campus.

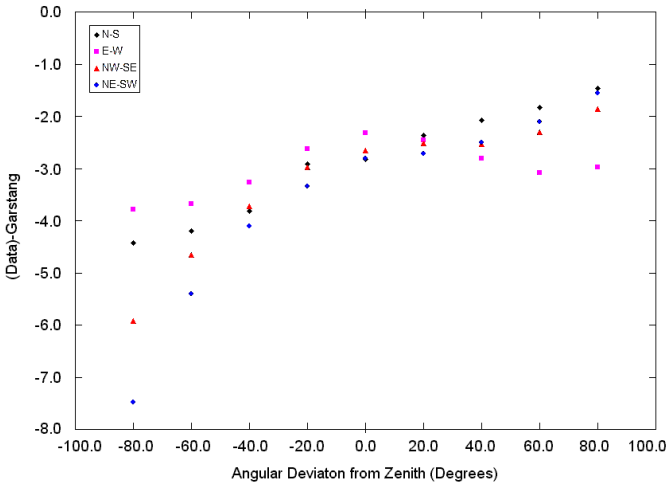


Figure 3b. The observed sky brightness (at Eagle Lake) minus the Garstang model. Notice that this site exhibits significant light pollution with an excess brightness of 3.0 mag/arcsec² at zenith and increasing excess brightness at off-zenith angles.

Abstracts of Papers and Posters Presented at the 99th Spring Meeting of the AAVSO, Held in Mendoza, Argentina, April 15–18, 2010

Introduction to Variable Star Astronomy

Sebastián Otero

Olazabal 3650-8 C, Buenos Aires, 1430, Argentina; varsao@hotmail.com

Abstract In this introduction we explain what a variable star is and what are its main characteristics. Variable star classification is described with images and light curves of each type, stressing that variability is—most of the time—an evolutionary stage in a star’s life. A general overview of the current status of this field of study and the always important role of the amateur astronomer—even in the automated surveys era—is presented. Finally, we take a first look at the visual observation method and give some exercises to be made during observing nights.

Current Hot Variable Star Topics

Arne A. Henden

AAVSO, 49 Bay State Road, Cambridge, MA 02138; arne@aavso.org

Abstract Transient events happen almost daily, many being novae, supernovae and other outbursting stars. In addition, several known variable stars are undergoing unusual events. This paper will highlight a number of these objects and show how you can observe them.

History of Variable Stars

Rafael Girola

Asociacion Civil EnDiAs, San Miguel, Prov. Buenos Aires, Argentina; rafaelgirola@yahoo.com.ar

Nestor Vinet

Asociacion Civil EnDiAs, San Miguel, Prov. Buenos Aires, Argentina; nestorvinet@yahoo.com.ar

Abstract Within the field of history of variable stars, we have focused on the history of Cepheid stars. Using graphics, we will describe historical evolutive behavior and its characteristics stressing on the Period Luminosity relation, and in consequence the importance of the research made by Miss Leavitt during the 20th century. We also will present an introduction to Fuzzy logic. For that

purpose, we will show examples of its application in different disciplines such as biology, industrial processes, and electronics. In this work we will leave open the possibility of applying this mathematical concept in the field of variable star classification, when the observer facing the traditional models meets the dilemma of decision.

Activities of the SEV/LIADA

Raúl Roberto Podestá

María Dolores Suárez de Podestá

B. Cono Sur-MZ-77 Casa 18, Formosa, 3600, Argentina; rrpodesta@hotmail.com

Abstract For the Ligo de Asronomia Iberoamericana (LIADA) 2009 was a busy year, and discussions were initiated for the creation of a Variable Star Section (la Sección de Estrellas Variables, SEV). In June 2009 SEV was formed, which is the “Variable Star Section, League of IberoAmerican Astronomy.” The growth was exponential, and observers from various countries began reporting their work. The SEV has produced a work program, developed it further, and is armed with a Web page, which shows all the observations reported. The courses on variable stars, through ON LINE, have had extraordinary success, thus fulfilling the SEV objectives for observers: dissemination of data, education, and technical and scientific training.

Mira Observations by José Brazilício

Alexandre Amorim

Antonia Domingos De Souza, 315, Florianópolis, 88047-585, Brazil; costeiral@yahoo.com

Abstract José Brazilício de Souza was musician, cosmography professor, and an amateur astronomer who lived in Florianópolis, Brazil. He made several visual observations: comets, solar, eclipses, planetary, and moon observations between 1882 and 1909. Among his data we found some Mira (o Cet) estimates. This paper shows his Mira records and a phased light curve using elements for 1881.

King Charles’ Star: A Multidisciplinary Approach to Dating Cassiopeiae A

Martin Lunn

martin.lunn@ymt.org.uk

Lila Rakoczy

rakoczy@hotmail.co.uk

Abstract Few astronomical phenomena have been as studied as the supernova known as Cassiopeiae A. Widely believed to have occurred in the latter half of the seventeenth century, it is also thought to have gone unrecorded. This paper will argue that Cas A did not go unobserved, but in fact was seen in Britain on May 29, 1630, and coincided with the birth of the future King Charles II of Great Britain. This “noon-day star” is an important feature of Stuart/Restoration propaganda, the significance of which has been widely acknowledged by historians and literary experts. The argument here, however, is that in addition the historical accounts provide credible evidence for a genuine astronomical event, the nature of which must be explained. Combining documentary analysis with an overview of the current scientific thinking on dating supernovae, the authors put forward their case for why Charles’ star should be recognized as a sighting of Cas A. Finally, it will be argued that a collaborative approach between the humanities and the sciences can be a valuable tool, not just in furthering our understanding of Cas A, but in the dating of supernovae in general.

Near-infrared Observations of Cepheid Variables in the Large Magellanic Cloud

Lucas Macri

5313 Riviera Court, College Station, TX 77845; macri.lucas@gmail.com

Abstract I present preliminary results of near-infrared observations of Cepheid variables in the Large Magellanic Cloud, obtained with the CPAPIR camera at the Cerro Tololo 1.5-m telescope.

The observations were carried out with two goals: (a) to better characterize the Cepheid Period-Luminosity (P-L) relation at near-infrared wavelengths, especially for periods below 10 days; (b) to determine if the P-L relations are linear or non-linear in these bandpasses.

Several analyses of OGLE-II observations of Cepheid variables in the Large Magellanic Cloud have detected a non-linearity or “break” in the slope of the optical (V and I) P-L relations at a period around 10 days. Theoretical models indicate the non-linearity may be due to changes in the interaction of the hydrogen ionization front and the stellar photosphere as a function of global stellar parameters, such as mass and metal abundance. Models predict that the non-linearity becomes most pronounced at abundances similar to that of the Large Magellanic Cloud.

In this talk, I will show representative light curves for a small subset of our nearly 1,200 Cepheid variables and I will present preliminary PL relations in the J and K bands as well as color-magnitude diagrams for Cepheid variables and field stars.

Minima of Some Eclipsing Binaries

Alexandre Amorim

Antonia Domingos De Souza, 315, Florianópolis, 88047-585, Brazil; costeiral@yahoo.com

Abstract This paper shows a list containing fourteen southern eclipsing binaries, not much observed, and sixty-two dates of minima. 394 visual observations were computed, considering that 86% of them were made by Alves and 14% by Amorim. The main goal is update the elements for each star, providing useful guide to future visual, photoelectric and CCD observations. All the dates were obtained by the bi-sectioned chords. The chosen binaries are: SY Ara, LU Ara, GW Car, SS Cen, BD Cen, T Cir, TT Cru, DT Lup, FK Lup, NP Pav, RV Tel, RR TrA, V Tuc, and RR Vel. Phased light curves of these binaries are available.

New Variable Stars in the Southern Cross

Victor Angel Buso

Entre Rios 2974, 2000 Rosario, Argentina

Abstract With a photographic survey, our program started in 1994 and gathering data from that time we discovered the variability of a star in the constellation Crux. This is the result of a digitalization program of photographs taken in Cristo Rey Observatory, started in 1994 and with CCD cameras. The data show that IRAS12521-6034 is a variable star. The survey has been continued by members of the Asociación Santafesina de Astronomía, and then we have found other stars suspected to be variables.

Didactics on Education in Astronomy

Sebastián Musso

Centro de Estudios Astronomicos de Mar del Plata, Mar del Plata, Prov. Buenos Aires, Argentina; sebastianmusso@hotmail.com

Abstract This work is not intended as a “how to,” guide or methodology for teaching astronomy. Rather, it is a compilation of experiences, a summary of those activities that have helped me in my task of popularizing science. In popularizing science, because I enjoy doing it so much, something special is transmitted that helps us reach those who try to spread the taste of the science we love.

Starting Research Projects at Buenaventura Suárez Observatory in San Luis Province (poster)

Eric González

Universidad de La Punta, San Luis, Argentina; ericgonzalez@ulp.edu.ar

Abstract The Buenaventura Suárez Observatory has several small telescopes acquired during the International Year of Astronomy (IYA2009) for public education. A brief description of the available equipment is presented, along with three research and public education programs to be developed starting on 2010.

New Equipment for Variable Star Research at the Instituto Copernico Observatory

Jaime García

Gutierrez Esq, Calle Jon Agrario, 5603 Rama Caida, Mendoza, Argentina; jgarcia@institutocopernico.org

Federico García

Calle 4 Nro. 642, Depto E E/126 Y 127, Berisso, 1923, Argentina; fgarcia@institutocopernico.org

Abstract New equipment was recently installed and is undergoing calibration at the Instituto Copernico's Observatory, in Rama Caéda, south of Mendoza. We will show briefly this equipment and the observatory's scientific and education goals.

Observational Techniques Workshop

Visual Observing Techniques

Sebastián Otero

Olazabal 3650-8 C, Buenos Aires, 1430, Argentina; varsao@hotmail.com

Abstract Obtaining high precision in visual observing takes more than just knowing the fractional method of brightness estimates. Different circumstances play an important—and even determining—role at the moment you make an estimate. This presentation lists several factors that need to be taken into account while making an observation: color of variable star and comparison stars, their brightnesses, sky background brightness, individual color sensitivity, right choice of the comparison stars and their position with respect to the variable are some of them. Different problems the observer may face with their respective possible solutions are also listed, along

with some advice to improve the observer's skills, supported by examples of the goals that can be achieved if you struggle to get the most out of your capabilities.

An Introduction to CCD Photometry of Variable Stars

Jaime García

*Gutierrez Esq, Calle Jon Agrario, 5603 Rama Caida, Mendoza, Argentina;
jgarcia@institutocopernico.org*

Abstract The aim of this presentation is introducing to the audience the use of the CCD camera for more than beautiful images, producing science with its own instruments. It details techniques for acquiring images in order to perform photometry on them.

Advanced CCD Observing Techniques

Arne A. Henden

AAVSO, 49 Bay State Road, Cambridge, MA 02138; arne@aavso.org

Abstract After you have learned the basics of using your CCD camera, you still need to learn the techniques necessary for quality photometry. This paper covers the basic essentials: choosing the correct aperture size, improving the precision of your measures, learning about signal/noise, defects like saturation, clouds and scintillation, beginning differential photometry, paying attention to the time of an observation, and transformation. Practical examples are given throughout.

Data Mining in Astronomy Workshop

An Introduction to Data Mining

Michael Koppelman

6019 Fairwood Drive, Minnetonka, MN 55345; michael@slackerastronomy.org

Abstract I will give a brief overview of what data mining is and the many data sources that are available to researchers. I will also show examples of data mining papers and discuss some of the techniques used in data mining research.

Tips to Succeed in Using the ASAS-3 Database

Sebastián Otero

Olazabal 3650-8 C, Buenos Aires, 1430, Argentina; varsao@hotmail.com

Abstract The ASAS-3 database—publicly available through the internet—allows us to obtain observations of millions of stars in the Southern hemisphere (up to Declination $+28^\circ$) between V-magnitude 6 and 14, but its use is not straightforward. There are things you need to know to avoid jumping to wrong conclusions about the data. There are things you need to take into account to choose which of the data in the website are best and which need to be avoided. Some tips to get the most out of this amazing database are given in this talk.

Mining for Rare Variable Stars in Photometric Databases

Doug Welch

100 Melville Street, Dundas, ON L9H 2A3, Canada

Abstract In this talk, I will provide examples of how to hunt rare but astrophysically-interesting stars such as Cepheids in eclipsing systems, double-mode Cepheids, and R CrB stars in the MACHO and NSVS databases. Some surveys are “mined out” for such systems now, but not all. Existing exoplanet surveys and future photometric database releases will ensure a healthy supply of new variable star “ore” including good prospects of finding new “Rosetta Stone” systems.

Data Reduction Workshop

Uncertainty Analysis in Photometric Observations

Michael Koppelman

6019 Fairwood Drive, Minnetonka, MN 55345; michael@slackerastronomy.org

Abstract Uncertainty analysis is an important part of observing. We take a brief look at formal uncertainty analysis for any observation set. We then address sources of uncertainty in photometric observations and discuss practical methods for applying uncertainty analysis to common photometric data sets.

Using the AAVSO International Database

Arne A. Henden

AAVSO, 49 Bay State Road, Cambridge, MA 02138; arne@aavso.org

Abstract The AAVSO International Database (AID) contains over eighteen million brightness estimates of thousands of variable stars, almost all made by amateur astronomers. We cover how these observations are submitted, the pipeline that all observations pass through, how observations can be retrieved from the database, and the basic tools for data visualization: the light curve generator and

data download, VSX, and Seqplot. Many of the flags, such as validation, are described. Analysis tools such as VStar are covered. References regarding other photometric and imaging datasets are given.

How to Use MAXIM DL for CCD Image Reduction

Federico García

Calle 4 Nro. 642, Depto E E/126 Y 127, Berisso, 1923, Argentina; fgarcia@institutocopernico.org

Abstract This goal of this talk is to present a standard way of performing CCD image calibration and reduction using MAXIM DL software. The presentation consists of two parts: the first, in which the steps to follow for image calibration are introduced, and the second, where it is explained how to perform the photometry using, in this case, a reference star to obtain magnitudes as a function of photon counts instead of determining it differentially.

Period Search Techniques in Variable Stars

Jaime García

Gutierrez Esq, Calle Jon Agrario, 5603 Rama Caida, Mendoza, Argentina; jgarcia@institutocopernico.org

Abstract There are several techniques of searching for periods in oscillatory phenomena like light variation in stars. All of them are focused in the study of light curves. In this talk we will introduce a new tool available through the AAVSO for the visualization and analysis of light curves, the software VSTAR.

An Introduction to PHOTOMETRICA

Michael Koppelman

6019 Fairwood Drive, Minnetonka, MN 55345; michael@slacker astronomy.org

Abstract PHOTOMETRICA is a web-based photometry tool that is part of the AAVSONet system. I will demonstrate how to use PHOTOMETRICA to do photometric analyses of time series data to search for variable stars, create light curves, and generate reports suitable for submission to the AAVSO.

Index to Volume 38

Author

Adkins, James Kevin, and Jennifer Birriel	
A Simple, Portable Apparatus to Measure Night Sky Brightness at Various Zenith Angles	221
Alton, Kevin B.	
A Unified Roche-Model Light Curve Solution for the W UMa Binary AC Bootis	57
Amorim, Alexandre	
Minima of Some Eclipsing Binaries (Abstract)	233
Mira Observations by Brazilício (Abstract)	231
Anon.	
Index to Volume 38	238
Billings, Gary	
Rapid Cadence Monitoring of ϵ Aurigae (Abstract)	142
Birriel, Jennifer, and Jaclyn Wheatley, Christine McMichael	
Documenting Local Night Sky Brightness Using Sky Quality Meters: An Interdisciplinary College Capstone Project and a First Step Toward Reducing Light Pollution	132
Birriel, Jennifer, and James Kevin Adkins	
A Simple, Portable Apparatus to Measure Night Sky Brightness at Various Zenith Angles	221
Boyd, David	
Two New Variable Stars in the Fields of Nova Cygni 2006 and Nova Cygni 2007	168
Boyd, David, and Tut Campbell, George Roberts	
The 2009 July Superoutburst of IL Vulpeculae	39
Brown, Samantha J., and O. F. Mills, Wayne Osborn, Vivian Hoette	
Ross 4—A Possible Recurrent Nova?	176
Buso, Victor Angel	
New Variable Stars in the Southern Cross (Abstract)	233
Campbell, Tut, and David Boyd, George Roberts	
The 2009 July Superoutburst of IL Vulpeculae	39
Collins, Donald F.	
Intrinsic Variability of Eclipsing Variable β Lyrae Measured With a Digital SLR Camera (Abstract)	144
Esteves, Samantha, in John R. Percy <i>et al.</i>	
Photometric Variability Properties of 21 T Tauri and Related Stars From AAVSO Visual Observations	151
Variability “Profiles” for T Tauri Variables and Related Objects From AAVSO Visual Observations (Abstract)	140
Foster, Grant	
T Ursae Minoris: From Mira to ??? (Abstract)	140
García, Federico	
How to Use MAXIM DL for CCD Image Reduction (Abstract)	237
García, Federico, and Jaime García	
New Equipment for Variable Star Research at the Instituto Copernico Observatory (Abstract)	234
García, Jaime	
An Introduction to CCD Photometry of Variable Stars (Abstract)	235
Period Search Techniques in Variable Stars (Abstract)	237
Girola, Rafael, and Nestor Vinet	
History of Variable Stars (Abstract)	230

Glasheen, Jou, in John R. Percy <i>et al.</i>	
Photometric Variability Properties of 21 T Tauri and Related Stars From AAVSO Visual Observations	151
Variability “Profiles” for T Tauri Variables and Related Objects From AAVSO Visual Observations (Abstract)	140
González, Eric	
Starting Research Projects at Buenaventura Suárez Observatory in San Luis Province (poster)	234
Hang, Mimi	
Debris Disks in the AB Doradus Moving Group (Abstract)	142
Heiser, Arnold M.	
Photometry of V578 Monocerotis	93
Henden, Arne A.	
Advanced CCD Observing Techniques (Abstract)	235
Current Hot Variable Star Topics (Abstract)	230
Using the AAVSO International Database (Abstract)	236
Henden, Arne A., in Matthew Templeton <i>et al.</i>	
Optical Time-Series Photometry of the Peculiar Nova CSS 081007:030559+054715	147
Hoette, Vivian, in Samantha J. Brown <i>et al.</i>	
Ross 4—A Possible Recurrent Nova?	176
Howell, Andy	
<i>BVR</i> Photometry of W Ursae Majoris Binary Systems and Lessons Learned (Abstract)	142
Howell, Steve B.	
Kepler Observations of Variable Stars (Abstract)	141
Hurdis, David A., and Tom Krajci	
Secular Variation of the Mode Amplitude-Ratio of the Double-Mode RR Lyrae Star NSVS 5222076	1
Kadooka, Mary Ann	
Hawaii Student/Teacher Astronomy Research (HI STAR) Outcomes (Abstract)	143
Koff, Robert, in Matthew Templeton <i>et al.</i>	
Optical Time-Series Photometry of the Peculiar Nova CSS 081007:030559+054715	147
Kok, Yitping	
Absolute Magnitudes and Distances of Recent Novae	193
Koppelman, Michael	
An Introduction to Data Mining (Abstract)	235
An Introduction to PHOTOMETRICA (Abstract)	237
Making Good Plots With EXCEL (Abstract)	145
Uncertainty Analysis in Photometric Observations (Abstract)	236
Krajci, Tom, and David A. Hurdis	
Secular Variation of the Mode Amplitude-Ratio of the Double-Mode RR Lyrae Star NSVS 5222076	1
Krajci, Tom, and Patrick Wils	
Photometry of the Dwarf Nova SDSS J094002.56+274942.0 in Outburst	33
Larsen, Kristine	
Scientists Look at 2012: Carrying on Margaret Mayall’s Legacy of Debunking Pseudoscience (Abstract)	139
Lin, Alfred, in John R. Percy <i>et al.</i>	
Photometric Variability Properties of 21 T Tauri and Related Stars From AAVSO Visual Observations	151
Variability “Profiles” for T Tauri Variables and Related Objects From AAVSO Visual Observations (Abstract)	140

Littlefield, Colin	
Observing Exoplanet Transits With Digital SLR Cameras	212
Long Junjiajia, and John R. Percy	
Further Studies of “Irregularity” in Pulsating Red Giants	161
Long, Junjiajia, in John R. Percy <i>et al.</i>	
Photometric Variability Properties of 21 T Tauri and Related Stars From AAVSO Visual Observations	151
Los, Edward J.	
Estimate of the Limiting Magnitudes of the Harvard College Observatory Plate Collection (Abstract)	144
Lunn, Martin, and Lila Rakoczy	
King Charles’ Star: A Multidisciplinary Approach to Dating Cassiopeiae A (Abstract)	231
Macri, Lucas	
Near-infrared Observations of Cepheid Variables in the Large Magellanic Cloud (Abstract)	232
Majaess, Danial J.	
RR Lyrae and Type II Cepheid Variables Adhere to a Common Distance Relation	100
Mashintsova, Marina, in John R. Percy <i>et al.</i>	
Photometric Variability Properties of 21 T Tauri and Related Stars From AAVSO Visual Observations	151
Variability “Profiles” for T Tauri Variables and Related Objects From AAVSO Visual Observations (Abstract)	140
McMichael, Christine, and Jennifer Birriel, Jaclyn Wheatley	
Documenting Local Night Sky Brightness Using Sky Quality Meters: An Interdisciplinary College Capstone Project and a First Step Toward Reducing Light Pollution	132
Mills, O. F., in Samantha J. Brown <i>et al.</i>	
Ross 4—A Possible Recurrent Nova?	176
Morel, Mati, and Alan Plummer	
The VSS RASNZ Variable Star Charts: a Story of Co-Evolution	123
Musso, Sebastian	
Didactics on Education in Astronomy (Abstract)	233
Nicholson, Martin	
Possible Misclassified Eclipsing Binary Stars Within the Detached Eclipsing Binary Light Curve Fitter (DEBiL) Data Set	113
Osborn, Wayne, in Samantha J. Brown <i>et al.</i>	
Ross 4—A Possible Recurrent Nova?	176
Otero, Sebastian	
Introduction to Variable Star Astronomy (Abstract)	230
Tips to Succeed in Using the ASAS-3 Database (Abstract)	235
Visual Observing Techniques (Abstract)	234
Paxson, Kevin B.	
Differential Ensemble Photometry by Linear Regression	202
Pazmino, John	
The Park in the Sky (Abstract)	145
Percy, John R., and Long Junjiajia	
Further Studies of “Irregularity” in Pulsating Red Giants	161
Percy, John R., and Samantha Esteves, Jou Glasheen, Alfred Lin, Junjiajia Long, Marina Mashintsova, Emil Terziev, Sophia Wu	
Photometric Variability Properties of 21 T Tauri and Related Stars From AAVSO Visual Observations	151

Percy, John R., and Samantha Esteves, Jou Glasheen, Alfred Lin, Marina Mashintsova, Sophia Wu Variability “Profiles” for T Tauri Variables and Related Objects From AAVSO Visual Observations (Abstract)	140
Plummer, Alan, and Mati Morel The VSS RASNZ Variable Star Charts: a Story of Co-Evolution	123
Podestá, Maria Dolores Suárez de, and Raul Roberto Podestá Activities of the SEV/LIADA (Abstract)	231
Podestá, Raul Roberto, and Maria Dolores Suárez de Podestá Activities of the SEV/LIADA (Abstract)	231
Rakoczy, Lila, and Martin Lunn King Charles’ Star: A Multidisciplinary Approach to Dating Cassiopeiae A (Abstract)	231
Roberts, George, and David Boyd, Tut Campbell The 2009 July Superoutburst of IL Vulpeculae	39
Sada, P. V. Two New Eclipsing Binary Systems: GSC 1393-1461 and GSC 2449-0654, and One New Flare Star: GSC 5604-0255	52
Samolyk, Gerard Recent CCD Minima of 185 Eclipsing Binary Stars	183
Recent Maxima of 64 Short Period Pulsating Stars	12
Recent Minima of 161 Eclipsing Binary Stars	85
Simonsen, Michael The Z CamPaign (Abstract)	140
Szkody, Paula GALEX and Optical Light Curves of LARPs (Abstract)	141
Templeton, Matthew, and Robert Koff, Patrick Wils, Arne A. Henden Optical Time-Series Photometry of the Peculiar Nova CSS 081007:030559+054715	147
Terziev, Emil, in John R. Percy <i>et al.</i> Photometric Variability Properties of 21 T Tauri and Related Stars From AAVSO Visual Observations	151
Vinet, Nestor, and Rafael Girola History of Variable Stars (Abstract)	230
Welch, Doug Mining for Rare Variable Stars in Photometric Databases (Abstract)	236
Welther, Barbara L. Mrs. Fleming’s “Q” Stars (Abstract)	145
Wheatley, Jaelyn, and Jennifer Birriel, Christine McMichael Documenting Local Night Sky Brightness Using Sky Quality Meters: An Interdisciplinary College Capstone Project and a First Step Toward Reducing Light Pollution	132
Williams, Peter F. NSV 19431 and YY Centauri—Two Mira Variables	45
Wils, Patrick, and Tom Krajci Photometry of the Dwarf Nova SDSS J094002.56+274942.0 in Outburst	33
Wils, Patrick, in Matthew Templeton <i>et al.</i> Optical Time-Series Photometry of the Peculiar Nova CSS 081007:030559+054715	147
Wu, Sophia, in John R. Percy <i>et al.</i> Photometric Variability Properties of 21 T Tauri and Related Stars From AAVSO Visual Observations	151
Variability “Profiles” for T Tauri Variables and Related Objects From AAVSO Visual Observations (Abstract)	140

Subject**AAVSO**

An Introduction to PHOTOMETRICA (Abstract)	
Michael Koppelman	237
Period Search Techniques in Variable Stars (Abstract)	
Jaime Garcíá	237
Recent CCD Minima of 185 Eclipsing Binary Stars	
Gerard Samolyk	183
Recent Maxima of 64 Short Period Pulsating Stars	
Gerard Samolyk	12
Recent Minima of 161 Eclipsing Binary Stars	
Gerard Samolyk	85
The VSS RASNZ Variable Star Charts: a Story of Co-Evolution	
Alan Plummer and Mati Morel	123

AAVSO INTERNATIONAL DATABASE

An Introduction to PHOTOMETRICA (Abstract)	
Michael Koppelman	237
Absolute Magnitudes and Distances of Recent Novae	
Yitping Kok	193
Further Studies of “Irregularity” in Pulsating Red Giants	
John R. Percy and Junjiajia Long	161
Optical Time-Series Photometry of the Peculiar Nova CSS 081007:030559+054715	
Matthew Templeton <i>et al.</i>	147
Photometric Variability Properties of 21 T Tauri and Related Stars From AAVSO Visual Observations	
John R. Percy <i>et al.</i>	151
Recent CCD Minima of 185 Eclipsing Binary Stars	
Gerard Samolyk	183
Recent Maxima of 64 Short Period Pulsating Stars	
Gerard Samolyk	12
Recent Minima of 161 Eclipsing Binary Stars	
Gerard Samolyk	85
T Ursae Minoris: From Mira to ??? (Abstract)	
Grant Foster	140
Using the AAVSO International Database (Abstract)	
Henden, Arne A.	236
Variability “Profiles” for T Tauri Variables and Related Objects From AAVSO Visual Observations (Abstract)	
John R. Percy <i>et al.</i>	140
The VSS RASNZ Variable Star Charts: a Story of Co-Evolution	
Alan Plummer and Mati Morel	123

AMPLITUDE ANALYSIS

T Ursae Minoris: From Mira to ??? (Abstract)

Grant Foster

140

ASTEROIDSTwo New Eclipsing Binary Systems: GSC 1393-1461 and GSC 2449-0654,
and One New Flare Star: GSC 5604-0255

P. V. Sada

52

ASTRONOMERS, AMATEUR; PROFESSIONAL-AMATEUR COLLABORATION

Activities of the SEV/LIADA (Abstract)

Raul Roberto Podestá and Maria Dolores Suárez de Podestá

231

Didactics on Education in Astronomy (Abstract)

Sebastian Musso

233

Introduction to Variable Star Astronomy (Abstract)

Sebastián Otero

230

Mira Observations by Brazilício (Abstract)

Alexandre Amorim

231

New Equipment for Variable Star Research at the Instituto Copernico Observatory
(Abstract)

Jaime García and Federico García

234

New Variable Stars in the Southern Cross (Abstract)

Victor Angel Buso

233

Using the AAVSO International Database (Abstract)

Henden, Arne A.

236

ASTRONOMY, HISTORY OF [See also ARCHAEOASTRONOMY; OBITUARIES]

History of Variable Stars (Abstract)

Rafael Girola and Nestor Vinet

230

King Charles' Star: A Multidisciplinary Approach to Dating Cassiopeiae A (Abstract)

Martin Lunn and Lila Rakoczy

231

Mira Observations by Brazilício (Abstract)

Alexandre Amorim

231

Mrs. Fleming's "Q" Stars (Abstract)

Barbara L. Welther

145

Scientists Look at 2012: Carrying on Margaret Mayall's Legacy of Debunking
Pseudoscience (Abstract)

Kristine Larsen

139

The VSS RASNZ Variable Star Charts: a Story of Co-Evolution

Alan Plummer and Mati Morel

123

ASTRONOMY, WOMEN IN

Mrs. Fleming's "Q" Stars (Abstract)

Barbara L. Welther

145

BLAZARS [See also VARIABLE STARS (GENERAL)]

Differential Ensemble Photometry by Linear Regression

Kevin B. Paxson

202

CATAclysmic Variables [See also VARIABLE STARS (GENERAL)]

The 2009 July Superoutburst of IL Vulpeculae David Boyd, Tut Campbell, and George Roberts	39
Photometry of the Dwarf Nova SDSS J094002.56+274942.0 in Outburst Tom Krajci and Patrick Wils	33
Ross 4—A Possible Recurrent Nova? Samantha J. Brown <i>et al.</i>	176
The Z CamPaign (Abstract) Michael Simonsen	140

CATALOGUES, DATABASES, SURVEYS

<i>B/RI</i> Photometry of W Ursae Majoris Binary Systems and Lessons Learned (Abstract) Andy Howell	142
Debris Disks in the AB Doradus Moving Group (Abstract) Mimi Hang	142
Estimate of the Limiting Magnitudes of the Harvard College Observatory Plate Collection (Abstract) Edward J. Los	144
Mining for Rare Variable Stars in Photometric Databases (Abstract) Doug Welch	236
Mrs. Fleming’s “Q” Stars (Abstract) Barbara L. Welther	145
Near-infrared Observations of Cepheid Variables in the Large Magellanic Cloud (Abstract) Lucas Macri	232
New Variable Stars in the Southern Cross (Abstract) Victor Angel Buso	233
Photometry of the Dwarf Nova SDSS J094002.56+274942.0 in Outburst Tom Krajci and Patrick Wils	33
Possible Misclassified Eclipsing Binary Stars Within the Detached Eclipsing Binary Light Curve Fitter (DEBiL) Data Set Martin Nicholson	113
Ross 4—A Possible Recurrent Nova? Samantha J. Brown <i>et al.</i>	176
Tips to Succeed Using the ASAS-3 Database (Abstract) Sebastián Otero	235
Two New Eclipsing Binary Systems: GSC 1393-1461 and GSC 2449-0654, and One New Flare Star: GSC 5604-0255 P. V. Sada	52
The VSS RASNZ Variable Star Charts: a Story of Co-Evolution Alan Plummer and Mati Morel	123
The Z CamPaign (Abstract) Michael Simonsen	140

CEPHEID VARIABLES [See also VARIABLE STARS (GENERAL)]

History of Variable Stars (Abstract) Rafael Girola and Nestor Vinet	230
--	-----

Near-infrared Observations of Cepheid Variables in the Large Magellanic Cloud (Abstract)	
Lucas Macri	232
RR Lyrae and Type II Cepheid Variables Adhere to a Common Distance Relation	
Daniel J. Majaess	100
CHARTS, VARIABLE STAR	
Possible Misclassified Eclipsing Binary Stars Within the Detached Eclipsing Binary Light Curve Fitter (DEBiL) Data Set	
Martin Nicholson	113
The VSS RASNZ Variable Star Charts: a Story of Co-Evolution	
Alan Plummer and Mati Morel	123
CHARTS; COMPARISON STAR SEQUENCES	
Possible Misclassified Eclipsing Binary Stars Within the Detached Eclipsing Binary Light Curve Fitter (DEBiL) Data Set	
Martin Nicholson	113
The VSS RASNZ Variable Star Charts: a Story of Co-Evolution	
Alan Plummer and Mati Morel	123
CLUSTERS, GLOBULAR	
RR Lyrae and Type II Cepheid Variables Adhere to a Common Distance Relation	
Daniel J. Majaess	100
COMETS	
Mira Observations by Brazilício (Abstract)	
Alexandre Amorim	231
COMPUTERS; COMPUTER PROGRAMS; INTERNET, WORLD WIDE WEB	
Activities of the SEV/LIADA (Abstract)	
Raul Roberto Podestá and Maria Dolores Suárez de Podestá	231
Advanced CCD Observing Techniques (Abstract)	
Henden, Arne A.	235
<i>BVR</i> Photometry of W Ursae Majoris Binary Systems and Lessons Learned (Abstract)	
Andy Howell	142
How to Use MAXIM DL for CCD Image Reduction (Abstract)	
Federico García	237
An Introduction to PHOTOMETRICA (Abstract)	
Michael Koppelman	237
Making Good Plots With EXCEL (Abstract)	
Michael Koppelman	145
Mrs. Fleming's "Q" Stars (Abstract)	
Barbara L. Welther	145
Period Search Techniques in Variable Stars (Abstract)	
Jaime García	237
A Simple, Portable Apparatus to Measure Night Sky Brightness at Various Zenith Angles	
Jennifer Birriel and James Kevin Adkins	221
COORDINATED OBSERVATIONS [MULTI-SITE, MULTI-WAVELENGTH OBSERVATIONS]	
The Z CamPaign (Abstract)	
Michael Simonsen	140

DATA MINING

Estimate of the Limiting Magnitudes of the Harvard College Observatory Plate Collection (Abstract)	
Edward J. Los	144
An Introduction to Data Mining (Abstract)	
Michael Koppelman	235
An Introduction to PHOTOMETRICA (Abstract)	
Michael Koppelman	237
Kepler Observations of Variable Stars (Abstract)	
Steve B. Howell	141
Mining for Rare Variable Stars in Photometric Databases (Abstract)	
Doug Welch	236
Tips to Succeed Using the ASAS-3 Database (Abstract)	
Sebastián Otero	235
Using the AAVSO International Database (Abstract)	
Henden, Arne A.	236

DELTA SCUTI STARS [See also VARIABLE STARS (GENERAL)]

Recent Maxima of 64 Short Period Pulsating Stars	
Gerard Samolyk	12
Two New Variable Stars in the Fields of Nova Cygni 2006 and Nova Cygni 2007	
David Boyd	168

ECLIPSING BINARIES [See also VARIABLE STARS (GENERAL)]

<i>BVR</i> Photometry of W Ursae Majoris Binary Systems and Lessons Learned (Abstract)	
Andy Howell	142
Intrinsic Variability of Eclipsing Variable β Lyrae Measured With a Digital SLR Camera (Abstract)	
Donald F. Collins	144
Minima of Some Eclipsing Binaries (Abstract)	
Alexandre Amorim	233
Photometry of V578 Monocerotis	
Arnold M. Heiser	93
Possible Misclassified Eclipsing Binary Stars Within the Detached Eclipsing Binary Light Curve Fitter (DEBiL) Data Set	
Martin Nicholson	113
Rapid Cadence Monitoring of ϵ Aurigae (Abstract)	
Gary Billings	142
Recent CCD Minima of 185 Eclipsing Binary Stars	
Gerard Samolyk	183
Recent Minima of 161 Eclipsing Binary Stars	
Gerard Samolyk	85
Two New Eclipsing Binary Systems: GSC 1393-1461 and GSC 2449-0654, and One New Flare Star: GSC 5604-0255	
P. V. Sada	52

A Unified Roche-Model Light Curve Solution for the W UMa Binary AC Bootis

Kevin B. Alton

57

EDUCATION

Documenting Local Night Sky Brightness Using Sky Quality Meters: An Interdisciplinary College Capstone Project and a First Step Toward Reducing Light Pollution

Jennifer Birriel, Jaclyn Wheatley, and Christine McMichael

132

EDUCATION, VARIABLE STARS IN

Didactics on Education in Astronomy (Abstract)

Sebastian Musso

233

Hawaii Student/Teacher Astronomy Research (HI STAR) Outcomes (Abstract)

Mary Ann Kadooka

143

New Equipment for Variable Star Research at the Instituto Copernico Observatory (Abstract)

Jaime Garcíá and Federico Garcíá

234

EXTRAGALACTIC

Near-infrared Observations of Cepheid Variables in the Large Magellanic Cloud (Abstract)

Lucas Macri

232

RR Lyrae and Type II Cepheid Variables Adhere to a Common Distance Relation

Daniel J. Majaess

100

FLARE STARS [See also VARIABLE STARS (GENERAL)]

Two New Eclipsing Binary Systems: GSC 1393-1461 and GSC 2449-0654, and One New Flare Star: GSC 5604-0255

P. V. Sada

52

GIANTS, NON-MIRA TYPE

Rapid Cadence Monitoring of ϵ Aurigae (Abstract)

Gary Billings

142

INDEX, INDICES

Index to Volume 38

Anon.

238

INSTRUMENTATION [See also CCD; VARIABLE STAR OBSERVING]

Advanced CCD Observing Techniques (Abstract)

Henden, Arne A.

235

Documenting Local Night Sky Brightness Using Sky Quality Meters: An Interdisciplinary College Capstone Project and a First Step Toward Reducing Light Pollution

Jennifer Birriel, Jaclyn Wheatley, and Christine McMichael

132

Intrinsic Variability of Eclipsing Variable β Lyrae Measured With a Digital SLR Camera (Abstract)

Donald F. Collins

144

An Introduction to CCD Photometry of Variable Stars (Abstract)

Jaime Garcíá

235

Making Good Plots With EXCEL (Abstract)

Michael Koppelman

145

Observing Exoplanet Transits With Digital SLR Cameras Colin Littlefield	212
A Simple, Portable Apparatus to Measure Night Sky Brightness at Various Zenith Angles Jennifer Birriel and James Kevin Adkins	221
IRREGULAR VARIABLES [See also VARIABLE STARS (GENERAL)]	
Further Studies of “Irregularity” in Pulsating Red Giants John R. Percy and Junjiajia Long	161
LIGHT POLLUTION	
Documenting Local Night Sky Brightness Using Sky Quality Meters: An Interdisciplinary College Capstone Project and a First Step Toward Reducing Light Pollution Jennifer Birriel, Jaclyn Wheatley, and Christine McMichael	132
The Park in the Sky (Abstract) John Pazmino	145
A Simple, Portable Apparatus to Measure Night Sky Brightness at Various Zenith Angles Jennifer Birriel and James Kevin Adkins	221
LUNAR	
Mira Observations by Brazilício (Abstract) Alexandre Amorim	231
MAGNETIC VARIABLES; POLARS [See also VARIABLE STARS (GENERAL)]	
GALEX and Optical Light Curves of LARPs (Abstract) Paula Szkody	141
MIRA VARIABLES [See also VARIABLE STARS (GENERAL)]	
Mira Observations by Brazilício (Abstract) Alexandre Amorim	231
NSV 19431 and YY Centauri—Two Mira Variables Peter F. Williams	45
T Ursae Minoris: From Mira to ??? (Abstract) Grant Foster	140
The VSS RASNZ Variable Star Charts: a Story of Co-Evolution Alan Plummer and Mati Morel	123
MODELS, STELLAR	
Debris Disks in the AB Doradus Moving Group (Abstract) Mimi Hang	142
A Unified Roche-Model Light Curve Solution for the W UMa Binary AC Bootis Kevin B. Alton	57
MULTI-WAVELENGTH OBSERVATIONS [See also COORDINATED OBSERVATIONS]	
GALEX and Optical Light Curves of LARPs (Abstract) Paula Szkody	141
Optical Time-Series Photometry of the Peculiar Nova CSS 081007:030559+054715 Matthew Templeton <i>et al.</i>	147
NOVAE; RECURRENT NOVAE; NOVA-LIKE [See also CATAclysmic VARIABLES]	
Absolute Magnitudes and Distances of Recent Novae Yitping Kok	193

<i>Index, JAAVSO Volume 38, 2010</i>	249
Current Hot Variable Star Topics (Abstract)	
Arne A. Henden	230
Mrs. Fleming's "Q" Stars (Abstract)	
Barbara L. Welther	145
Optical Time-Series Photometry of the Peculiar Nova CSS 081007:030559+054715	
Matthew Templeton <i>et al.</i>	147
Ross 4—A Possible Recurrent Nova?	
Samantha J. Brown <i>et al.</i>	176
OBSERVATORIES	
New Equipment for Variable Star Research at the Instituto Copernico Observatory (Abstract)	
Jaime Garcíá and Federico Garcíá	234
The Park in the Sky (Abstract)	
John Pazmino	145
Starting Research Projects at Buenaventura Suárez Observatory in San Luis Province (poster)	
Eric González	234
PERIOD ANALYSIS; PERIOD CHANGES	
The 2009 July Superoutburst of IL Vulpeculae	
David Boyd, Tut Campbell, and George Roberts	39
Further Studies of "Irregularity" in Pulsating Red Giants	
John R. Percy and Junjiajia Long	161
Intrinsic Variability of Eclipsing Variable β Lyrae Measured With a Digital SLR Camera (Abstract)	
Donald F. Collins	144
An Introduction to PHOTOMETRICA (Abstract)	
Michael Koppelman	237
Minima of Some Eclipsing Binaries (Abstract)	
Alexandre Amorim	233
Mira Observations by Brazilício (Abstract)	
Alexandre Amorim	231
NSV 19431 and YY Centauri—Two Mira Variables	
Peter F. Williams	45
Optical Time-Series Photometry of the Peculiar Nova CSS 081007:030559+054715	
Matthew Templeton <i>et al.</i>	147
Period Search Techniques in Variable Stars (Abstract)	
Jaime Garcíá	237
Photometric Variability Properties of 21 T Tauri and Related Stars From AAVSO Visual Observations	
John R. Percy <i>et al.</i>	151
Photometry of V 578 Monocerotis	
Arnold M. Heiser	93

Photometry of the Dwarf Nova SDSS J094002.56+274942.0 in Outburst Tom Krajci and Patrick Wils	33
Rapid Cadence Monitoring of ϵ Aurigae (Abstract) Gary Billings	142
Recent Maxima of 64 Short Period Pulsating Stars Gerard Samolyk	12
Recent CCD Minima of 185 Eclipsing Binary Stars Gerard Samolyk	183
Recent Minima of 161 Eclipsing Binary Stars Gerard Samolyk	85
Secular Variation of the Mode Amplitude-Ratio of the Double-Mode RR Lyrae Star NSVS 5222076 David A. Hurdis and Tom Krajci	1
Two New Eclipsing Binary Systems: GSC 1393-1461 and GSC 2449-0654, and One New Flare Star: GSC 5604-0255 P. V. Sada	52
Two New Variable Stars in the Fields of Nova Cygni 2006 and Nova Cygni 2007 David Boyd	168
A Unified Roche-Model Light Curve Solution for the W UMa Binary AC Bootis Kevin B. Alton	57
Variability “Profiles” for T Tauri Variables and Related Objects From AAVSO Visual Observations (Abstract) John R. Percy <i>et al.</i>	140

PHOTOMETRY

Advanced CCD Observing Techniques (Abstract) Henden, Arne A.	235
Photometry of V578 Monocerotis Arnold M. Heiser	93
RR Lyrae and Type II Cepheid Variables Adhere to a Common Distance Relation Daniel J. Majaess	100
Uncertainty Analysis in Photometric Observations (Abstract) Michael Koppelman	236

PHOTOMETRY, CCD

Absolute Magnitudes and Distances of Recent Novae Yitping Kok	193
Advanced CCD Observing Techniques (Abstract) Henden, Arne A.	235
<i>BVR</i> Photometry of W Ursae Majoris Binary Systems and Lessons Learned (Abstract) Andy Howell	142
Differential Ensemble Photometry by Linear Regression Kevin B. Paxson	202
Intrinsic Variability of Eclipsing Variable β Lyrae Measured With a Digital SLR Camera (Abstract) Donald F. Collins	144

An Introduction to CCD Photometry of Variable Stars (Abstract)	
Jaime Garcíá	235
An Introduction to PHOTOMETRICA (Abstract)	
Michael Koppelman	237
Observing Exoplanet Transits With Digital SLR Cameras	
Colin Littlefield	212
Optical Time-Series Photometry of the Peculiar Nova	
CSS 081007:030559+054715	
Matthew Templeton <i>et al.</i>	147
Photometry of the Dwarf Nova SDSS J094002.56+274942.0 in Outburst	
Tom Krajci and Patrick Wils	33
Rapid Cadence Monitoring of ϵ Aurigae (Abstract)	
Gary Billings	142
Recent CCD Minima of 185 Eclipsing Binary Stars	
Gerard Samolyk	183
Recent Maxima of 64 Short Period Pulsating Stars	
Gerard Samolyk	12
Recent Minima of 161 Eclipsing Binary Stars	
Gerard Samolyk	85
Secular Variation of the Mode Amplitude-Ratio of the Double-Mode RR Lyrae Star	
NSVS 5222076	
David A. Hurdís and Tom Krajci	1
T Ursae Minoris: From Mira to ??? (Abstract)	
Grant Foster	140
The 2009 July Superoutburst of IL Vulpeculae	
David Boyd, Tut Campbell, and George Roberts	39
Two New Variable Stars in the Fields of Nova Cygni 2006 and Nova Cygni 2007	
David Boyd	168
A Unified Roche-Model Light Curve Solution for the W UMa Binary AC Bootis	
Kevin B. Alton	57
PHOTOMETRY, INFRARED	
Debris Disks in the AB Doradus Moving Group (Abstract)	
Mimi Hang	142
PHOTOMETRY, NEAR-INFRARED	
Near-infrared Observations of Cepheid Variables in the Large Magellanic Cloud (Abstract)	
Lucas Macri	232
PHOTOMETRY, PHOTOELECTRIC	
A Unified Roche-Model Light Curve Solution for the W UMa Binary AC Bootis	
Kevin B. Alton	57
PHOTOMETRY, PHOTOGRAPHIC	
Estimate of the Limiting Magnitudes of the Harvard College Observatory Plate	
Collection (Abstract)	
Edward J. Los	144

Mrs. Fleming's "Q" Stars (Abstract)	
Barbara L. Welther	145
New Variable Stars in the Southern Cross (Abstract)	
Victor Angel Buso	233
Ross 4—A Possible Recurrent Nova?	
Samantha J. Brown <i>et al.</i>	176
PHOTOMETRY, VISUAL	
Absolute Magnitudes and Distances of Recent Novae	
Yitping Kok	193
Further Studies of "Irregularity" in Pulsating Red Giants	
John R. Percy and Junjiajia Long	161
Introduction to Variable Star Astronomy (Abstract)	
Sebastián Otero	230
NSV 19431 and YY Centauri—Two Mira Variables	
Peter F. Williams	45
Photometric Variability Properties of 21 T Tauri and Related Stars From AAVSO Visual Observations	
John R. Percy <i>et al.</i>	151
T Ursae Minoris: From Mira to ??? (Abstract)	
Grant Foster	140
Variability "Profiles" for T Tauri Variables and Related Objects From AAVSO Visual Observations (Abstract)	
John R. Percy <i>et al.</i>	140
Visual Observing Techniques (Abstract)	
Sebastián Otero	234
PLANETS	
Debris Disks in the AB Doradus Moving Group (Abstract)	
Mimi Hang	142
Mira Observations by Brazilício (Abstract)	
Alexandre Amorim	231
Scientists Look at 2012: Carrying on Margaret Mayall's Legacy of Debunking Pseudoscience (Abstract)	
Kristine Larsen	139
PLANETS, EXTRASOLAR	
Debris Disks in the AB Doradus Moving Group (Abstract)	
Mimi Hang	142
Kepler Observations of Variable Stars (Abstract)	
Steve B. Howell	141
Observing Exoplanet Transits With Digital SLR Cameras	
Colin Littlefield	212
POETRY, THEATER, DANCE, SOCIETY	
Didactics on Education in Astronomy (Abstract)	
Sebastián Musso	233
The Park in the Sky (Abstract)	

<i>Index, JAAVSO Volume 38, 2010</i>	253
John Pazmino	145
Scientists Look at 2012: Carrying on Margaret Mayall's Legacy of Debunking Pseudoscience (Abstract)	
Kristine Larsen	139
Starting Research Projects at Buenaventura Suárez Observatory in San Luis Province (poster)	
Eric González	234
REMOTE OBSERVING	
The 2009 July Superoutburst of IL Vulpeculae	
David Boyd, Tut Campbell, and George Roberts	39
RR LYRAE STARS [See also VARIABLE STARS (GENERAL)]	
RR Lyrae and Type II Cepheid Variables Adhere to a Common Distance Relation	
Daniel J. Majaess	100
Recent Maxima of 64 Short Period Pulsating Stars	
Gerard Samolyk	12
Secular Variation of the Mode Amplitude-Ratio of the Double-Mode RR Lyrae Star NSVS 5222076	
David A. Hurdis and Tom Krajci	1
S DORADUS VARIABLES [See also VARIABLE STARS (GENERAL)]	
Two New Variable Stars in the Fields of Nova Cygni 2006 and Nova Cygni 2007	
David Boyd	168
SATELLITE OBSERVATIONS	
Debris Disks in the AB Doradus Moving Group (Abstract)	
Mimi Hang	142
GALEX and Optical Light Curves of LARPs (Abstract)	
Paula Szkody	141
Kepler Observations of Variable Stars (Abstract)	
Steve B. Howell	141
Optical Time-Series Photometry of the Peculiar Nova CSS 081007:030559+054715	
Matthew Templeton <i>et al.</i>	147
SATELLITES; SATELLITE MISSIONS [See also COORDINATED OBSERVATIONS]	
GALEX and Optical Light Curves of LARPs (Abstract)	
Paula Szkody	141
SCIENTIFIC WRITING, PUBLICATION OF DATA	
Making Good Plots With EXCEL (Abstract)	
Michael Koppelman	145
SELF-CORRELATION ANALYSIS	
Further Studies of "Irregularity" in Pulsating Red Giants	
John R. Percy and Junjiajia Long	161
Photometric Variability Properties of 21 T Tauri and Related Stars From AAVSO Visual Observations	
John R. Percy <i>et al.</i>	151
Variability "Profiles" for T Tauri Variables and Related Objects From AAVSO Visual Observations (Abstract)	
John R. Percy <i>et al.</i>	140

SEMIREGULAR VARIABLES [See also VARIABLE STARS (GENERAL)]

- T Ursae Minoris: From Mira to ??? (Abstract)
Grant Foster 140

SOLAR

- Mira Observations by Brazilício (Abstract)
Alexandre Amorim 231
- Scientists Look at 2012: Carrying on Margaret Mayall's Legacy of Debunking
Pseudoscience (Abstract)
Kristine Larsen 139

SPECTRA, SPECTROSCOPY

- Mrs. Fleming's "Q" Stars (Abstract)
Barbara L. Welther 145

STATISTICAL ANALYSIS

- Absolute Magnitudes and Distances of Recent Novae
Yitping Kok 193
- BVR* Photometry of W Ursae Majoris Binary Systems and Lessons Learned (Abstract)
Andy Howell 142
- Differential Ensemble Photometry by Linear Regression
Kevin B. Paxson 202
- GALEX and Optical Light Curves of LARPs (Abstract)
Paula Szkody 141
- History of Variable Stars (Abstract)
Rafael Girola and Nestor Vinet 230
- How to Use MAXIM DL for CCD Image Reduction (Abstract)
Federico García 237
- An Introduction to PHOTOMETRICA (Abstract)
Michael Koppelman 237
- Kepler Observations of Variable Stars (Abstract)
Steve B. Howell 141
- Near-infrared Observations of Cepheid Variables in the Large Magellanic Cloud (Abstract)
Lucas Macri 232
- Optical Time-Series Photometry of the Peculiar Nova CSS 081007:030559+054715
Matthew Templeton *et al.* 147
- Period Search Techniques in Variable Stars (Abstract)
Jaime García 237
- Possible Misclassified Eclipsing Binary Stars Within the Detached Eclipsing Binary
Light Curve Fitter (DEBiL) Data Set
Martin Nicholson 113
- RR Lyrae and Type II Cepheid Variables Adhere to a Common Distance Relation
Daniel J. Majaess 100
- T Ursae Minoris: From Mira to ??? (Abstract)
Grant Foster 140
- The Z CamPaign (Abstract)
Michael Simonsen 140

<i>Index, JAAVSO Volume 38, 2010</i>	255
Uncertainty Analysis in Photometric Observations (Abstract)	
Michael Koppelman	236
A Unified Roche-Model Light Curve Solution for the W UMa Binary AC Bootis	
Kevin B. Alton	57
Variability “Profiles” for T Tauri Variables and Related Objects From AAVSO	
Visual Observations (Abstract)	
John R. Percy <i>et al.</i>	140
SUPERNOVAE [See also VARIABLE STARS (GENERAL)]	
Current Hot Variable Star Topics (Abstract)	
Arne A. Henden	230
King Charles’ Star: A Multidisciplinary Approach to Dating Cassiopeiae A (Abstract)	
Martin Lunn and Lila Rakoczy	231
SUSPECTED VARIABLES [See also VARIABLE STARS (GENERAL)]	
New Variable Stars in the Southern Cross (Abstract)	
Victor Angel Buso	233
Ross 4—A Possible Recurrent Nova?	
Samantha J. Brown <i>et al.</i>	176
SX PHOENICIS VARIABLES [See also VARIABLE STARS (GENERAL)]	
RR Lyrae and Type II Cepheid Variables Adhere to a Common Distance Relation	
Daniel J. Majaess	100
T TAURI STARS [See also VARIABLE STARS (GENERAL)]	
Photometric Variability Properties of 21 T Tauri and Related Stars From AAVSO	
Visual Observations	
John R. Percy <i>et al.</i>	151
Variability “Profiles” for T Tauri Variables and Related Objects From AAVSO	
Visual Observations (Abstract)	
John R. Percy <i>et al.</i>	140
TERRESTRIAL	
Scientists Look at 2012: Carrying on Margaret Mayall’s Legacy of Debunking	
Pseudoscience (Abstract)	
Kristine Larsen	139
UNKNOWN; UNSTUDIED VARIABLES	
Kepler Observations of Variable Stars (Abstract)	
Steve B. Howell	141
New Variable Stars in the Southern Cross (Abstract)	
Victor Angel Buso	233
VARIABLE STAR OBSERVING ORGANIZATIONS	
Activities of the SEV/LIADA (Abstract)	
Raul Roberto Podestá and Maria Dolores Suárez de Podestá	231
The VSS RASNZ Variable Star Charts: a Story of Co-Evolution	
Alan Plummer and Mati Morel	123
VARIABLE STAR OBSERVING [See also INSTRUMENTATION]	
Activities of the SEV/LIADA (Abstract)	
Raul Roberto Podestá and Maria Dolores Suárez de Podestá	231

Advanced CCD Observing Techniques (Abstract) Henden, Arne A.	235
Current Hot Variable Star Topics (Abstract) Arne A. Henden	230
Didactics on Education in Astronomy (Abstract) Sebastián Musso	233
How to Use MAXIM DL for CCD Image Reduction (Abstract) Federico Garcíá	236
An Introduction to CCD Photometry of Variable Stars (Abstract) Jaime Garcíá	235
An Introduction to Data Mining (Abstract) Michael Koppelman	235
An Introduction to PHOTOMETRICA (Abstract) Michael Koppelman	237
Introduction to Variable Star Astronomy (Abstract) Sebastián Otero	230
Minima of Some Eclipsing Binaries (Abstract) Alexandre Amorim	233
New Equipment for Variable Star Research at the Instituto Copernico Observatory (Abstract) Jaime Garcíá and Federico Garcíá	234
The Park in the Sky (Abstract) John Pazmino	145
Period Search Techniques in Variable Stars (Abstract) Jaime Garcíá	237
RR Lyrae and Type II Cepheid Variables Adhere to a Common Distance Relation Daniel J. Majaess	100
A Simple, Portable Apparatus to Measure Night Sky Brightness at Various Zenith Angles Jennifer Birriel and James Kevin Adkins	221
Starting Research Projects at Buenaventura Suarez Observatory in San Luis Province (poster) Eric González	234
Uncertainty Analysis in Photometric Observations (Abstract) Michael Koppelman	236
Using the AAVSO International Database (Abstract) Henden, Arne A.	236
The VSS RASNZ Variable Star Charts: a Story of Co-Evolution Alan Plummer and Mati Morel	123
Visual Observing Techniques (Abstract) Sebastián Otero	234
The Z CamPaign (Abstract) Michael Simonsen	140

VARIABLE STARS (GENERAL)

Estimate of the Limiting Magnitudes of the Harvard College Observatory Plate Collection (Abstract)	
Edward J. Los	144
History of Variable Stars (Abstract)	
Rafael Girola and Nestor Vinet	230
Introduction to Variable Star Astronomy (Abstract)	
Sebastián Otero	230
Kepler Observations of Variable Stars (Abstract)	
Steve B. Howell	141
Mining for Rare Variable Stars in Photometric Databases (Abstract)	
Doug Welch	236
Tips to Succeed Using the ASAS-3 Database (Abstract)	
Sebastián Otero	235
Variability “Profiles” for T Tauri Variables and Related Objects From AAVSO Visual Observations (Abstract)	
John R. Percy <i>et al.</i>	140

VARIABLE STARS (INDIVIDUAL); OBSERVING TARGETS

[U Ant] Further Studies of “Irregularity” in Pulsating Red Giants	
John R. Percy and Junjiajia Long	161
[V Aps] Further Studies of “Irregularity” in Pulsating Red Giants	
John R. Percy and Junjiajia Long	161
[VW Aql] Further Studies of “Irregularity” in Pulsating Red Giants	
John R. Percy and Junjiajia Long	161
[SY Ara] Minima of Some Eclipsing Binaries (Abstract)	
Alexandre Amorim	233
[LU Ara] Minima of Some Eclipsing Binaries (Abstract)	
Alexandre Amorim	233
[SU Aur] Photometric Variability Properties of 21 T Tauri and Related Stars From AAVSO Visual Observations	
John R. Percy <i>et al.</i>	151
[SV Aur] Further Studies of “Irregularity” in Pulsating Red Giants	
John R. Percy and Junjiajia Long	161
[ϵ Aur] Rapid Cadence Monitoring of ϵ Aurigae (Abstract)	
Gary Billings	142
[AC Boo] A Unified Roche-Model Light Curve Solution for the W UMa Binary AC Bootis	
Kevin B. Alton	57
[UX Cam] Further Studies of “Irregularity” in Pulsating Red Giants	
John R. Percy and Junjiajia Long	161
[W CMa] Further Studies of “Irregularity” in Pulsating Red Giants	
John R. Percy and Junjiajia Long	161
[RZ Cap] Recent Maxima of 64 Short Period Pulsating Stars	
Gerard Samolyk	12

[R Car] The VSS RASNZ Variable Star Charts: a Story of Co-Evolution Alan Plummer and Mati Morel	123
[RT Car] Further Studies of “Irregularity” in Pulsating Red Giants John R. Percy and Junjiajia Long	161
[GW Car] Minima of Some Eclipsing Binaries (Abstract) Alexandre Amorim	233
[WW Cas] Further Studies of “Irregularity” in Pulsating Red Giants John R. Percy and Junjiajia Long	161
[AA Cas] Further Studies of “Irregularity” in Pulsating Red Giants John R. Percy and Junjiajia Long	161
[IZ Cas] Further Studies of “Irregularity” in Pulsating Red Giants John R. Percy and Junjiajia Long	161
[PY Cas] Further Studies of “Irregularity” in Pulsating Red Giants John R. Percy and Junjiajia Long	161
[V723 Cas] Differential Ensemble Photometry by Linear Regression Kevin B. Paxson	202
[SS Cen] Minima of Some Eclipsing Binaries (Abstract) Alexandre Amorim	233
[YY Cen] NSV 19431 and YY Centauri—Two Mira Variables Peter F. Williams	45
[AD Cen] Further Studies of “Irregularity” in Pulsating Red Giants John R. Percy and Junjiajia Long	161
[BD Cen] Minima of Some Eclipsing Binaries (Abstract) Alexandre Amorim	233
[V1213 Cen] Absolute Magnitudes and Distances of Recent Novae Yitping Kok	193
[V5583 Cen] Absolute Magnitudes and Distances of Recent Novae Yitping Kok	193
[ST Cep] Further Studies of “Irregularity” in Pulsating Red Giants John R. Percy and Junjiajia Long	161
[YZ Cep] Photometric Variability Properties of 21 T Tauri and Related Stars From AAVSO Visual Observations John R. Percy <i>et al.</i>	151
[DI Cep] Photometric Variability Properties of 21 T Tauri and Related Stars From AAVSO Visual Observations John R. Percy <i>et al.</i>	151
[DM Cep] Further Studies of “Irregularity” in Pulsating Red Giants John R. Percy and Junjiajia Long	161
[o Cet] Mira Observations by Brazilício (Abstract) Alexandre Amorim	231
[T Cha] Photometric Variability Properties of 21 T Tauri and Related Stars From AAVSO Visual Observations John R. Percy <i>et al.</i>	151

[T Cir] Minima of Some Eclipsing Binaries (Abstract) Alexandre Amorim	233
[R CrA] Photometric Variability Properties of 21 T Tauri and Related Stars From AAVSO Visual Observations John R. Percy <i>et al.</i>	151
[T CrA] Photometric Variability Properties of 21 T Tauri and Related Stars From AAVSO Visual Observations John R. Percy <i>et al.</i>	151
[TT Cru] Minima of Some Eclipsing Binaries (Abstract) Alexandre Amorim	233
[SV Cyg] Further Studies of “Irregularity” in Pulsating Red Giants John R. Percy and Junjiajia Long	161
[T Cyg] Further Studies of “Irregularity” in Pulsating Red Giants John R. Percy and Junjiajia Long	161
[V2467 Cyg] Absolute Magnitudes and Distances of Recent Novae Yitping Kok	193
[V449 Cyg] Further Studies of “Irregularity” in Pulsating Red Giants John R. Percy and Junjiajia Long	161
[CT Del] Further Studies of “Irregularity” in Pulsating Red Giants John R. Percy and Junjiajia Long	161
[AB Dor association] Debris Disks in the AB Doradus Moving Group (Abstract) Mimi Hang	142
[UW Dra] Further Studies of “Irregularity” in Pulsating Red Giants John R. Percy and Junjiajia Long	161
[AQ Dra] Photometric Variability Properties of 21 T Tauri and Related Stars From AAVSO Visual Observations John R. Percy <i>et al.</i>	151
[AT Dra] Further Studies of “Irregularity” in Pulsating Red Giants John R. Percy and Junjiajia Long	161
[WY Gem] Further Studies of “Irregularity” in Pulsating Red Giants John R. Percy and Junjiajia Long	161
[BU Gem] Further Studies of “Irregularity” in Pulsating Red Giants John R. Percy and Junjiajia Long	161
[GN Her] Further Studies of “Irregularity” in Pulsating Red Giants John R. Percy and Junjiajia Long	161
[OP Her] Further Studies of “Irregularity” in Pulsating Red Giants John R. Percy and Junjiajia Long	161
[DG Hya] Recent Maxima of 64 Short Period Pulsating Stars Gerard Samolyk	12
[TT Leo] Further Studies of “Irregularity” in Pulsating Red Giants John R. Percy and Junjiajia Long	161
[WX LMi] GALEX and Optical Light Curves of LARPs (Abstract) Paula Szkody	141

[RU Lup] Photometric Variability Properties of 21 T Tauri and Related Stars From AAVSO Visual Observations John R. Percy <i>et al.</i>	151
[DT Lup] Minima of Some Eclipsing Binaries (Abstract) Alexandre Amorim	233
[FK Lup] Minima of Some Eclipsing Binaries (Abstract) Alexandre Amorim	233
[GQ Lup] Photometric Variability Properties of 21 T Tauri and Related Stars From AAVSO Visual Observations John R. Percy <i>et al.</i>	151
[HT Lup] Photometric Variability Properties of 21 T Tauri and Related Stars From AAVSO Visual Observations John R. Percy <i>et al.</i>	151
[T Lyr] Further Studies of “Irregularity” in Pulsating Red Giants John R. Percy and Junjiajia Long	161
[X Lyr] Further Studies of “Irregularity” in Pulsating Red Giants John R. Percy and Junjiajia Long	161
[XY Lyr] Further Studies of “Irregularity” in Pulsating Red Giants John R. Percy and Junjiajia Long	161
[HK Lyr] Further Studies of “Irregularity” in Pulsating Red Giants John R. Percy and Junjiajia Long	161
[β Lyr] Intrinsic Variability of Eclipsing Variable β Lyrae Measured With a Digital SLR Camera (Abstract) Donald F. Collins	144
[V578 Mon] Photometry of V578 Monocerotis Arnold M. Heiser	93
[TY Oph] Further Studies of “Irregularity” in Pulsating Red Giants John R. Percy and Junjiajia Long	161
[V2672 Oph] Absolute Magnitudes and Distances of Recent Novae Yitping Kok	193
[T Ori] Photometric Variability Properties of 21 T Tauri and Related Stars From AAVSO Visual Observations John R. Percy <i>et al.</i>	151
[RY Ori] Photometric Variability Properties of 21 T Tauri and Related Stars From AAVSO Visual Observations John R. Percy <i>et al.</i>	151
[UX Ori] Photometric Variability Properties of 21 T Tauri and Related Stars From AAVSO Visual Observations John R. Percy <i>et al.</i>	151
[BF Ori] Photometric Variability Properties of 21 T Tauri and Related Stars From AAVSO Visual Observations John R. Percy <i>et al.</i>	151
[BL Ori] Further Studies of “Irregularity” in Pulsating Red Giants John R. Percy and Junjiajia Long	161

[BN Ori] Photometric Variability Properties of 21 T Tauri and Related Stars From AAVSO Visual Observations John R. Percy <i>et al.</i>	151
[EX Ori] Further Studies of “Irregularity” in Pulsating Red Giants John R. Percy and Junjiajia Long	161
[V350 Ori] Photometric Variability Properties of 21 T Tauri and Related Stars From AAVSO Visual Observations John R. Percy <i>et al.</i>	151
[NP Pav] Minima of Some Eclipsing Binaries (Abstract) Alexandre Amorim	233
[TU Phe] Photometric Variability Properties of 21 T Tauri and Related Stars From AAVSO Visual Observations John R. Percy <i>et al.</i>	151
[RZ Psc] Photometric Variability Properties of 21 T Tauri and Related Stars From AAVSO Visual Observations John R. Percy <i>et al.</i>	151
[ST Psc] Further Studies of “Irregularity” in Pulsating Red Giants John R. Percy and Junjiajia Long	161
[TX Psc] Further Studies of “Irregularity” in Pulsating Red Giants John R. Percy and Junjiajia Long	161
[U Pup] The VSS RASNZ Variable Star Charts: a Story of Co-Evolution Alan Plummer and Mati Morel	123
[NX Pup] Photometric Variability Properties of 21 T Tauri and Related Stars From AAVSO Visual Observations John R. Percy <i>et al.</i>	151
[V351 Pup] Absolute Magnitudes and Distances of Recent Novae Yitping Kok	193
[V4633 Sgr] Absolute Magnitudes and Distances of Recent Novae Yitping Kok	193
[V5581 Sgr] Absolute Magnitudes and Distances of Recent Novae Yitping Kok	193
[V5582 Sgr] Absolute Magnitudes and Distances of Recent Novae Yitping Kok	193
[AK Sco] Photometric Variability Properties of 21 T Tauri and Related Stars From AAVSO Visual Observations John R. Percy <i>et al.</i>	151
[V856 Sco] Photometric Variability Properties of 21 T Tauri and Related Stars From AAVSO Visual Observations John R. Percy <i>et al.</i>	151
[τ^1 Ser] Further Studies of “Irregularity” in Pulsating Red Giants John R. Percy and Junjiajia Long	161
[RR Tau] Photometric Variability Properties of 21 T Tauri and Related Stars From AAVSO Visual Observations John R. Percy <i>et al.</i>	151

[RY Tau] Photometric Variability Properties of 21 T Tauri and Related Stars From AAVSO Visual Observations John R. Percy <i>et al.</i>	151
[CP Tau] Further Studies of “Irregularity” in Pulsating Red Giants John R. Percy and Junjiajia Long	161
[RV Tel] Minima of Some Eclipsing Binaries (Abstract) Alexandre Amorim	233
[X TrA] Further Studies of “Irregularity” in Pulsating Red Giants John R. Percy and Junjiajia Long	161
[RR TrA] Minima of Some Eclipsing Binaries (Abstract) Alexandre Amorim	233
[V Tuc] Minima of Some Eclipsing Binaries (Abstract) Alexandre Amorim	233
[VY UMa] Further Studies of “Irregularity” in Pulsating Red Giants John R. Percy and Junjiajia Long	161
[T UMi] T Ursae Minoris: From Mira to ??? (Abstract) Grant Foster	140
[RR Vel] Minima of Some Eclipsing Binaries (Abstract) Alexandre Amorim	233
[DY Vul] Further Studies of “Irregularity” in Pulsating Red Giants John R. Percy and Junjiajia Long	161
[IL Vul] The 2009 July Superoutburst of IL Vulpeculae David Boyd, Tut Campbell, and George Roberts	39
[185 Eclipsing Binaries] Recent CCD Minima of 185 Eclipsing Binary Stars Gerard Samolyk	183
[161 Eclipsing Binaries] Recent Minima of 161 Eclipsing Binary Stars Gerard Samolyk	85
[64 RR Lyr and δ Sct stars] Recent Maxima of 64 Short Period Pulsating Stars Gerard Samolyk	12
[3C 66A] Differential Ensemble Photometry by Linear Regression Kevin B. Paxson	202
[Cas A] King Charles’ Star: A Multidisciplinary Approach to Dating Cassiopeiae A (Abstract) Martin Lunn and Lila Rakoczy	231
[CSS 081007:030559+054715] Optical Time-Series Photometry of the Peculiar Nova CSS 081007:030559+054715 Matthew Templeton <i>et al.</i>	147
[GSC 1393-1461] Two New Eclipsing Binary Systems: GSC 1393-1461 and GSC 2449-0654, and One New Flare Star: GSC 5604-0255 P. V. Sada	52
[GSC 2449-0654] Two New Eclipsing Binary Systems: GSC 1393-1461 and GSC 2449-0654, and One New Flare Star: GSC 5604-0255 P. V. Sada	52

[GSC 5604-0255] Two New Eclipsing Binary Systems: GSC 1393-1461 and GSC 2449-0654, and One New Flare Star: GSC 5604-0255 P. V. Sada	52
[HD 189733b] Observing Exoplanet Transits With Digital SLR Cameras Colin Littlefield	212
[HIP 18859] Debris Disks in the AB Doradus Moving Group (Abstract) Mimi Hang	142
[IRAS 12521-6034] New Variable Stars in the Southern Cross (Abstract) Victor Angel Buso	233
[NSV 1436] Ross 4—A Possible Recurrent Nova? Samantha J. Brown <i>et al.</i>	176
[NSV 19431] NSV 19431 and YY Centauri—Two Mira Variables Peter F. Williams	45
[NSVS 5222076] Secular Variation of the Mode Amplitude-Ratio of the Double-Mode RR Lyrae Star NSVS 5222076 David A. Hurdis and Tom Krajci	1
[Ross 4] Ross 4—A Possible Recurrent Nova? Samantha J. Brown <i>et al.</i>	176
[SDSS 1031+20] GALEX and Optical Light Curves of LARPs (Abstract) Paula Szkody	141
[SDSS 1212+01] GALEX and Optical Light Curves of LARPs (Abstract) Paula Szkody	141
[SDSS J094002.56+274942.0] Photometry of the Dwarf Nova SDSS J094002.56+274942.0 in Outburst Tom Krajci and Patrick Wils	33
[VSXJ 202751.9+414727] Two New Variable Stars in the Fields of Nova Cygni 2006 and Nova Cygni 2007 David Boyd	168
[VSXJ 211145.0+444530] Two New Variable Stars in the Fields of Nova Cygni 2006 and Nova Cygni 2007 David Boyd	168
X-RAY SOURCES	
Optical Time-Series Photometry of the Peculiar Nova CSS 081007:030559+054715 Matthew Templeton <i>et al.</i>	147

NOTES